

UNCLASSIFIED

AD NUMBER

AD873169

LIMITATION CHANGES

TO:

Approved for public release; distribution is unlimited. Document partially illegible.

FROM:

Distribution authorized to U.S. Gov't. agencies and their contractors; Critical Technology; JUN 1970. Other requests shall be referred to Air Force Weapons Laboratory, WLCT, Kirtland AFB, NM 87117. Document partially illegible. This document contains export-controlled technical data.

AUTHORITY

afwl, ltr, 30 nov 1971

THIS PAGE IS UNCLASSIFIED

AFWL-TR-70-20

AFWL-TR-
70-20

20

AD 163. —
DDG FILE COPY
AD873169

ANALYTICAL MODEL FOR HIGH EXPLOSIVE MUNITIONS STORAGE

H. L. Schreyer

L. E. Romesberg

Mechanics Research, Inc.
Albuquerque, New Mexico

TECHNICAL REPORT NO. AFWL-TR-70-20

June 1970

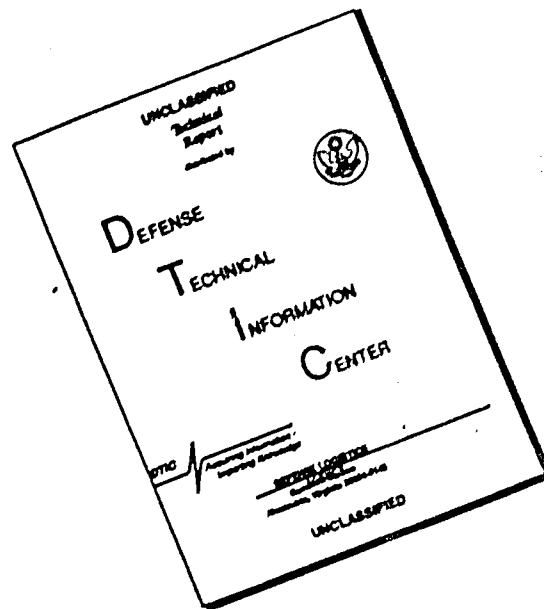
AIR FORCE WEAPONS LABORATORY
Air Force Systems Command
Kirtland Air Force Base
New Mexico

DDC
RECEIVED
AUG 23 1970
A

This document is subject to special export controls and each transmittal to foreign governments or foreign nationals may be made only with prior approval of AFWL (WLCT) , Kirtland AFB, NM, 87117.

258

DISCLAIMER NOTICE



THIS DOCUMENT IS BEST QUALITY AVAILABLE. THE COPY FURNISHED TO DTIC CONTAINED A SIGNIFICANT NUMBER OF PAGES WHICH DO NOT REPRODUCE LEGIBLY.

ANALYTICAL MODEL FOR HIGH EXPLOSIVE MUNITIONS STORAGE

H. L. Schreyer

L. E. Romesberg

Mechanics Research, Inc.
Albuquerque, New Mexico

TECHNICAL REPORT NO. AFWL-TR-70-20

This document is subject to special export controls and each transmittal to foreign governments or foreign nationals may be made only with prior approval of AFWL (WJCT), Kirtland AFB, NM 87117. Distribution is limited because of the technology discussed in the report.

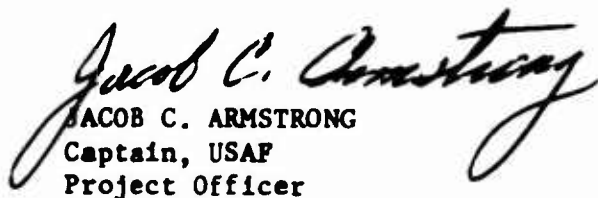
FOREWORD

This report was prepared by Mechanico Research, Inc., Albuquerque, New Mexico, under Contract F29601-69-C-0034. The research was performed under Project 1597, Task 12.

Inclusive dates of research were February 1969 through March 1970. The report was submitted 24 March 1970, by the Air Force Weapons Laboratory Project Officer, Captain Jacob C. Armstrong (WLCT).

Information in this report is embargoed under the U.S. Export Control Act of 1949, administered by the Department of Commerce. This report may be released by departments or agencies of the U.S. Government to departments or agencies of foreign governments with which the United States has defense treaty commitments, subject to approval of AFWL (WLCT).

This report has been reviewed and is approved.


JACOB C. ARMSTRONG
Captain, USAF
Project Officer


CLARENCE E. TESKE
Major, USAF
Chief, Aerospace Facilities Branch


CLIFF M. WHITEHEAD
Colonel, USAF
Chief, Civil Engineering Division

ABSTRACT

Analytical models and subsequent computer codes have been developed for predicting peak overpressure, positive unit impulse, the distribution and impact velocity of bomb fragments, crater dimensions and ejecta thickness from the detonations of typical bomb stacks used by the Air Force. These models consider aboveground barricaded stacks with an equivalent net weight high-explosive range of 10 to 500 tons of TNT. The peak overpressure and impulse from a detonation are obtained by modifying the known results of a bare hemispherical charge to take into account the stack and barricade geometries and the interaction effect of bombs. Fragment dispersion patterns are predicted by combining experimental results for single bombs and using the trajectory equations for the motion of a steel fragment in air. By using basic principles and experimental data, crater and ejecta dimensions are predicted. Based on output from the computer codes, illustrative examples are given together with recommendations for future tests to obtain needed data. Programs for optimizing munition storage areas are also suggested.

(Distribution Limitation Statement No. 2)

This page intentionally left blank.

CONTENTS

<u>Section</u>		<u>Page</u>
I.	INTRODUCTION	1
II.	BLAST EFFECTS	4
	1. Introduction	4
	2. Bare Charge Parameters	5
	3. Bomb Effect	9
	4. Stack Geometry Effect	10
	5. Barricade Effect	27
	6. Summary	33
III.	FRAGMENTATION	34
	1. Introduction	34
	2. Statement of Problem	34
	3. Scope of Investigation	35
	4. Analytical Fragment Model, Single Bomb	37
	a. Fragment Parameters	37
	b. Fragment Trajectories	39
	c. Fragment Ballistic Coefficients	45
	d. Coordinate System	48
	e. Barricade Geometry Considerations	52
	f. Distribution of Fragments	55
	5. Analytical Fragment Model, Stack of Bombs	59
	6. Summary	61
IV.	CRATERING	62
	1. Introduction	62

<u>Section</u>	<u>Page</u>
2. The Effect of Charge Shape	64
a. Preliminary Comments	64
b. Basic Assumptions	64
c. Cratering Factor	68
d. Charge Shape and Nondimensional Variables	69
3. Crater and Ejecta Formations	74
a. Basic Shape Parameters	74
b. Energy Considerations	82
c. Dimensional Considerations	86
d. Energy Dissipation	89
4. Summary	95
V. ILLUSTRATIVE EXAMPLES	99
1. Introduction	99
2. Results from Blast Pressure Program	100
3. Fragment Distributions	109
4. Apparent Crater and Ejecta Dimensions	115
5. Summary	120
VI. RECOMMENDED INVESTIGATIONS	121
1. Introduction	121
2. Pressure and Impulse Data	122
a. Single Bombs	122
b. Bomb Stacks	122
c. Barricades	123
3. Fragment Data	124

<u>Section</u>	<u>Page</u>
4. Crater Data	125
5. Optimization of Storage Areas	127
VII. CONCLUSIONS	129
Appendix I	131
Appendix II	165
Appendix III	220
References	235

ILLUSTRATIONS

<u>Figure</u>		<u>Page</u>
1	Shock Wave Parameters for Hemispherical TNT Surface Explosion at Sea Level	6
2	Bomb Stack Dimensions	15
3	Overpressure Ratio x FAR vs Distance from Charge Center	17
4	Impulse Ratio x FAR vs Distance from Charge Center	18
5	Comparison of Predicted Overpressure and Impulse Ratios to BRL Data for Cubical Shaped Explosive Stack	22
6	Edge Pressure/Face Pressure and Edge Impulse/Face Impulse vs Scaled Distance from Charge Center	26
7	Geometry Effect and Interpolation Technique	28
8	Exterior Leakage Pressure vs Scaled Distance	30
9	Representative Fragmentation Data for the Explosion of a Single Bomb	36
10	Polar and Departure Angles for a Bomb Fragment	38
11	Trajectory of a Fragment	40
12	Typical Bomb Stack Barricade	49
13	Coordinate System for a Regular Barricade Enclosing a Single Bomb	50
14	General Barricade Configuration	54
15	Approximate Impact Areas	57
16	Fragmentation Survey Plan for Phase II of the "Big Papa" Tests	60
17	Notation for Typical Charge Shape	66
18	A Set of Four Charge Shapes	72
19	Idealized crater and Ejecta Parameters	75

<u>Figure</u>		<u>Page</u>
20	Maximum Crater Slope	77
21	Centroids of Crater and Ejecta Elements	81
22	Trajectory of an Element	83
23	Pressure vs Range for Various Charge and Barricade Combinations	101
24	Pressure Isobars for Various Charge and Barricade Combinations	106
25	Typical Fragment Trajectories for a Fixed Value of Azimuth Angle and Incremental Departure Angles	110
26	Impact Conditions vs Range at Selected Azimuth Angles for Sample Problem	112
27	Apparent Crater Dimensions in Soil vs Charge Weight	116
28	Nondimensional Ejecta Shapes as a Function of Earth Media Parameter β	118
29	Apparent Crater Dimensions in Basalt Rock vs Charge Weight	119
30	Typical Input Data Card for Program Blast	156
31	Stack and Barricade Geometry Parameters	157
32	Typical Input Data for Program FRAGM	207

TABLES

<u>Table</u>		<u>Page</u>
I	Polynomial Coefficients for Determining Peak Overpressure and Scaled Positive Impulse for a Bare Hemispherical Charge	8
II	Peak Overpressures (PSI) Yielded by 50-lb. RDX Composition C-3 Charges	12
III	Positive Impulse (PSI-MS) Yielded by 50-lb RDX Composition C-3 Charges	13
IV	Experimentally Based Coefficients for Determining Pressure Ratios and Impulse Ratios as Functions of FAR	20
V	Polynomial Coefficients for B, C, D, F, G, and H	21
VI	Polynomial Coefficients for the Ratios Edge Pressure/Face Pressure and Edge Impulse/Face Impulse	25
VII	Polynomial Coefficients for Pressure Ratio Vs Z Polynomials for Barricade Effect	32

ABBREVIATIONS AND SYMBOLS

A	Cross-sectional area of fragment perpendicular to the direction of propagation, ft. ²
B	Region defined by geometry of explosive charge
B _L	Bottom half of region of explosive charge
B, C, D	Coefficients for (P/P _{sphere}) polynomial in FAR
C _D	Drag coefficient
C _F	Cratering factor
C _{Fo}	Crater factor for a reference charge
C _O ^F	C _F /C _{Fo}
C _O , C ₁ , ...	Coefficients for B, C, D, F, G, and H polynomials
D _a	Apparent depth of crater, ft.
E _D	Energy dissipated in the form of heat
E _G	Total kinetic energy of the earth elements, ft. lb.
E _s	Kinetic energy delivered to earth surface, ft. lb.
E ^D	Energy dissipation ratio
E _T	Total kinetic energy of a charge, ft. lb.
EFNB	Effective number of bombs in a stack
F _D	Drag force on fragment, lbs.
F _D ^X	Drag force in X-direction, lbs.

F_D^Y	Drag force in Y-direction, lbs.
F_G	Force of gravity, lbs.
F, G, H	Coefficients for (I/I_{sphere}) polynomial in FAR
FAR	Face area ratio
H	Vertical distance from centroid of crater volume element to centroid of ejecta volume element, ft.
H_e	Height of ejecta, ft.
I	Scaled positive impulse, $\text{psi-ms/lb.}^{1/3}$
K	Ratio of energy at surface for a yield W divided by energy at surface for a reference charge yield W_0
L	Distance to horizontal plane through center of mass, ft.
[L]	total length dimension
[M]	Fundamental mass dimension
$N_{\theta_1, \theta_2}^{\beta_1, \beta_2}$	Number of fragments in the region $\theta_1 \leq \theta \leq \theta_2$, $\beta_1 \leq \beta \leq \beta_2$
P	Peak overpressure, psi
R	Distance from burst point, ft.
R_a	Apparent radius of crater, ft.
R_c	Radius to center of mass of crater volume element, ft.
R_e	Radius to center of mass of ejecta volume element, ft.

$R_{j-1,j}, R_{j,j+1}$	Lower and upper boundaries of impact area A_j
R_1, R_2, \dots	Ordered impact ranges for nearest, next nearest, etc., impact points
$\tilde{R}_1, \tilde{R}_2, \tilde{R}_3$	Distance from burst point to points of barricade, ft.
SD	Stack depth, ft.
SH	Stack height, ft.
SL	Stack length, ft.
T	W/W_0
[T]	Fundamental time dimension
V	Speed of fragment, ft./sec.
\dot{V}	Time rate change of velocity, ft./sec. ²
V_e	Volume of ejecta, ft. ³
V_L	Volume of bottom half of charge, ft. ³
\vec{V}_0	Velocity vector at time = zero, ft./sec.
W	Weapon yield, equivalent weight of TNT
W_L	Weapon yield for a charge shape with center of mass at L, lbs. of TNT
W_0	Yield of a reference charge, lb. of TNT
X	Horizontal distance for an element trajectory, ft.
Z	Scaled distance, ft./lb. ^{1/3}
Z_e	Vertical height to center of mass ejecta volume element, ft.
Z_1, Z_2, Z_3	Height of barricade at $\tilde{R}_1, \tilde{R}_2, \tilde{R}_3$ respectively, ft.

a	Coefficient in polynomial \hat{x}
a_0	Acceleration in vertical direction, ft./sec. ²
a_0, a_1, \dots	Coefficients for polynomial in P
b	Coefficient in polynomial \hat{x}
b_0, b_1, \dots	Coefficients for polynomial in I
c	Ballistic coefficient, 1/ft.
c_0, c_1, \dots	Coefficients for polynomials B, C, D, F, G, and H
d_0, d_1, \dots	Coefficients for polynomial EDGE PRESSURE/FACE PRESSURE
e	Kinetic energy per unit mass, ft./lb.
\bar{e}_B	Unit vector in direction of center line out of nose of bomb
e_s	Energy per unit mass delivered at earth surface, ft./lb.
e_0	Initial kinetic energy per unit mass, ft./lb.
\bar{e}_0	Unit vector in direction \bar{V}_0
e_0, e_1, \dots	Coefficients for polynomial EDGE IMPULSE/FACE IMPULSE
$\bar{e}_1, \bar{e}_2, \bar{e}_3$	Unit vectors in directions X, Y, and Z respectively.
f	Non-dimensional function of ϕ
f'	Unknown function
f_0, f_1, \dots	Coefficients for polynomial for pressure ratio for barricade effect
g	Gravity constant, ft./sec. ²
i_s	Positive unit impulse, psi-ms

k	Constant
l	Length of sides for a steel cube, ft.
m	Mass of fragment, slugs
t	Time, sec.
v	Velocity in vertical direction, ft./sec.
v_o	Initial speed of particles in charge, ft./sec.
w_F	Weight of fragment, lb.
w_{FG}	Weight of fragment, grams
x	Distance along X-direction, ft.
\ddot{x}	Acceleration in X-direction, ft./sec. ²
\hat{x}	Crater depth as a function of R, ft.
x_c	Coordinate to center of mass of element of crater volume, ft.
y	Distance along Y-direction, ft.
\ddot{y}	Acceleration in Y-direction, ft./sec. ²
y_o	Height of bomb above impact point, ft.
z	Distance above earth surface, ft.
\ddot{z}	Acceleration in vertical direction, ft./sec. ²
z_{CG}	Vertical distance to center of mass of explosive, ft.
z_{CG}^o	Height of center of mass of reference charge, ft.
z_o	Vertical position at time = 0, ft.

α	Angle between horizontal line and tangent to trajectory, radians
$\dot{\alpha}$	Time rate change of α , radians/sec.
α_{impact}	Impact angle for fragment, degrees
β	Departure angle from burst point measured from horizontal, degrees
$\hat{\beta}$	Soil parameters
β_1, β_2	Lower and upper bounds on a region of β respectively
γ	Angle between centerline out nose of bomb and initial velocity of fragment, degrees
γ_A	Weight density of air, lb./ft. ³
δ	Angle between azimuth angle θ and barricade wall
ΔV_c	Element of volume of the crater, ft. ³
ΔV_e	Element of volume of the ejecta, ft. ³
Δx	Incremental change in x
Δy	Incremental change in y
$\Delta \alpha$	Incremental change in α
$\Delta \beta$	Increment of β
$\Delta \theta$	Increment of θ
$\dot{\epsilon}$	Strain rate
ζ	Constant
θ	Angle between line out center of barricade opening and horizontal direction of fragment
θ_B	Angle between line out center of barricade opening and centerline out nose of bomb

θ_1, θ_2	Lower and upper bound on a region of θ respectively
μ	Constant for energy computations
ν	Non-dimensional variable, generalized viscosity
ν'	Soil viscosity
ρ	Mass density of soil
ρ_A	Density of air, slugs/ft. ³
σ	Soil parameter
τ	Stress
ϕ	Angle between R_2 and barricade wall
ψ	Angle between R_1 and barricade wall
$\Psi(\gamma)$	Number of fragments per steradian
Ψ_{12}	Average number of fragments per steradian in a solid angle

This page intentionally left blank.

SECTION I

INTRODUCTION

One of the major problems at many Air Force installations is the storage of large quantities of munitions. Safety considerations for protection of personnel and material in the event of accidental detonation, although overriding, are in direct conflict with economics, i.e., large clear zones require considerable real estate with resulting long roads and utility lines. If munitions storage clearance requirements could be reduced without endangering safety requirements, significant economic gains could be realized.

Full-scale tests of munitions storage concepts have been conducted and have yielded valuable information leading toward more rational munitions storage criteria. Such tests are, however, expensive and exceedingly time consuming. Availability of analytical procedures which could be used with some confidence to predict the effects of detonation of a stack of munitions would be invaluable in analyzing new storage concepts, or in rational, effective planning of such future full scale tests as may be required. This study is a step toward development of such procedures.

The most significant parameters in determining munitions detonation hazards include peak overpressure, unit impulse, mass and velocity of projectiles formed from bomb fragments and their distribution, crater dimensions, and the probable ejecta distribution. This report outlines an analytical model that adequately

predicts these parameters for the range of 25,000 to 500,000 pounds net weight of high explosives. Associated with the report are computer programs that perform the numerical analysis required for the models. Even though the most recent sources have been consulted, it was considered advisable to construct the model and the computer programs in a manner that would easily allow alterations as new experimental and theoretical work became available.

Section II considers the peak overpressure and unit impulse emanating from bomb stacks, both barricaded and unbarricaded. Section III handles fragmentation while Section IV discusses cratering. The corresponding computer programs are listed and described in Appendices I, II and III respectively. Examples of results obtained from the computer programs are presented in Section V. As a result of the extensive literature survey that was conducted and from the formation of the analytical models, it became apparent that further investigations, both experimental and analytical, in certain critical areas would be highly beneficial. Such a program is outlined in Section VI.

Throughout the report, an attempt has been made to use a judicious combination of basic principles and results from small and full-scale tests. Such an approach is considered necessary if the results are to be used for typical situations that currently confront the Air Force. Furthermore, the use of fundamental concepts implies that new situations can be handled with some degree of confidence. However, it should always be kept in mind that soil conditions, for example, can change with time and

accordingly, even well designed experiments produce data with a considerable amount of scatter. Accordingly, a certain amount of engineering judgment is required in connection with the results of this study.

SECTION II

BLAST EFFECTS

1. INTRODUCTION

The objective of this section is to develop an analytical model which will predict the environment produced by the air blast from a high explosive detonation. The primary parameters to be investigated are the peak overpressure and positive impulse experienced at all points on the surface surrounding a high-order surface detonation. The effects to be investigated include: a) the effect of substituting conventional Air Force bombs for TNT in the explosive stack; b) the effect on the peak overpressure-scaled distance P-Z and scaled positive impulse-scaled distance I-Z relationships produced by the explosive stack geometry, and c) the effect on the P-Z and I-Z relationships produced by a barricade surrounding the explosive stack on three sides (standard open-end barricade). The scaled distance Z is defined to be the distance R from the point of detonation divided by the equivalent charge weight in pounds of TNT to the one-third power $W^{1/3}$

$$Z = R/W^{1/3} \quad (1)$$

The scaled positive impulse I is defined to be the positive unit impulse i_s divided by the equivalent charge weight in pounds of TNT to the one-third power $W^{1/3}$

$$I = i_s/W^{1/3} \quad (2)$$

The general approach followed is to develop a model to predict the P-Z and I-Z relationships for a surface detonation of a hemispherical stack of high explosive TNT, and then to modify these relationships to account for the individual effects listed above. The effect produced by changing the point of detonation in the stack is assumed to be negligible. (See Reference 1).

2. BARE CHARGE PARAMETERS

The initial task in the development is to model the environment produced by a surface detonation of a bare, i.e., unbarri-caded, hemispherical stack of TNT, with respect to peak overpressure and scaled positive impulse. Curves describing the peak overpressure-scaled distance relationship for high explosive surface detonations are available throughout the literature. These relationships have been developed through many years of full scale testing and are widely accepted. Discrepancies do appear in the literature when comparing the relationships published by one testing agency with those published by another; however, these discrepancies are of a relatively small order. The relationships selected for the model development (See Figure 1) are published in Reference 2.

To carry out the objectives of this section, it is necessary to have these results available in a numerical form. The procedure used in modeling the P-Z and I-Z relationships is as follows: a) Points on the P-Z and I-Z curves are selected; b) the coordinates (P, Z) and (I, Z) of these points are transformed

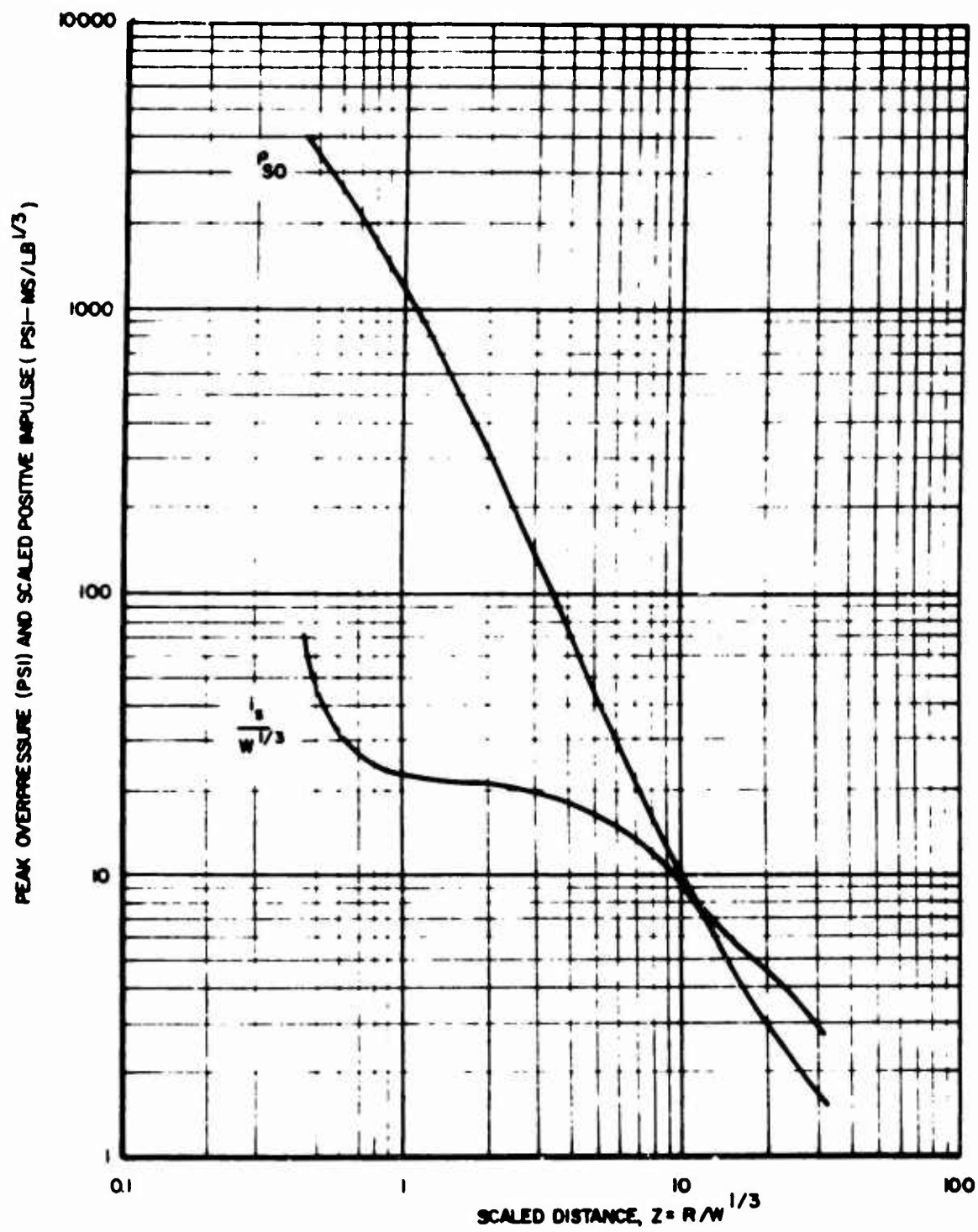


Figure 1. Shock Wave Parameters for Hemispherical TNT Surface Explosion at Sea Level

by computing the natural logarithm of each coordinate so that the coordinates $(\ln P, \ln Z)$ and $(\ln I, \ln Z)$ are obtained;
 c) the coordinates $(\ln P, \ln Z)$ and $(\ln I, \ln Z)$ are used in a least squares polynomial curve fit program to obtain relationships of the form

$$\ln P = a_0 + a_1 (\ln Z) + a_2 (\ln Z)^2 + \dots \text{ and} \quad (3)$$

$$\ln I = b_0 + b_1 (\ln Z) + b_2 (\ln Z)^2 + \dots \quad (4)$$

d) the polynomial coefficients obtained from the curve fit program are then used to evaluate the value of peak overpressure P and scaled positive impulse I at the desired values of scaled distance Z .

This procedure yields results which are in very close agreement with the original relationships (curves). The maximum error in the predicted peak overpressure-scaled distance relationship is less than 7% for $.5 < Z < 10 \text{ ft/lb}^{1/3} (P > 10 \text{ psi})$, less than 3% for $10 < Z < 45 \text{ ft/lb}^{1/3} (1.0 > P > 10 \text{ psi})$ and less than 5.0% for $45 < Z < 500 \text{ ft/lb}^{1/3} (P < 1.0 \text{ psi})$. The maximum error in the predicted scaled positive impulse-scaled distance relationship is less than 6% for $.5 < Z < 10 \text{ ft/lb}^{1/3} (I > 10.0 \text{ psi-ms/lb}^{1/3})$, less than 5% for $10 < Z < 75 \text{ ft/lb}^{1/3} (10.0 > I > 1.0 \text{ psi-ms/lb}^{1/3})$ and less than 15% for $75 < Z < 500 \text{ ft/lb}^{1/3} (I < 1.0 \text{ psi-ms/lb}^{1/3})$.

The resulting coefficients for determining the overpressure and scaled positive impulse according to Equations (3) and (4) are given in Table I.

TABLE I

POLYNOMIAL COEFFICIENTS FOR DETERMINING PEAK OVERPRESSURE
AND SCALED POSITIVE IMPULSE FOR A BARE HEMISPHERICAL CHARGE

$$\begin{aligned} a_0 &= 10.7036810 \times 10^1 \\ a_1 &= -0.1663724 \times 10^1 \\ a_2 &= -0.2516481 \times 10^0 \\ a_3 &= -0.1137714 \times 10^0 \\ a_4 &= +0.3818405 \times 10^{-1} \\ a_5 &= +0.5035198 \times 10^{-1} \\ a_6 &= -0.2756970 \times 10^{-1} \\ a_7 &= +0.5557968 \times 10^{-2} \\ a_8 &= -0.5108014 \times 10^{-3} \\ a_9 &= +3.1795565 \times 10^{-4} \end{aligned}$$

$$\begin{aligned} b_0 &= +0.3129288 \times 10^1 \\ b_1 &= -0.1295979 \times 10^0 \\ b_2 &= +0.4112452 \times 10^0 \\ b_3 &= -0.7687394 \times 10^0 \\ b_4 &= +0.4969224 \times 10^0 \\ b_5 &= -0.1684197 \times 10^0 \\ b_6 &= +0.2805656 \times 10^{-1} \\ b_7 &= -0.1791292 \times 10^{-2} \end{aligned}$$

3. BOMB EFFECT

The effect produced by substituting conventional Air Force bombs for TNT in the explosive stack has been studied by several authors for many years. This effect is accounted for in the model development through the use of a bomb factor. This factor is multiplied by the total explosive weight in the bomb stack to yield an equivalent weight of TNT. The bomb factor includes the confined explosion effect, the surface reflectivity effect, and the individual bomb geometry effect. Typical bomb factors can be found in Reference 3. No attempt has been made to account for the explosion confinement effect caused by stacking bombs. There will be some confinement effect caused by surrounding a bomb by other bombs. However, since there apparently is no empirical or theoretical data available, this effect cannot be accounted for in the present model.

4. STACK GEOMETRY EFFECT

It is a well accepted fact that the geometry of the explosive stack has a great effect on the peak overpressure and positive impulse at positions "close" to the stack. This effect diminishes with distance from the stack. Even though this fact is well known and accepted, there is very little data available in the current literature which quantitatively describes such a variation.

Apparently Reference 4 describes one of the few attempts to measure the effect of the geometry of charges on peak overpressure and positive impulse. The report is composed basically of peak overpressure and positive impulse measurements using eight charge shapes composed of 50 pounds of RDX composition C-3 explosive which is equivalent to 54.5 pounds of TNT.

It will be assumed that a "standard" high explosive bomb stack can be approximated by a solid stack of explosives with a rectangular solid shape. Therefore, the only shapes considered by the above mentioned report which are pertinent to the model development are the cubical shaped charge and the plate shaped charge. The length of a side of the cubical shaped charge used in the test was 9.6 in. x 9.6 in. while the plate dimensions were 54.1 in. x 9.0 in. x 1.8 in. Pressure and impulse measurements were made at 35 ft., 45 ft., 60 ft., 70 ft., and 80 ft., from the center of the charges, along lines perpendicular

to each face and through the charge center for the cube and the plate, and along lines through the edge and the charge center in a horizontal plane for the cube. These distances from the charge center correspond to scaled distances of 9.22, 11.85, 15.80, 18.43, and 21.06 ft/lb^{1/3}, respectively. The average peak overpressures and positive impulses measured at the above locations for the sphere, cube and plate are shown in Tables II and III, respectively (See Tables 1a, 1b, 2a, 2b, 7a, and 7b of Reference 4).

The author of Reference 4 commented that the accuracy of the data did not warrant an attempt at curve fitting. Since the development of the geometry effect portion of the model is based solely on the data from this one report, steps were taken to smooth out some of the inaccuracies of the test data. To reduce the effect on readings by individual differences in recording instruments, system circuitry, and drift from zero calibration point before testing, the ratio of measurements for shaped charges divided by measurements from spherical charge rather than actual measurements was used. In other words, the model development deals with the effect of going from a spherical charge to a rectangular charge (i.e., cube and plate) rather than dealing with the rectangular charges at face value.

A parametric study performed on the data revealed that a reasonable approach to the model development would be to analyze the data with respect to an "area ratio" scheme. The reasons

TABLE II

PEAK OVERPRESSURES (PSI) YIELDED BY 50-LB. RDX COMPOSITION C-3 CHARGES

Distance From Charge Center (ft)	Sphere (1)	Cube Horizontal Face		PLATE			
				Largest Face Vertical		Largest Face Horizontal	
		(2)	(3)	Long Axis (4)	┐ Long Axis (5)	Long Axis (6)	┐ Long Axis (7)
35	10.2	11.8	13.6	11.2	18.0	8.5	10.1
45	7.7	7.5	9.6	8.1	13.6	6.8	6.6
60	4.8	3.9	5.7	5.1	6.6	5.2	4.5
70	-----	-----	-----	4.0	4.6	4.0	3.4
80	2.9	2.1	3.1	3.4	3.0	3.3	2.8

TABLE III

POSITIVE IMPULSE (PSI-MS) YIELDED BY 50-LB RDX COMPOSITION C-3 CHARGES

Distance From Charge Center (ft)	Sphere (1)	Cube Face (2)	Cube Horizontal Edge (3)	PLATE			
				Largest Face Vertical		Largest Face Horizontal	
				Long Axis (4)	┘ Long Axis (5)	Long Axis (6)	┘ Long Axis (7)
35	30.2	29.0	37.8	31.4	40.3	32.8	30.5
45	28.7	21.1	30.2	34.1	37.3	28.1	25.8
60	20.8	14.8	22.8	21.3	24.4	22.4	19.7
70	----	----	----	23.2	21.2	20.9	18.9
80	15.0	20.4	17.2	17.0	18.2	18.8	15.6

for adopting this scheme for a rectangular charge are as follows:

- a. The total energy released to the surrounding atmosphere by a charge resting on a surface should be proportional to the total surface area exposed to the atmosphere (this excludes the face of the charge which is in contact with the surface),
- b. The energy experienced by a point, which lies on a line perpendicular to one of the exposed faces of the charge and through the charge center, should be proportional to the total energy released by the detonation of the charge times the ratio of the charge face area nearest to the point to the total charge surface area exposed to the atmosphere. This ratio is hereafter referred to as the "face area ratio" (FAR), and is computed as follows (See Figure 2):

$$FAR_{P_1} = \frac{SH \times SD}{2(SH \times SD) + 2(SH \times SL) + (SL \times SD)} \quad (5a)$$

$$FAR_{P_2} = \frac{SH \times SL}{2(SH \times SD) + 2(SH \times SL) + (SL \times SD)} \quad (5b)$$

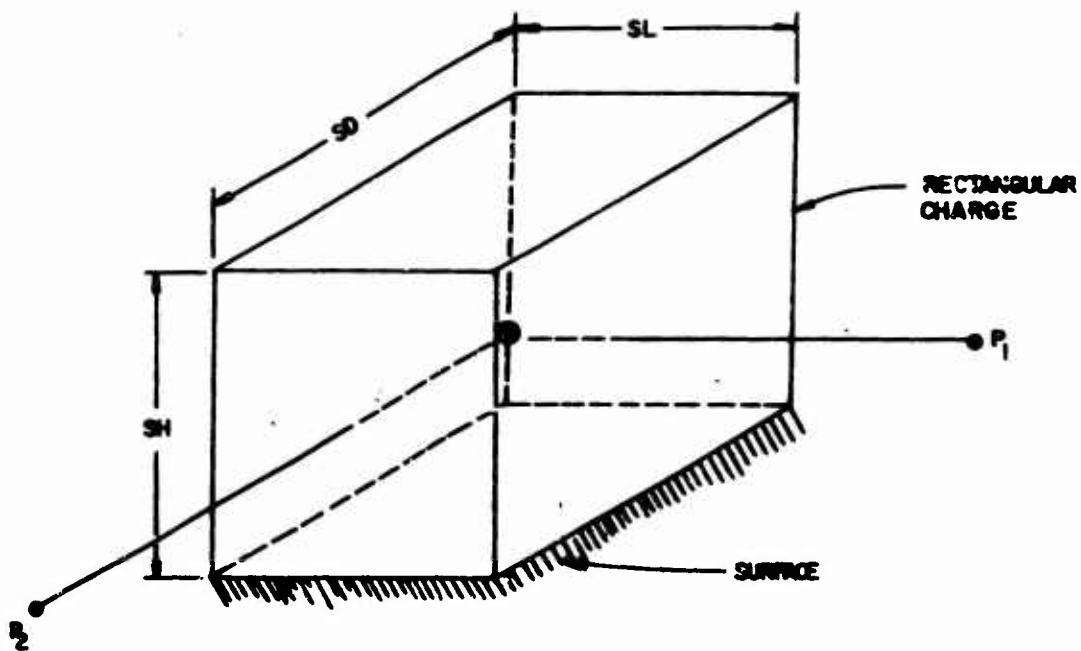


Figure 2. Bomb Stack Dimensions

The values of FAR, which correspond to the charge orientations and measurement directions for the cube and plate data of Tables II and III, are $FAR_2 = 0.20$, $FAR_4 = 0.0147$, $FAR_5 = 0.440$, $FAR_6 = 0.0227$, and $FAR_7 = 0.1365$, where the subscripts correspond to the numbered columns of both Tables. The magnitude of FAR will always be greater than 0.00 and less than 0.50. The data in columns 4 and 6 of Tables II and III are ignored in the analysis because it is felt that the values of FAR, for these conditions, are much lower than will ever be experienced in an actual bomb stack. Figure 3 shows the product of overpressure ratios (face overpressure from rectangular stacks divided by overpressure from spherical stack) and FAR plotted against distance from stack center. Figure 4 shows similar curves for impulse ratios. Note that for large distances from charge center these curves approach the value of FAR in each case. These curves not only vary with the value of FAR, but also with the distance from the charge center. At each value of R, or the corresponding value of scaled distance Z, however, a relationship between pressure ratio or impulse ratio and FAR can be established for the three curves shown in each figure. These relationships can be expressed in the form

$$\frac{P}{P_{\text{sphere}}} = B + C (FAR) + D (FAR)^2 \quad (6a)$$

$$\frac{I}{I_{\text{sphere}}} = F + G (FAR) + H (FAR)^2 \quad (6b)$$

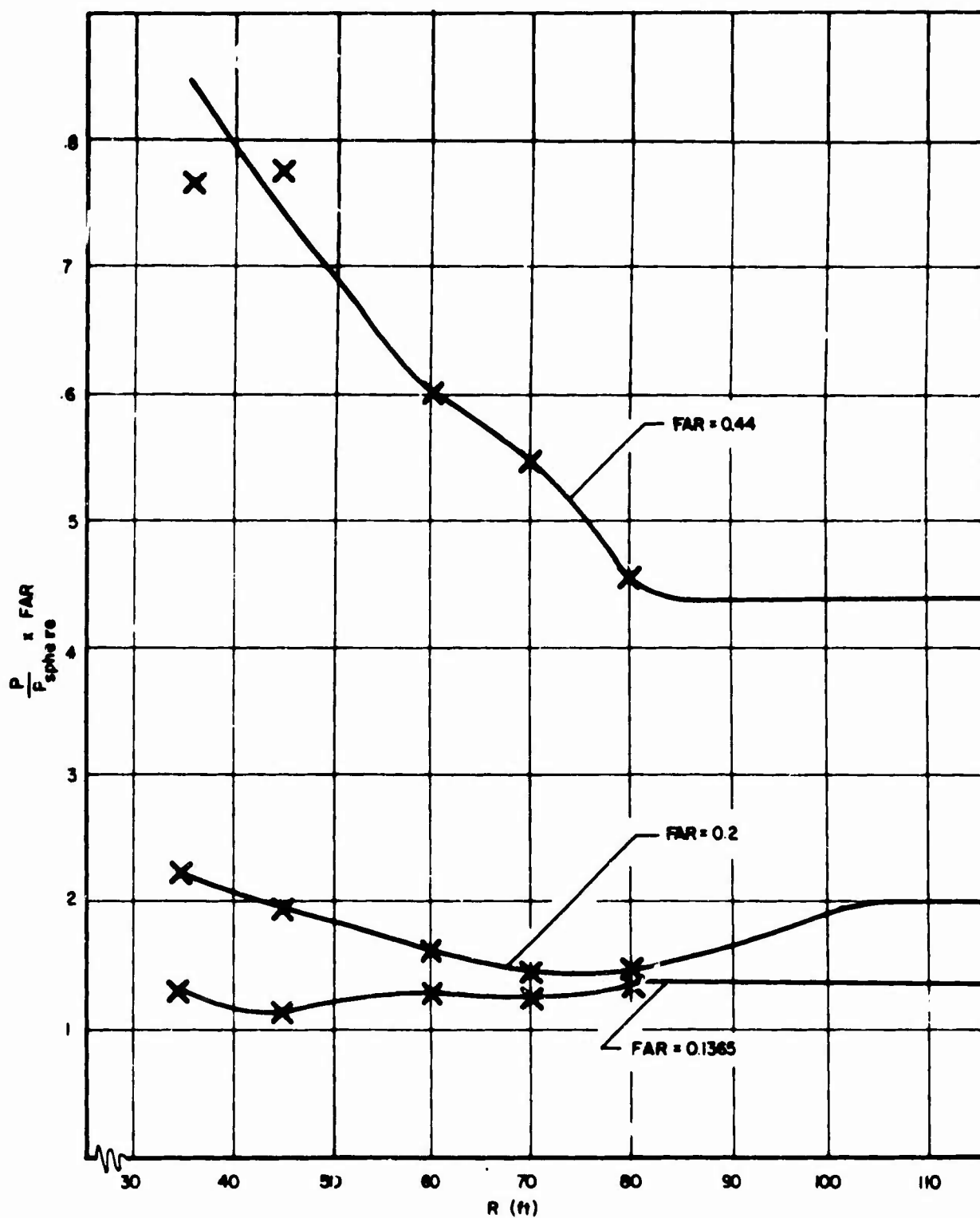


Figure 3. Overpressure Ratio x FAR vs. Distance from Charge Center

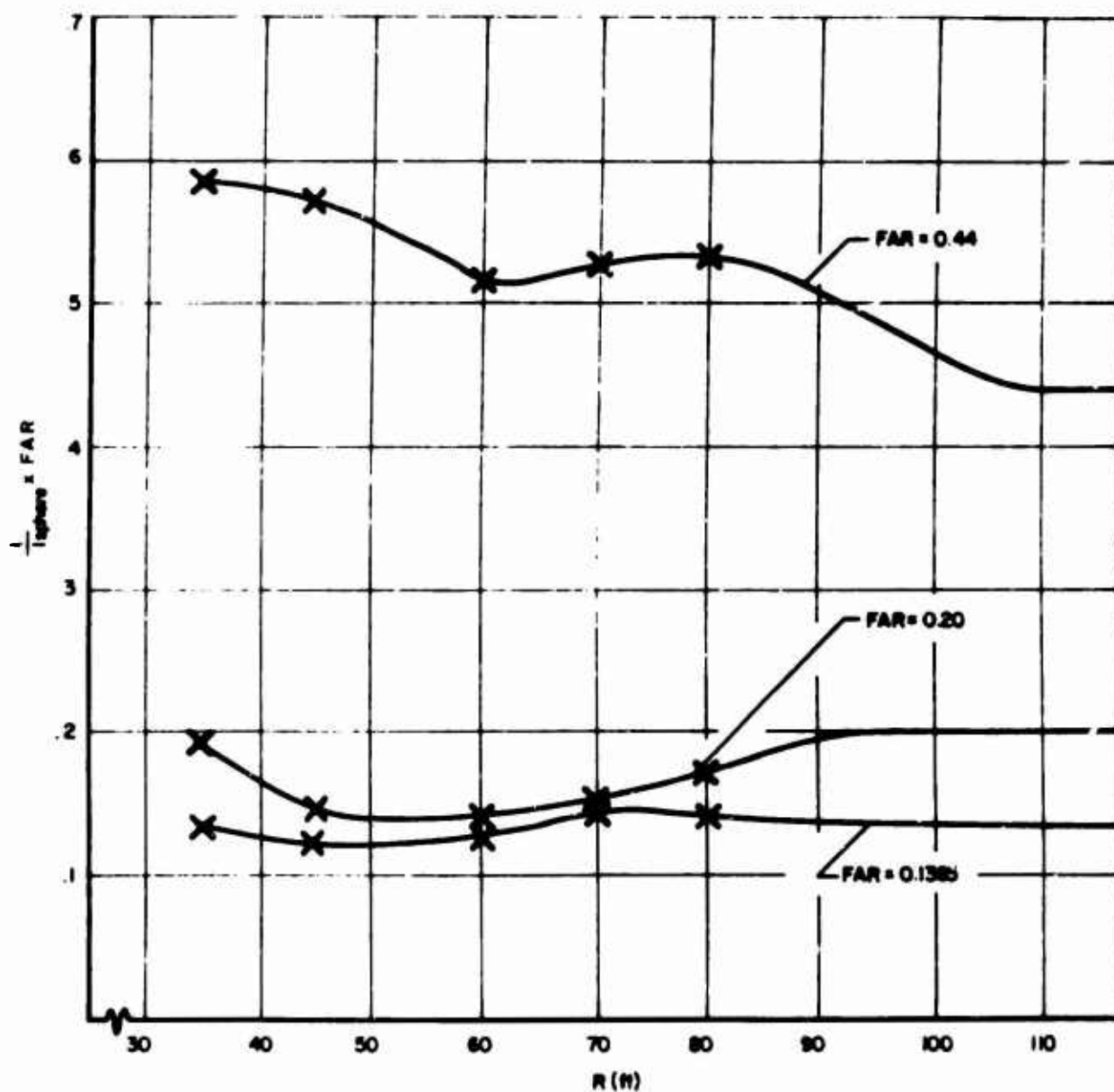


Figure 4. Impulse Ratio x FAR vs. Distance from Charge Center

where B, C, D, F, G, and H are coefficients which can be solved exactly for any fixed value of Z since in each case there are three unknowns and three equations.

In these relations data from charge shapes with different equivalent amounts of TNT can be used since the scaled distance Z can be used.

The solutions to these equations for the values of R or Z given in Tables II and III are shown in Table IV which indicates that B, C, D, F, G, and H vary with the value of Z. It was assumed that fifth order polynomials would adequately describe this variation in Z. A least squares polynomial curve fit program was used to fit the available data from Reference 4. Also, the geometry effect must vanish for large Z. Hence there were six data points available for the curve fitting routine (Table IV).

Denote the general form of these polynomials by

$$B, C, D, F, G, H = C_0 + C_1Z + C_2Z^2 + C_3Z^3 + C_4Z^4 + C_5Z^5 \quad (7)$$

The computed values of the coefficients are given in Table V.

Figure 5 gives the overpressure and impulse ratios based on Equations (6) and (7) for points along a line perpendicular to the center of one of the vertical faces of a cubical shaped explosive stack, that is, FAR = 0.2. Note that the predicted curves fit the data of Reference 4 quite accurately as well as approaching the value 1 for large Z. This is to be

TABLE IV

EXPERIMENTALLY BASED COEFFICIENTS FOR DETERMINING PRESSURE RATIOS AND
IMPULSE RATIOS AS FUNCTIONS OF FAR

Z	PRESSURE RATIO			IMPULSE RATIO		
	B	C	D	F	G	H
9.22	0.6867	1.5682	2.8168	1.3273	- 3.3782	7.7146
11.85	0.7166	0.5313	3.7778	1.6941	- 8.0431	16.2422
15.80	1.5938	-6.7473	14.2048	1.9596	- 9.9504	18.5522
18.43	1.7854	-8.6501	16.8589	2.2068	-11.0673	19.9411
21.06	1.9419	-9.4443	16.7771	1.7877	- 7.3553	13.7497
(large)	1.0000	0.0000	0.0000	1.0000	0.0000	0.0000

TABLE V

POLYNOMIAL COEFFICIENTS FOR B, C, D, F, G AND H

	C_0	C_1	C_2	C_3	C_4	C_5
B	19.9156	- 5.4922	0.5693	-0.0266	0.0006	0.0000
C	-161.9033	47.4129	-4.9886	0.2355	-0.0051	0.0000
D	272.6186	-77.9697	8.2005	-0.3888	0.0085	0.0001
F	5.9069	- 1.7159	0.2183	-0.0117	0.0003	0.0000
G	- 1.3016	4.6739	-0.9968	0.0645	-0.0017	0.0000
H	- 8.1686	- 4.9228	1.4370	-0.0910	0.0027	0.0000

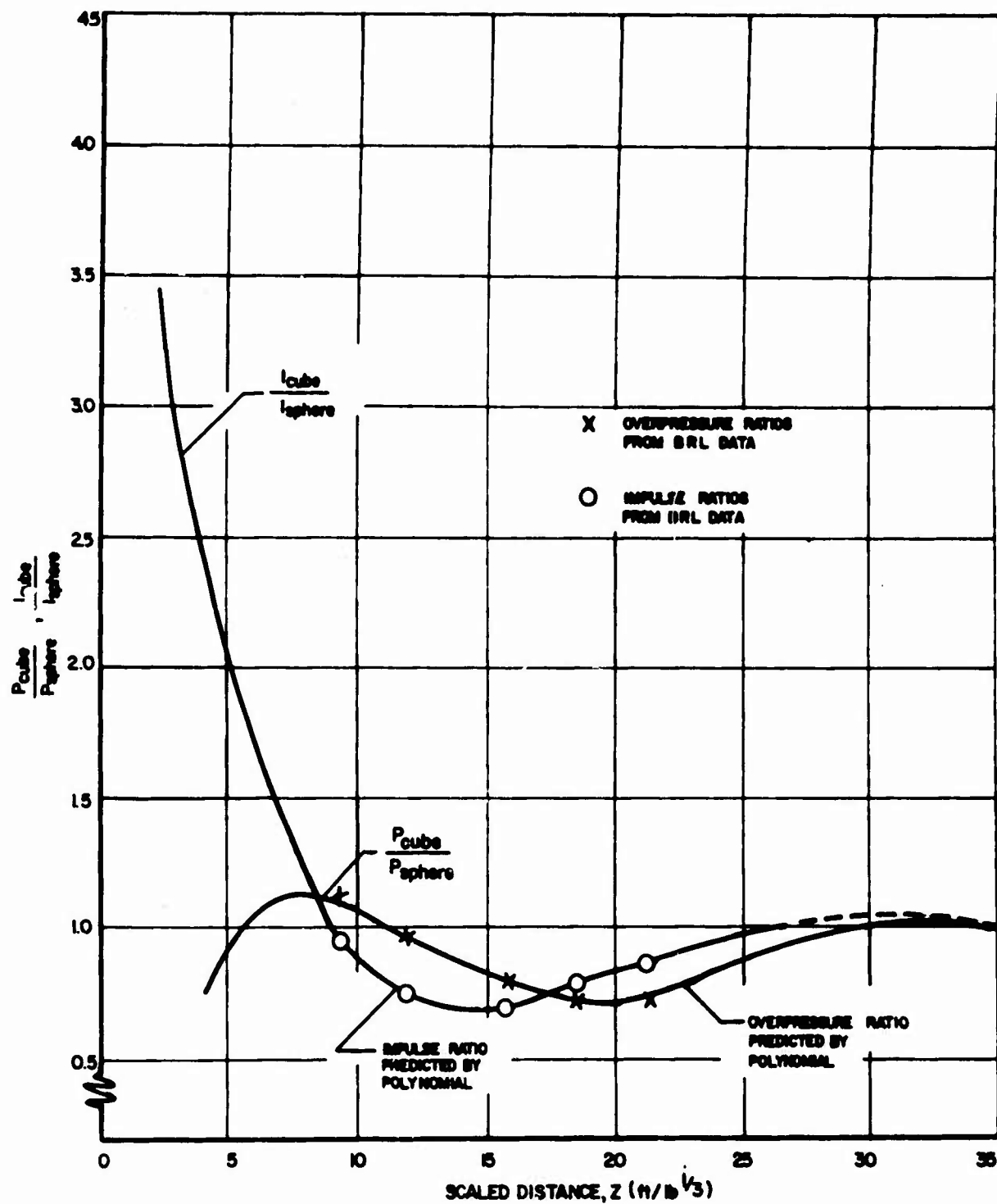


Figure 5. Comparison of Predicted Overpressure and Impulse Ratios to BRL Data for Cubical Shaped Explosive Stack.

expected since these points were used in determining the coefficients. A similar conclusion holds when $FAR = 0.44$ and $FAR = 0.1365$. The polynomial expressions are necessary for determining the overpressure and impulse ratios for values of Z and FAR not given explicitly by Reference 4.

Reasonable results for extrapolations to values of Z in the region $Z > 9$ can be expected because of the experimental data that is available. However, for values of Z less than 9 the predicted values may not be very accurate.

To obtain approximate values for the actual peak overpressure and positive impulse for positions along a line perpendicular to the center of a vertical stack face, the overpressure and positive impulse ratios are multiplied by the peak overpressure and positive impulse respectively. These are obtained from the polynomial fit for curves associated with the surface detonation of a hemispherical stack at the same values of scaled distance Z . Although the overpressure and impulse ratios involve spherical charges, the results from a hemispherical detonation are used to convert these ratios to true peak overpressures and positive impulses. The basic reason for using data associated with a hemispherical charge is that the positive impulse is larger than that associated with a spherical charge for the same value of Z . Presumably this would yield conservative values of positive impulse, which is especially needed in the region $Z < 9$ where no experimental data is available.

It is assumed that there is very little difference in peak overpressure and positive impulse between the center line mentioned above and the corresponding line on the surface vertically below the center line. Such an assumption will be implicitly assumed from now on for all other horizontal lines emanating from the center of a rectangular stack.

Now that the overpressure and impulse at positions out from the center of a vertical face of a rectangular stack have been modeled, the next step is to predict these parameters out from the vertical edges. The only data available on which this development can be based are the data shown in column 3 in Table II and Table III.

The technique employed in the development of the edge peak overpressure and scaled impulse versus scaled distance was to establish edge to face peak overpressure and edge to face positive impulse relationships as functions of scaled distance. This was achieved by dividing the values in column 3 of Tables II and III by the values in column 2 of the corresponding tables, thereby establishing coordinates for five points for the ratio relationships. These coordinates were put into a least squares polynomial curve fit program to obtain the polynomial coefficients for the polynomials in Z to describe the ratio relationships. Table VI shows the polynomial coefficients for the relationships that yield the ratio of edge peak overpressure to face peak overpressure and edge impulse to face impulse. Figure 6 shows these relationships as functions of scaled distance.

TABLE VI

POLYNOMIAL COEFFICIENTS FOR THE RATIOS
EDGE PRESSURE/FACE PRESSURE AND
EDGE IMPULSE/FACE IMPULSE

$$\frac{\text{EDGE PRESSURE}}{\text{FACE PRESSURE}} = \sum_{i=0}^6 d_i z^i$$

$$d_0 = -0.5442047 \times 10^{-1}$$

$$d_1 = -0.3279577 \times 10^{-2}$$

$$d_2 = 0.3172064 \times 10^{-1}$$

$$d_3 = -0.2700095 \times 10^{-2}$$

$$d_4 = 0.8668014 \times 10^{-4}$$

$$d_5 = -0.1294399 \times 10^{-5}$$

$$d_6 = 0.7019624 \times 10^{-8}$$

$$\frac{\text{EDGE IMPULSE}}{\text{FACE IMPULSE}} = \sum_{i=0}^4 e_i z^i$$

$$e_0 = -0.3879756 \times 10^0$$

$$e_1 = 0.2953776 \times 10^0$$

$$e_2 = -0.1519496 \times 10^{-1}$$

$$e_3 = 0.2943603 \times 10^{-3}$$

$$e_4 = -0.1946069 \times 10^{-5}$$

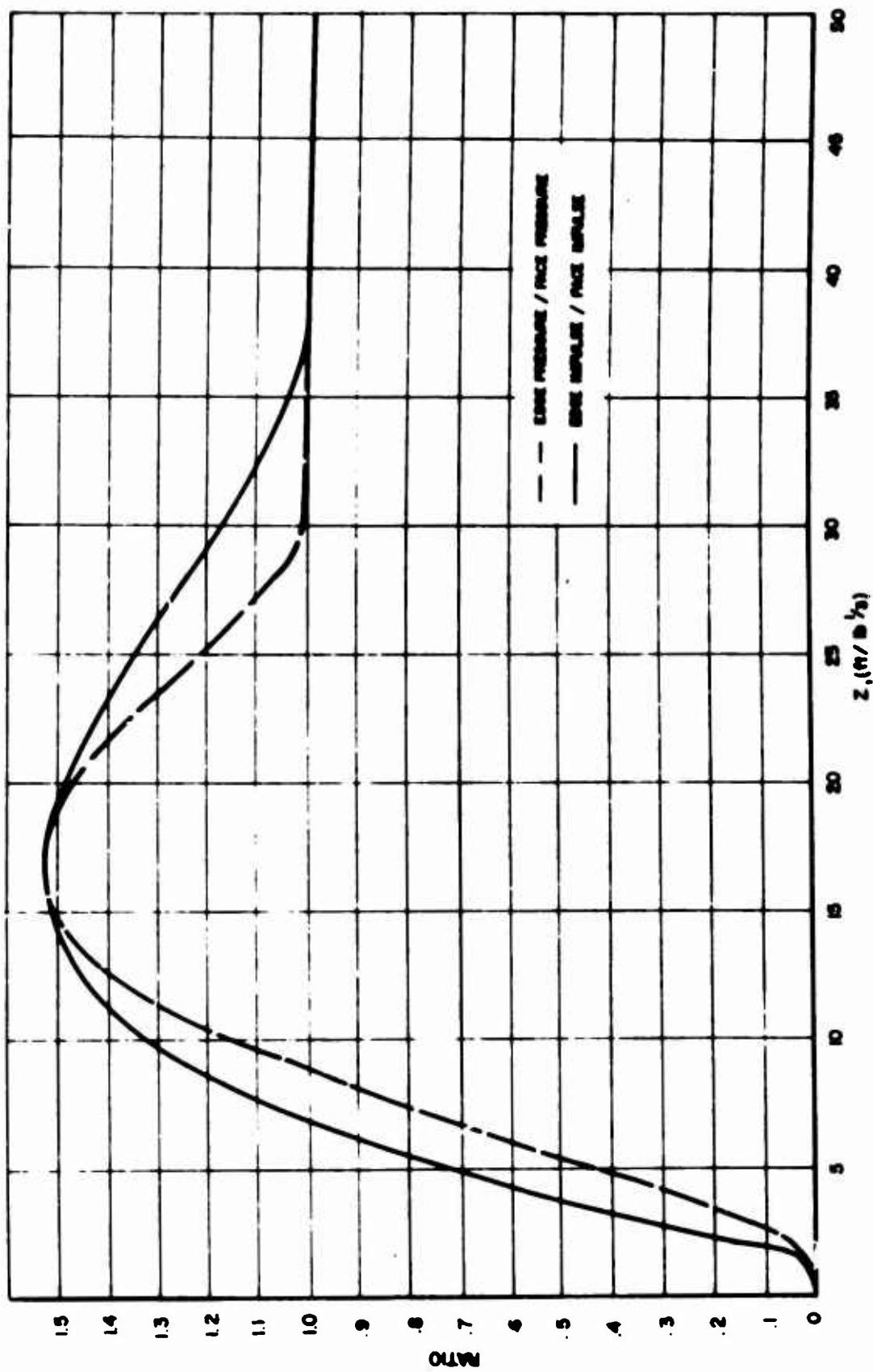


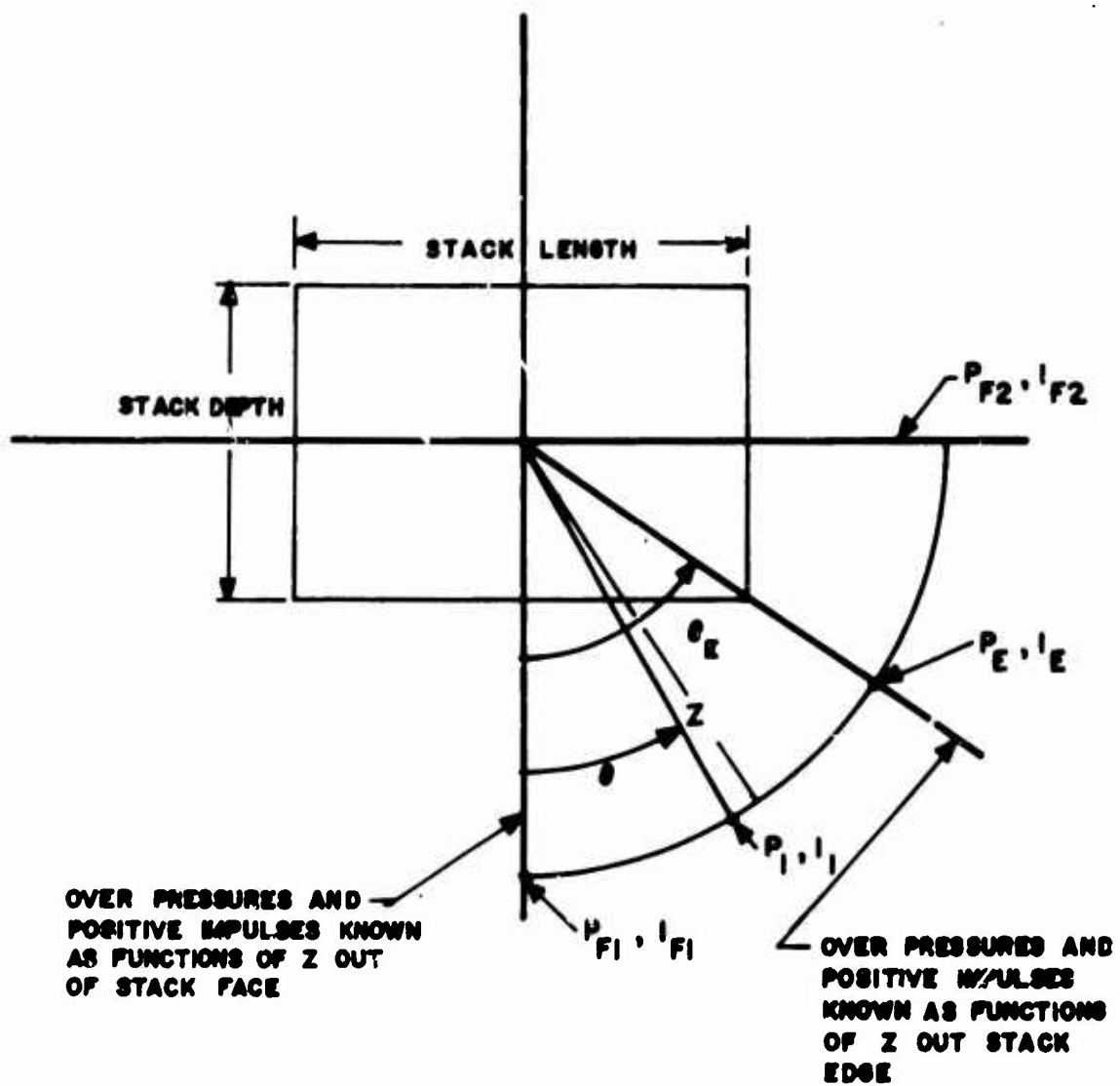
Figure 6. Edge Pressure/Face Pressure and Edge Impulse/Face Impulse vs. Scaled Distance from Charge Center.

These relationships were established from data for a cubical shaped charge where the pressures and impulses off of the faces as functions of Z are equal. The technique employed in the model for predicting edge overpressures and impulses for stacks which are not cubical (i.e., face pressure and impulse as functions of Z are not equal for adjoining faces) is to multiply the ratios, at a given value of Z , by the average face value of peak overpressure and impulse at the same value of Z .

Now that the peak overpressure and positive impulse relationships as functions of Z have been established along lines perpendicular to the stack faces through the stack center, and along lines extending from the stack center through the stack edges (all lines in a horizontal plane) the parameter values along intermediate lines through the stack center can be established by linear interpolation. This technique is illustrated in Figure 7.

5. BARRICADE EFFECT

It is a well known and accepted fact that a barricade in close proximity to an explosive detonation will significantly affect the peak overpressure and positive impulses at positions "close" to the barricade. Although there has been considerable study dealing with qualitative (i.e., amount of destruction) effects produced by barricaded explosive charges, there has not been much study concerning quantitative (i.e., actual pressure and impulse measurement) effects produced by barricaded explosive charges in the current literature.



$$P_I = \frac{z}{\theta_E} (P_E - P_{F1}) + P_{F1}$$

$$I_I = \frac{z}{\theta_E} (I_E - I_{F1}) + I_{F1}$$

Figure 7. Geometry Effect and Interpolation Technique

The only reference revealed by the literature search which deals directly with the effects produced by a standard (i.e., three adjoining walls perpendicular to each other) barricade is Reference 2. This report gives incident pressures as a function of scaled distance (See Figure 8) for various directions of propagation from a three sided barricade. The barricade length to depth ratio is approximately one (1) and the weight of charge to volume of structure ratio (W/V) (pounds of TNT/ft.³) is in the range 0.2 to 2.0. For very large or small W/V values, the incident pressure versus scaled distance in all directions of propagation from a barricade will be very nearly equal to the results for an unharricaded charge. Results of barricade effects on positive impulse versus scaled distance for various directions of propagation from the barricade considered are not reported here or elsewhere in the literature.

The technique employed in the development of this portion of the model was to establish peak overpressure ratio relationships for the four directions from the barricade center shown in Figure 8 as functions of scaled distance. This was accomplished by dividing the pressure values from the curve for an unconfined surface burst shown in Figure 8 by the pressure values from the curves for the four directions from the barricade center at selected values of scaled distance. These point coordinates were then put into a least squares polynomial curve fit program to obtain coefficients for fourth order polynomials in terms of scaled distance Z which describe the overpressure ratios for

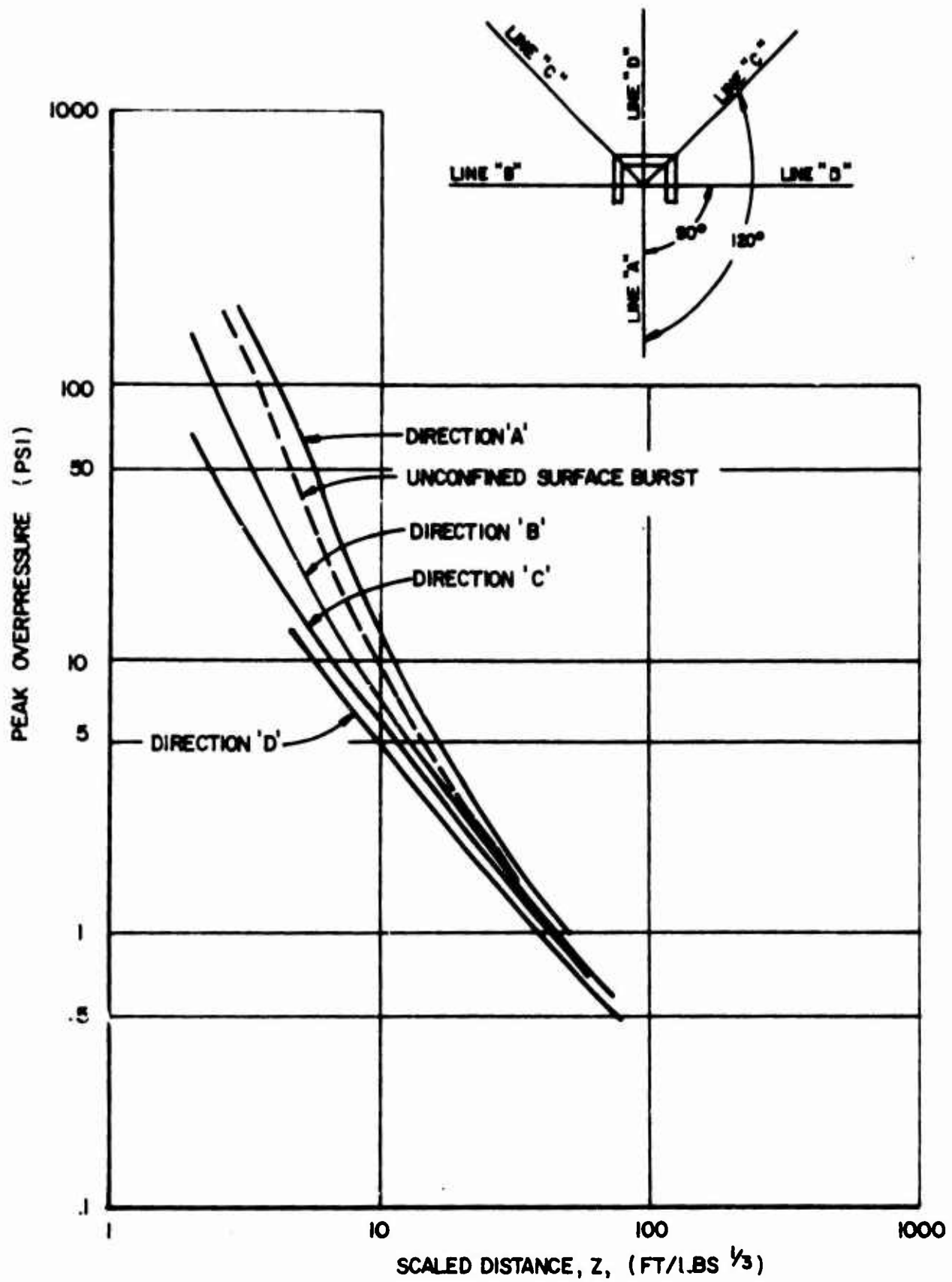


Figure 8. Exterior Leakage Pressure vs Scaled Distance

each of the four directions from the barricade center shown in Figure 8. The polynomial coefficients are shown in Table VII.

Pressure ratio relationships for directions between those shown are established through linear interpolation as was done in the geometry effects model development.

Since the barricade effect on positive impulse cannot be established because of the lack of reliable data, the model assumes that positive impulse is affected in the same way as is the pressure. Therefore, the above developed overpressure ratio relationships are reused as positive impulse ratio relationships.

The technique to establish the peak overpressure and positive impulse produced by a barricaded explosive detonation is to evaluate the above ratio relationships at the desired direction and scaled distance from the barricade and multiply the computed ratio value by the overpressure and impulse of the bare charge at the same value of scaled distance. If geometry effects are included in the problem, the computed ratio value is multiplied by the peak overpressure and positive impulse which has been previously modified to account for the stack geometry effect.

It should be emphasized that this approach assumes that the explosive stack and barricade are rectangular with stack and barricade sides parallel to each other, that the same vertical line passes through the center of the stack and the barricade, that the ratio of barricade length to barricade depth is approximately equal to one, and that the ratio of the weight of charge to the volume of barricade (lbs/ft^3) is in the range of 0.2 to 2.0.

TABLE VII
POLYNOMIAL COEFFICIENTS FOR PRESSURE RATIO VS. Z POLYNOMIALS FOR BARRICADE EFFECT

Direction From Barricade Center	f_0	f_1	f_2	f_3	f_4
Out Barricade Open End (Line A Figure 7)	0.1569062×10^1	$-0.2554407 \times 10^{-1}$	0.5148503×10^{-3}	$-0.4569341 \times 10^{-5}$	0.1281275×10^{-7}
Out Barricade Side (Line B Figure 7)	0.3327308×10^0	0.4917871×10^{-1}	$-0.1202383 \times 10^{-2}$	0.1121702×10^{-4}	$-0.3175593 \times 10^{-7}$
Out Barricade Corner (Line C Figure 7)	0.8900162×10^{-1}	0.6300556×10^{-1}	$-0.1518243 \times 10^{-2}$	0.1415396×10^{-4}	$-0.4012012 \times 10^{-7}$
Out Barricade Back (Line D Figure 7)	0.1533184×10^0	0.3944894×10^{-1}	$-0.7604483 \times 10^{-3}$	0.6033857×10^{-5}	$-0.1556003 \times 10^{-7}$

$$\text{Pressure Ratio} = \sum_{i=0}^4 f_i z^i$$

6. SUMMARY

This section has outlined the theory, experimental data and assumptions that have been utilized in developing a workable model for predicting peak overpressures and positive impulses associated with a barricaded HE detonation. The basic approach was to use well known results from detonations of bare hemispherical TNT charges and to modify these results to account for the effects of bombs, rectangular stack configurations and barricades. For those areas where a certain amount of uncertainty prevailed, a conservative approach was adopted so that the predicted values would be larger than what might be actually experienced in practice.

The computer program which follows the theory outlined in this section is described in Appendix I.

SECTION III

FRAGMENTATION

1. INTRODUCTION

The purpose of the fragmentation portion of the program is to formulate an analytical model to describe the fragment dispersion pattern resulting from the explosion of barricaded munitions. The model must consider the dispersions and patterns in terms of fragment velocities, weights, trajectories and ranges.

2. STATEMENT OF PROBLEM

The fragment dispersion pattern of a barricaded explosion is affected primarily by the parameters: a) initial fragment velocity, b) fragment mass, c) spatial position on the bomb, d) initial departure angle, e) fragment trajectories, f) bomb stack geometry, g) and barricade geometry. The analytical model developed with these parameters must yield fragment dispersion patterns that are at least comparable to dispersion data from barricaded explosive tests. The model must be able to yield the range and the striking velocity of the fragments in order to determine the danger of sympathetic detonation of adjacent bomb stacks.

3. SCOPE OF INVESTIGATION

The basic approach for predicting the above parameters for the explosion of a barricaded bomb stack is to proceed from known fragment behavior for a single bomb. Representative single bomb fragment data that are available (References 5-7) for a large variety of bombs is shown in Figure 9. These data consist of: a) the number of fragments per steradian (solid angle), b) the average fragment mass (grams), as a function of the polar angle measured from the nose of the bomb.

Once the initial fragment velocity and fragment weight are known, the trajectory range and striking velocity may be predicted for various angles of departure. These data are first generated for the explosion of a barricaded single bomb and is then correlated with fragment survey data from experimental bomb stack tests such as the "BIG PAPA" tests (Reference 1). The correlation with experimental fragment survey data yields interaction coefficients which indicate the number of single bombs required to yield the fragment data from the stack tests.

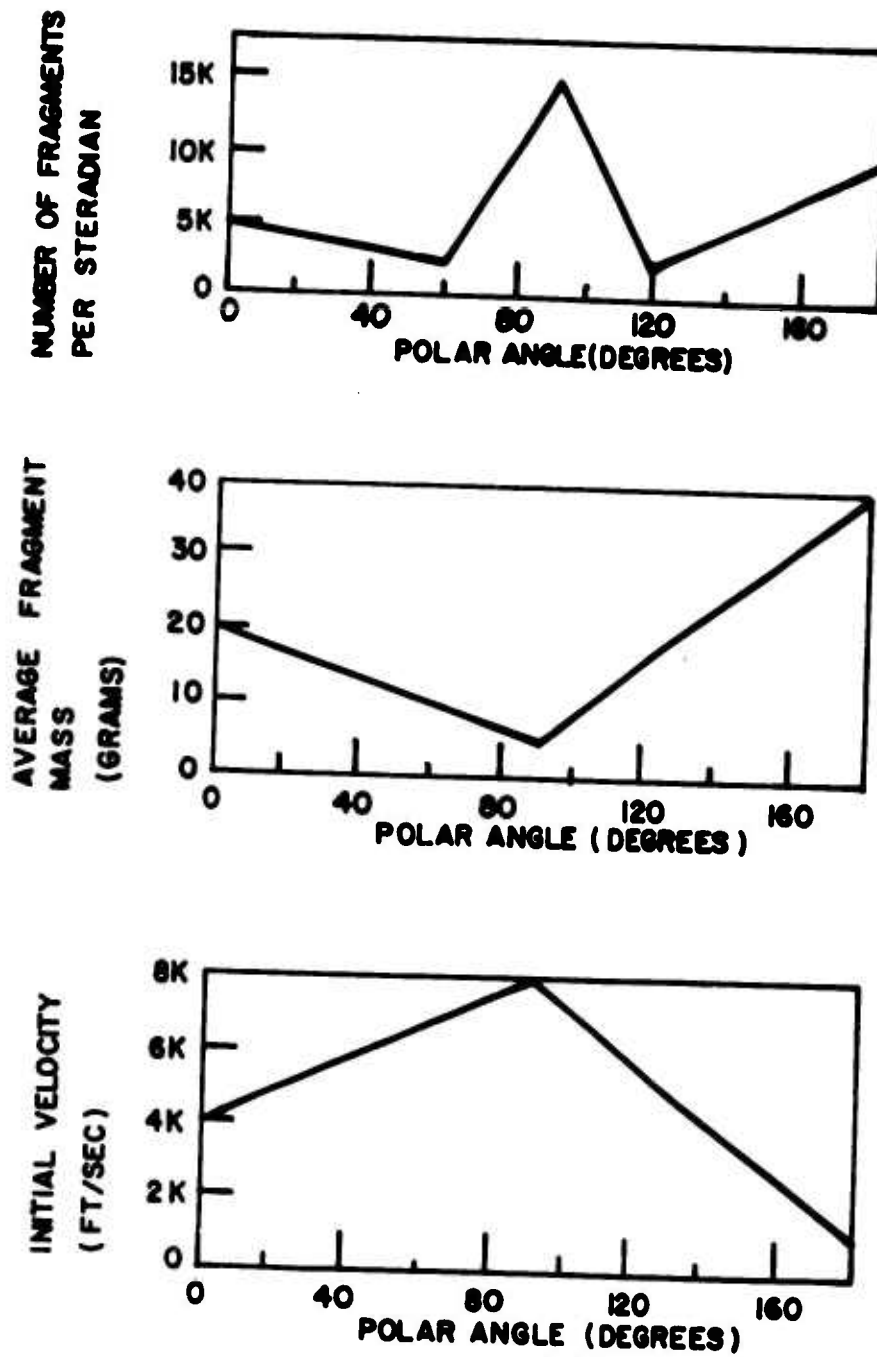


Figure 9. Representative Fragmentation Data
For The Explosion of a Single Bomb.

4. ANALYTICAL FRAGMENT MODEL FOR A SINGLE BOMB

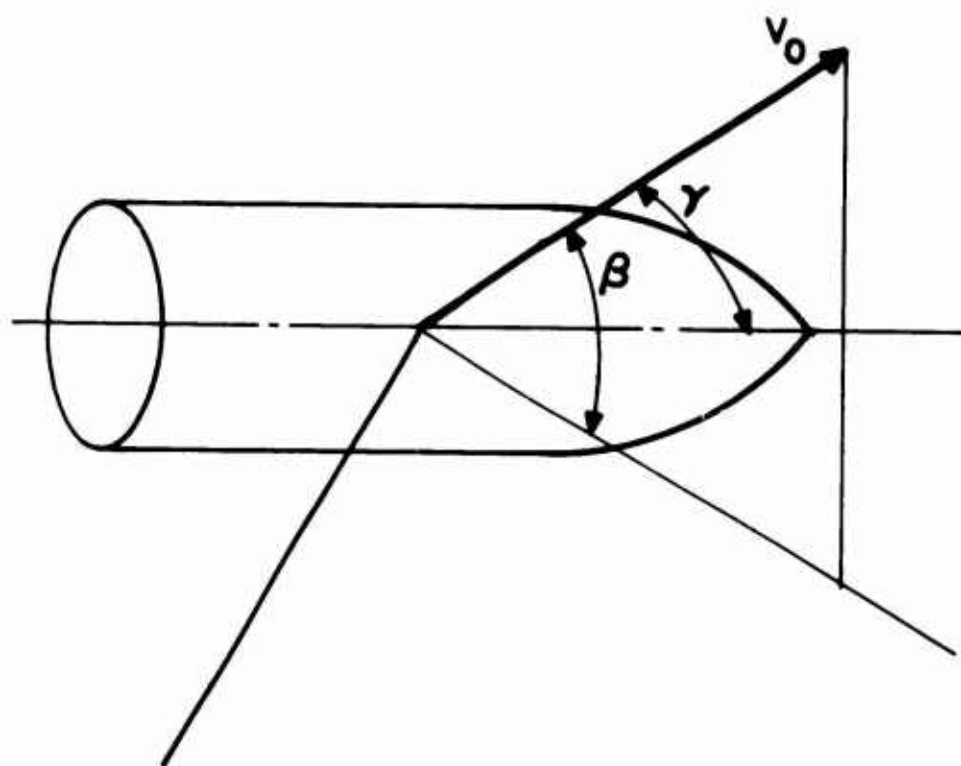
a. Fragment Parameters

To develop a model for a bomb stack, it is necessary to first consider the dispersion pattern for a single bomb. The parameters that are required include the mass and initial velocity of the fragments and the number of fragments per steradian that are emitted from the bomb.

Gurney's Theory and Mott and Shapiro's Theory (Reference 7) are available for predicting the initial fragment velocity and mass distribution respectively. Both of these theories have been favorably correlated with experimental data. A significant disadvantage of these theories is that there is no method for predicting how the mass of the fragments vary along the length of the bomb. Hence, a distribution would have to be assumed or the average fragment mass determined from Mott's equation could be used.

Since experimental fragment data for several bombs are available in the literature, as shown in Figure 9, it was considered appropriate to use this information as needed in the model instead of using an exclusively theoretical approach.

By using the data from fragment tests on single bombs, the following parameters are known as functions of the polar angle γ (Figure 10): a) fragment mass, b) fragment initial velocity, c) fragment mass distribution along the



$$0 \leq \gamma \leq \pi$$

$$-\pi/2 \leq \beta \leq \pi/2$$

Figure 10. Polar and Departure Angles
for a Bomb Fragment.

bomb, d) and number of fragments per steradian or solid angle. It is assumed that each fragment initially departs along the line through the bomb center and the point on the bomb casing at which the fragment is located. The angle that this line makes with the horizontal plane is denoted as the departure angle β .

b. Fragment Trajectories

The trajectory equations are necessary to: a) determine if fragments clear the barricade, b) predict the fragment range and impact velocity, c) predict the number of fragments/unit area and mass/unit area as a function of azimuth angle and range from blast. It will be assumed in the model that if fragments do not clear the barricade, they are stopped and no longer considered.

The range and impact velocity will be predicted by using basic equations of mechanics for the trajectory in a finite difference form.

The trajectory of a fragment is shown in Figure 11. The equations below are taken from References 8 and 9 and modified for purposes of this study.

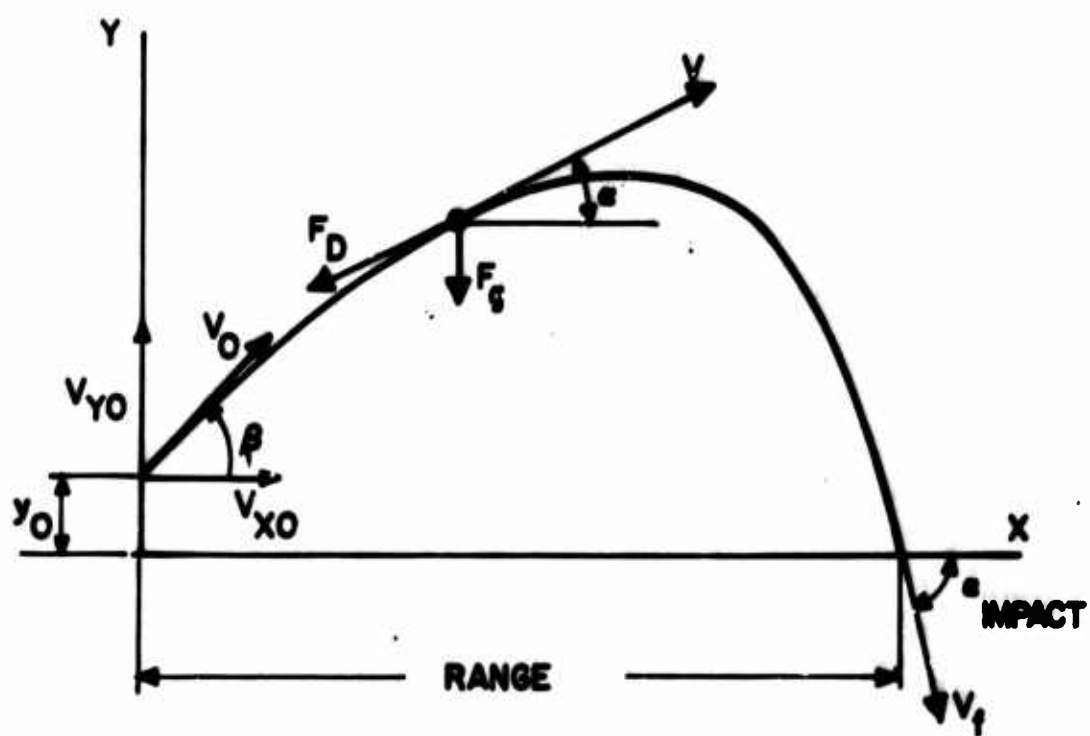


Figure 11. Trajectory of a Fragment.

The forces that act on a body in flight are the drag F_D and the force of gravity F_g . Assume that the magnitude of the drag force, acting in the direction opposite to the velocity, is given by

$$F_D = 1/2 \rho_A A C_D V^2 \quad (8)$$

where

ρ_A = density of air, slugs/ft.³

A = cross-sectional area perpendicular to the direction of propagation, ft.²

C_D = drag coefficient which is a function of shape

V = speed of fragment, ft./sec.

The components of the drag force in the X and Y directions are given respectively by

$$F_D^X = -F_D \cos \alpha \quad (9a)$$

$$F_D^Y = -F_D \sin \alpha \quad (9b)$$

where α , as shown in Figure 11, is the angle between the horizontal line and the tangent to the trajectory and varies such that

$$\beta \geq \alpha \geq -\alpha_{\text{impact}} \quad (10)$$

The magnitude of the force due to gravity is given by

$$F_g = mg \quad (11)$$

where

m = mass of fragment, slugs

g = gravitational constant, ft./sec.²

Newton's law yields the following equations of motion:

$$m\ddot{x} = F_D^X \quad (12a)$$

$$m\ddot{y} = F_D^Y - F_g \quad (12b)$$

where

\ddot{x} = acceleration in X-direction

\ddot{y} = acceleration in Y-direction

If the ballistic coefficient c is defined by

$$c = \frac{\rho_A A C_D}{2m} \quad (13)$$

then Equations (12a) and (12b) become

$$\ddot{x} = -cv^2 \cos\alpha \quad (14a)$$

$$\ddot{y} = -cv^2 \sin\alpha - g \quad (14b)$$

Since

$$\frac{dx}{dt} = V \cos \alpha \quad (15a)$$

$$\frac{dy}{dt} = V \sin \alpha \quad (15b)$$

Equations (14a) and (14b) become

$$\frac{d(V \cos \alpha)}{dt} = -cV^2 \cos \alpha \quad (16a)$$

$$\frac{d(V \sin \alpha)}{dt} = -cV^2 \sin \alpha - g \quad (16b)$$

By performing the indicated time derivatives, these equations can be written in the form

$$\dot{V} \cos \alpha - V \dot{\alpha} \sin \alpha = -cV^2 \cos \alpha \quad (17a)$$

$$\dot{V} \sin \alpha + V \dot{\alpha} \cos \alpha = -cV^2 \sin \alpha - g \quad (17b)$$

By multiplying Equation (17b) by $\cos \alpha$ and Equation (17a) by $-\sin \alpha$ and adding, we get the following equation

$$V \dot{\alpha} = -g \cos \alpha \quad (18)$$

or

$$d\alpha = \frac{-g \cos \alpha}{V} dt \quad (19)$$

Inverting this equation yields

$$dt = \frac{-V}{g \cos \alpha} d\alpha \quad (20)$$

By combining Equations (16a) and (20), we get

$$d(V \cos \alpha) = \frac{cV^3}{g} d\alpha \quad (21)$$

Multiply Equation (20) on the left hand side by $\left(\frac{dx}{dt}\right)$ and on the right by its equivalent $(V \cos \alpha)$ from Equation (15a)

$$dx = \frac{-V^2}{g} d\alpha \quad (22)$$

Similarly from Equations (15b) and (20)

$$dy = \frac{-V^2 \tan \alpha}{g} d\alpha \quad (23)$$

In summary, the governing equations for the time, velocity and coordinates of the fragment, with α chosen to be the independent variable, are

$$dt = \frac{V}{g \cos \alpha} d\alpha \quad (24a)$$

$$d(V \cos \alpha) = \frac{cV^3}{g} d\alpha \quad (24b)$$

$$dx = \frac{-V^2}{g} d\alpha \quad (24c)$$

$$dy = \frac{-V^2}{g} \tan \alpha d\alpha \quad (24d)$$

The initial conditions are

$$\alpha|_{t=0} = \beta \quad (25a)$$

$$v|_{t=0} = v_0 \quad (25b)$$

$$x|_{t=0} = 0 \quad (25c)$$

$$y|_{t=0} = y_0 \quad (25d)$$

For a numerical solution of V , x and y in terms of α , Equations (24b), (24c) and (24d) are written in a finite difference form as follows:

$$\Delta V = V \left(\tan \alpha + \frac{cV^2}{g \cos \alpha} \right) \Delta \alpha \quad (26a)$$

$$\Delta x = \frac{-V^2}{g} \Delta \alpha \quad (26b)$$

$$\Delta y = \frac{-V^2}{g} \tan \alpha \Delta \alpha \quad (26c)$$

After each increment in α , the coordinates of the fragment can be determined and the computation stopped once the particle strikes the barricade or the ground.

c. Fragment Ballistic Coefficients

In order to integrate the trajectory equations of the previous section, the ballistic coefficient c must

be determined for each fragment. It is more convenient to express Equation (13) in the form

$$c = \frac{\gamma_A C_D A}{2w_F} \quad (27)$$

where

γ_A = weight density of air, lb./ft.³

w_F = weight of fragment, lb.

The weight density of air is assumed known. C_D is expected to take on values ranging from 0.3 to 2.0 and will be assumed constant for any fragment. Reference 10 indicates a value of 0.6 for the drag coefficient, C_D , as most appropriate for random steel fragments from an exploded bomb case. The remaining term that is needed is the ratio A/w_F .

Since there is some disagreement as to appropriate values for this ratio, consider, for purposes of illustration only, a steel cube where the length of any edge is l . Then the cross-sectional area A must lie in the region

$$l^2 \leq A \leq 3l^2 \cos(54^\circ 44')$$

If the density is taken to be 500 lb./ft.³, then

$$w_F = 500l^3$$

and

$$l = \left[\frac{w_F}{500} \right]^{1/3}$$

The range for the area to weight ratio is then given by

$$\frac{.0159}{w_F^{1/3}} \leq \frac{A}{w_F} \leq \frac{.0275}{w_F^{1/3}} \left(\frac{ft^2}{lb} \right)$$

For irregular fragments such as those formed by the rupture of a bomb case, the area to weight ratio would be expected to be larger. An average value of

$$\frac{A}{w_F} = \frac{.0345}{w_F^{1/3}} \left(\frac{ft^2}{lb} \right) \quad (28a)$$

or

$$\frac{A}{w_{FG}} = \frac{.232}{w_{FG}^{1/3}} \left(\frac{ft^2}{lb} \right) \quad (28b)$$

has been suggested by Reference 11 where w_{FG} is the weight of the fragment in grams. This average value has been used in connection with the numerical analysis for the trajectory portion of the program in which case the fragment ballistic coefficient becomes

$$c = .00532/w_{FG}^{1/3} \quad (29)$$

d. Coordinate System

Most typical bomb stack barricades are rectangular with three closed sides and one open as shown in Figure 12. For convenience, we adopt the coordinate system shown in Figure 13 where $\theta = 0$ corresponds to the line coming from the center of the bomb out the open side of the barricade. As before, β is the angle that a given line makes with the horizontal plane. The bomb is assumed to be horizontal and θ_B denotes the orientation of the polar axis of the bomb.

The number of fragments per steradian that are emitted from a bomb (Figure 9) is given as a function of the polar angle γ . Since the analysis will be performed using the coordinates θ and β it is necessary to obtain a relation which expresses γ in terms of these two coordinates. This is easily handled using vector algebra.

In connection with Figure 13, let \bar{e}_1 , \bar{e}_2 , and \bar{e}_3 be unit base vectors in the directions X, Y, and Z respectively. Denote a unit vector in the direction of \bar{V}_0 by \bar{e}_0 and a unit vector out the nose of the bomb by \bar{e}_B . Then

$$\bar{e}_0 = \cos\beta \cos\theta \bar{e}_1 + \cos\beta \sin\theta \bar{e}_2 + \sin\beta \bar{e}_3 \quad (30a)$$

$$\bar{e}_B = \cos\theta_B \bar{e}_1 + \sin\theta_B \bar{e}_2 \quad (30b)$$

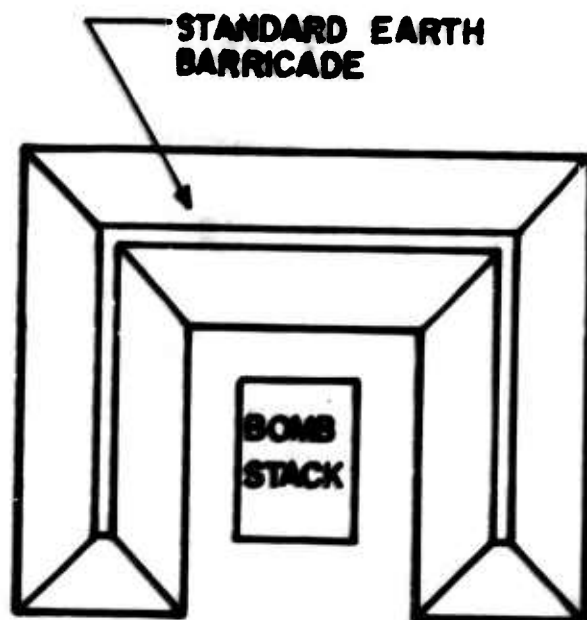


Figure 12. Typical Bomb Stack Barricade.

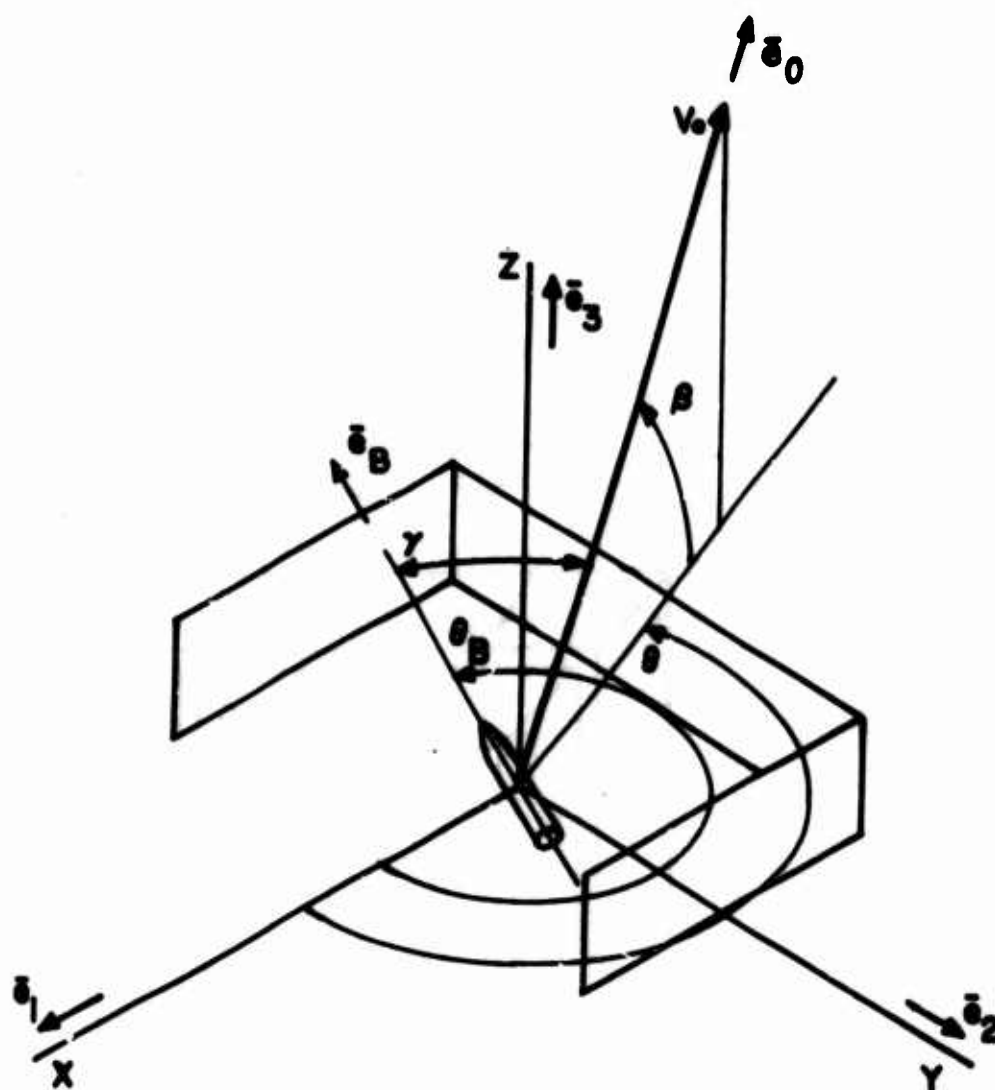


Figure 13. Coordinate System for a Regular Barricade Enclosing a Single Bomb.

Using the definition of the cross-product,

$$|\bar{e}_0 \times \bar{e}_B| = |\bar{e}_0| |\bar{e}_B| \sin \gamma \quad (31)$$

Since the magnitudes of \bar{e}_0 and \bar{e}_B are both one, this relation yields

$$\gamma = \arcsin \{ \sin^2 \beta + \cos^2 \beta \sin^2 (\theta - \theta_B) \}^{1/2} \quad (32)$$

Let $\Psi(\gamma)$ denote the number of fragments per steradian ejected by the bomb. Then the total number of fragments ejected out an arbitrary region is given by

$$N = \int \Psi(\gamma) d\omega \quad (33)$$

where the element of steradian $d\omega$ is given by

$$d\omega = \cos \beta d\theta d\beta \quad (34)$$

For the region bounded by the coordinates $\theta = \theta_1$,

$\theta = \theta_2$, $\beta = \beta_1$ and $\beta = \beta_2$, the total number of fragments would be

$$N_{\substack{\theta_1, \theta_2 \\ \beta_1, \beta_2}} = \int_{\beta_1}^{\beta_2} \int_{\theta_1}^{\theta_2} \Psi(\gamma) \cos \beta d\theta d\beta \quad (35)$$

If the average number of fragments per steradian over this region is denoted by Ψ_{12} , then the total number of fragments would be

$$N_{\substack{\theta_1, \theta_2 \\ \beta_1, \beta_2}} = \Psi_{12} (\theta_2 - \theta_1) (\sin \beta_2 - \sin \beta_1) \quad (36)$$

Usually the coordinates of a region such as the one defined above are given by

$$\theta_2 = \theta + \frac{\Delta\theta}{2} \quad (37a)$$

$$\theta_1 = \theta - \frac{\Delta\theta}{2} \quad (37b)$$

$$\beta_2 = \beta + \frac{\Delta\beta}{2} \quad (37c)$$

$$\beta_1 = \beta - \frac{\Delta\beta}{2} \quad (37d)$$

If $\Delta\theta$ and $\Delta\beta$ are small enough, it would be reasonable to choose as average values for the initial velocity, number of fragments, and fragment mass, those values given in Figure 9 for the polar angle $\gamma(\theta, \beta)$. These parameters could then be used in connection with the trajectory equations derived previously to determine probable impact velocities and coordinates.

e. Barricade Geometry Considerations

To include barricade geometry affects, a more general barricade composed of straight wall segments was considered. This introduces very little additional complicating features and allows some flexibility so that optimization of barricade design could be considered in the future.

The geometry of the wall segments of the barricade is described in terms of cylindrical coordinates R , θ , and Z with the origin placed at the bomb center. It is

assumed that the wall remains intact as far as the fragments are concerned so that if the fragment strikes a barricade wall, it stops. Thus, for particular azimuth and departure angles, the existence of a wall for that azimuth must first be determined; if a wall is present its height must be known so that the question of whether or not the fragments have cleared that portion of the barricade can be answered.

The problem to be solved is illustrated in Figure 14. For a given azimuth angle of trajectory θ , the distance to the wall \tilde{R}_3 must be determined. The known quantities are \tilde{R}_1 , \tilde{R}_2 , θ_1 , θ_2 , and the height of the barricade z_1 , z_2 , and z_3 . Since two sides (\tilde{R}_1 , \tilde{R}_2) and the included angle ($\Delta\theta$) are known, the law of tangents can be used to find ϕ and ψ :

$$\phi = \frac{1}{2} (180 - \Delta\theta) + \tan^{-1} \left\{ \left[\frac{\tilde{R}_1 - \tilde{R}_2}{\tilde{R}_1 + \tilde{R}_2} \right] \tan \frac{1}{2} (180 - \Delta\theta) \right\} \quad (38a)$$

$$\psi = \frac{1}{2} (180 - \Delta\theta) - \tan^{-1} \left\{ \left[\frac{\tilde{R}_1 - \tilde{R}_2}{\tilde{R}_1 + \tilde{R}_2} \right] \tan \frac{1}{2} (180 - \Delta\theta) \right\} \quad (38b)$$

The included angle between \tilde{R}_3 and the barricade wall is then

$$\delta = 180 - (\phi + (\theta_2 - \theta)) \quad (39)$$

The law of sines for a plane triangle can then be used to obtain the required distance to the barricade

$$\tilde{R}_3 = \tilde{R}_2 \frac{\sin \phi}{\sin \gamma} \quad (40)$$

f. Distribution of Fragments

The previous sections have outlined a method for computing the impact point and velocity for a group of fragments which are assumed to have identical mass and velocity. The total number of fragments in this group depend on the azimuth angle θ , departure angle β and the size of the region defined by θ_1 , θ_2 , β_1 and β_2 . In actual fact all of these fragments will not land at one spot but in general, they will be distributed over some area. The following discussion presents a method that should give reasonable results that can be compared with experimental data.

For a given θ , a series of impact ranges will be determined together with corresponding values of mass, number of fragments and impact velocities. The number of impact ranges will correspond directly to the number of increments used to cover the range of β . Suppose the ranges are ordered in an increasing sequence

$$0 \leq R_1 \leq R_2 \leq \dots \leq R_J \leq \dots \leq R_N.$$

To illustrate the procedure, consider the fragment parameters associated with the range R_2 . A reasonable approximation

is to distribute these fragments over the area bounded by the coordinates $R_{1,2}$, $R_{2,3}$, θ_1 and θ_2 (See Figure 15) where

$$\theta_1 = \theta - \frac{\Delta\theta}{2} \quad (41a)$$

$$\theta_2 = \theta + \frac{\Delta\theta}{2} \quad (41b)$$

$$R_{1,2} = \frac{R_1 + R_2}{2} \quad (41c)$$

$$R_{2,3} = \frac{R_2 + R_3}{2} \quad (41d)$$

The area A_2 covered by such a segment is

$$A_2 = \frac{1}{2} (R_{2,3}^2 - R_{1,2}^2) \Delta\theta \quad (42)$$

Similarly, the area associated with the range R_J would be

$$A_J = \frac{1}{2} (R_{J,J+1}^2 - R_{J-1,J}^2) \Delta\theta \quad (43)$$

where

$$R_{J-1,J} = \frac{1}{2} (R_{J-1} + R_J) \quad (44a)$$

$$R_{J,J+1} = \frac{1}{2} (R_J + R_{J+1}) \quad (44b)$$

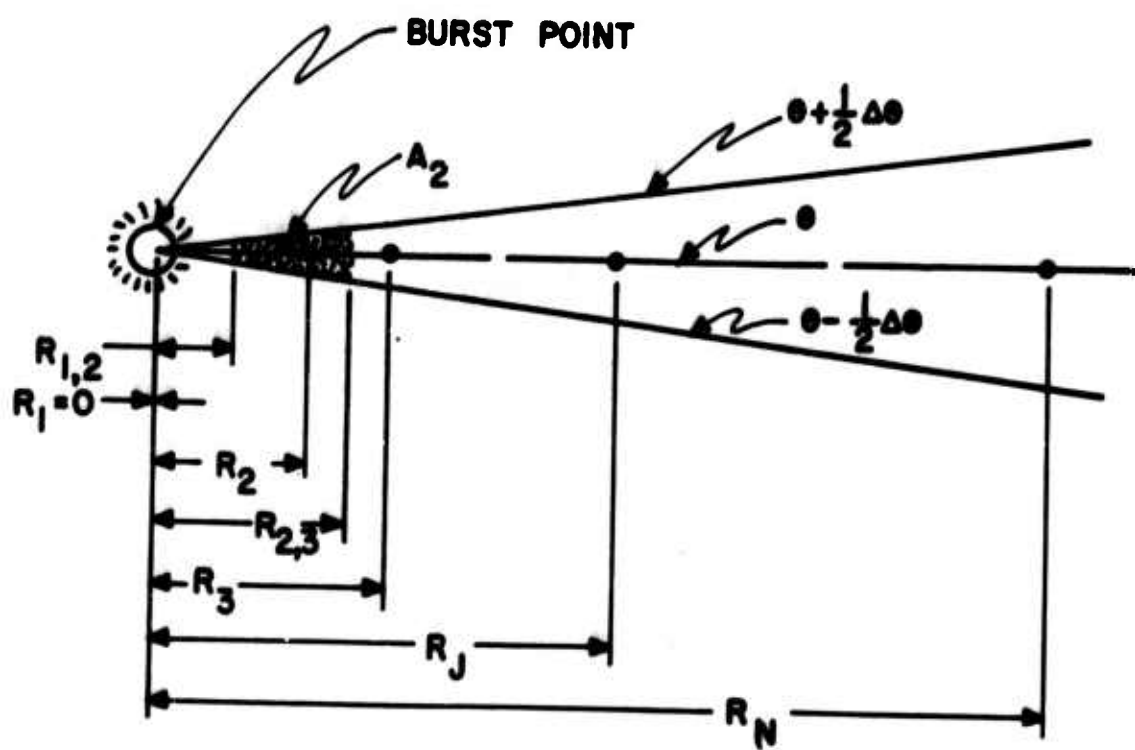


Figure 15. Approximate Impact Areas.

For the furthest impact point R_N , choose

$$R_{N-1,N} = \frac{1}{2} (R_{N-1} + R_N) \quad (45a)$$

$$R_{N,N+1} = 2R_N - R_{N-1,N} \quad (45b)$$

With the impact areas defined by Equation (43), both the number of fragments and the total weight per unit area can be determined by dividing the total number of fragments and the total weight landing at a particular range by the corresponding area, that is,

$$\left(\frac{\text{Number}}{\text{Unit Area}} \right)_J = (\text{Number of fragments landing at } R_J) / A_J \quad (46a)$$

$$\left(\frac{\text{Weight}}{\text{Unit Area}} \right)_J = \left(\frac{\text{Number}}{\text{Unit Area}} \right)_J (\text{Average weight of fragment landing at } R_J) \quad (46b)$$

5. ANALYTICAL FRAGMENT MODEL FOR A STACK OF BOMBS

The fragmentation model developed in the preceding discussion will yield fragment dispersions for a single bomb. The theory is expected to hold for a stack of bombs where the origin of the coordinate system is placed at the center of the stack. However, interaction effects should produce a number of fragments for a given impact area somewhat less than the product of the number of bombs and the number of fragments produced by a single bomb. The exact effect must be determined experimentally.

An illustration of the fragment survey areas from Phase II of the BIG PAPA Tests is shown in Figure 16. For each one of the fragment survey areas, fragments were counted and weighed. By computing the number of fragments and their weights for the same area, a "correlation" or "effective number of bombs" factor may be computed for each area. Hopefully, the variation of the correlation factor from survey area to survey area would lie within a tolerable limit. With the "effective number of bombs" EFNB, determined, the fragment distribution for a single bomb can be multiplied by EFNB to obtain the distribution pattern for the stack of bombs.

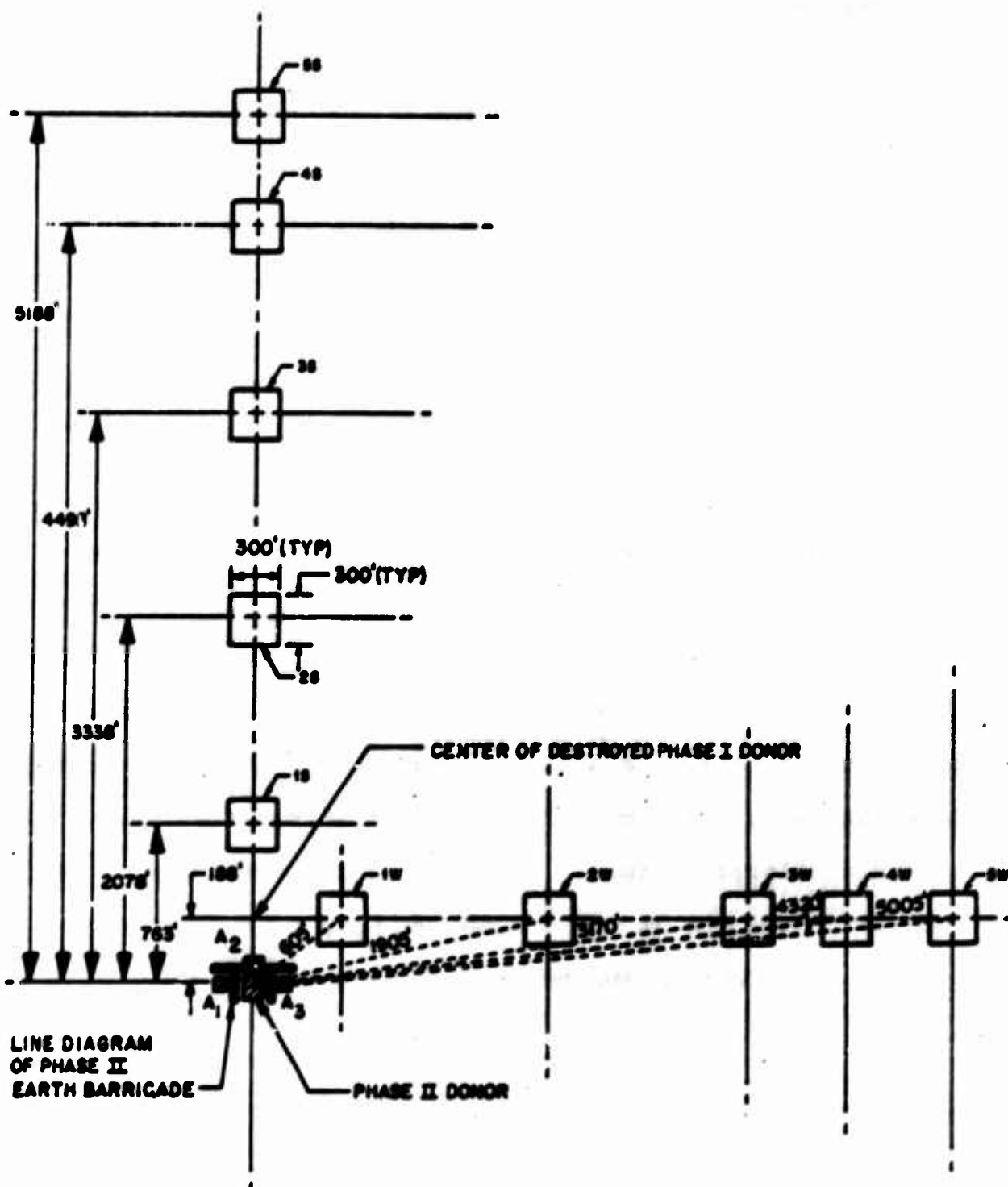


Figure 16. Fragmentation Survey Plan for Phase II of the Big Papa Tests.

6. SUMMARY

This section has presented a model that predicts the impact velocity and distribution of fragments for a barricaded or unbarricaded bomb stack.

Data in the form of initial fragment velocity, size and distribution for each bomb, which is available in References 5 and 6, is used. The fragments that are ejected within a small area of the bombcase are assumed to have identical initial conditions as far as the trajectory equations are concerned. Average values for the mass and initial velocities of the fragments are used together with a ballistic coefficient that was determined experimentally. If the group of fragments clear the barricade then the point and velocity of impact can be determined. For comparison with experimental data, this group of fragments is assumed to be distributed over an adjacent area determined by the increments in azimuth angles and points of impact of other groups of fragments along the same azimuth angle.

The same procedure is used for a stack of bombs except that the total number of bombs must be modified to account for interaction effects. The degree of modification must be determined empirically from existing experimental data.

The computer program that follows the theory of this section is described in Appendix II.

SECTION IV

CRATERING

1. INTRODUCTION

A considerable amount of data have been accumulated that relate the size of craters to the yield of explosives, primarily for bare spherical and hemispherical charges. Most of the work accomplished prior to 1961 has been summarized in Reference 12. Crater measurements of later detonations of major importance have been made and include "Operation Snow Ball" (Reference 13), "Operation Distant Plain" (References 14 and 15) and "Operation Sailor Hat" (Reference 16). These shots cover a wide range of explosive yield and soil types, a fact which produced a considerable amount of diversity in crater sizes.

Predicting the shape of explosion-produced craters and the distribution of the ejected material has been a matter of some concern for several years (References 17-20). Generally, the approach has been to assume a non-dimensional relation between characteristic dimensions of the crater and the explosive yield raised to some power. The resulting relation, called a scaling law, is then used to extrapolate to new regions of interest.

These scaling laws, even though set up to form a "best possible" fit for existing data, must be modified for changes in earth media. Furthermore, it has become rather apparent from the shots at the Suffield Experimental Station and from

"Operation Sailor Hat" that any one scaling law will produce reasonable results over a limited yield range.

The charge shapes in the tests mentioned above are exclusively spherical or hemispherical. Results for other shapes such as rectangular parallelepipeds that would be of more significance for this report are almost non-existent except for the "BIG PAPA" test (Reference 1).

In light of the almost total absence of analytical work in this area and because of the different shaped charge of interest in this project, specifically that associated with bomb stacks, it seemed appropriate to develop an elementary model using basic principles of mechanics. Although the approach adopted in this section freely uses past empirical relations, such an analysis could form the basis of a more rigorous development in the future if experiments could be devised to adequately determine the governing parameters.

As for the past sections, all charges will be assumed to be resting on the surface.

2. THE EFFECT OF CHARGE SHAPE

a. Preliminary Comments

When an explosion is detonated, the total available energy is divided into various categories: blast wave, heat, and kinetic energy of the material itself to mention the most obvious ones. Apparently the blast wave does not contribute to cratering, but rather, it causes a shock wave to be instigated in the earth (Reference 21). The major source of cratering action must then be the kinetic energy of the explosive material. By momentum transfer, energy is transferred to the earth media elements located on the surface and adjacent to the explosive, and by propagation within the neighboring region, earth particles are ejected and a crater is formed.

Because of the confining effect of the explosive material on itself, it seems plausible that the initial direction of propagation of explosive elements would be towards the surface of the explosive. Furthermore, because of air friction, interaction with other elements and so forth, the velocity of each element would decrease with time. Hence, those elements closest to the earth would be the most effective as far as cratering is concerned.

b. Basic Assumptions

The above observations suggest that it is appropriate to make several simplifying assumptions to make an investi-

gation of charge shape amenable to analysis. Because of the preliminary nature of this work, the following assumptions are made with the full knowledge that they may be unjustified; however, the resulting analysis should yield a reasonable approximation:

approximation:

(1) Assumption 1

Just the bottom half of the charge contributes to the cratering phenomenon.

(2) Assumption 2

The velocities of all elements in the bottom half of the charge are the same immediately after detonation and are directed vertically downward. This implies that if v_0 is the initial speed of all elements in the charge, then the initial kinetic energy per unit mass

$$e_0 = \frac{1}{2} v_0^2 \quad (47)$$

is independent of position.

(3) Assumption 3

The friction force is constant and is the same within and outside the original outline of the charge.

Such an assumption yields a couple of interesting results. First it can be shown that the kinetic energy/unit mass e decays linearly with distance by letting z denote the distance of an element above the surface at any time t (See Figure 17). From Newton's Law, the acceleration is constant

$$\ddot{z} = a_0 \quad (48)$$

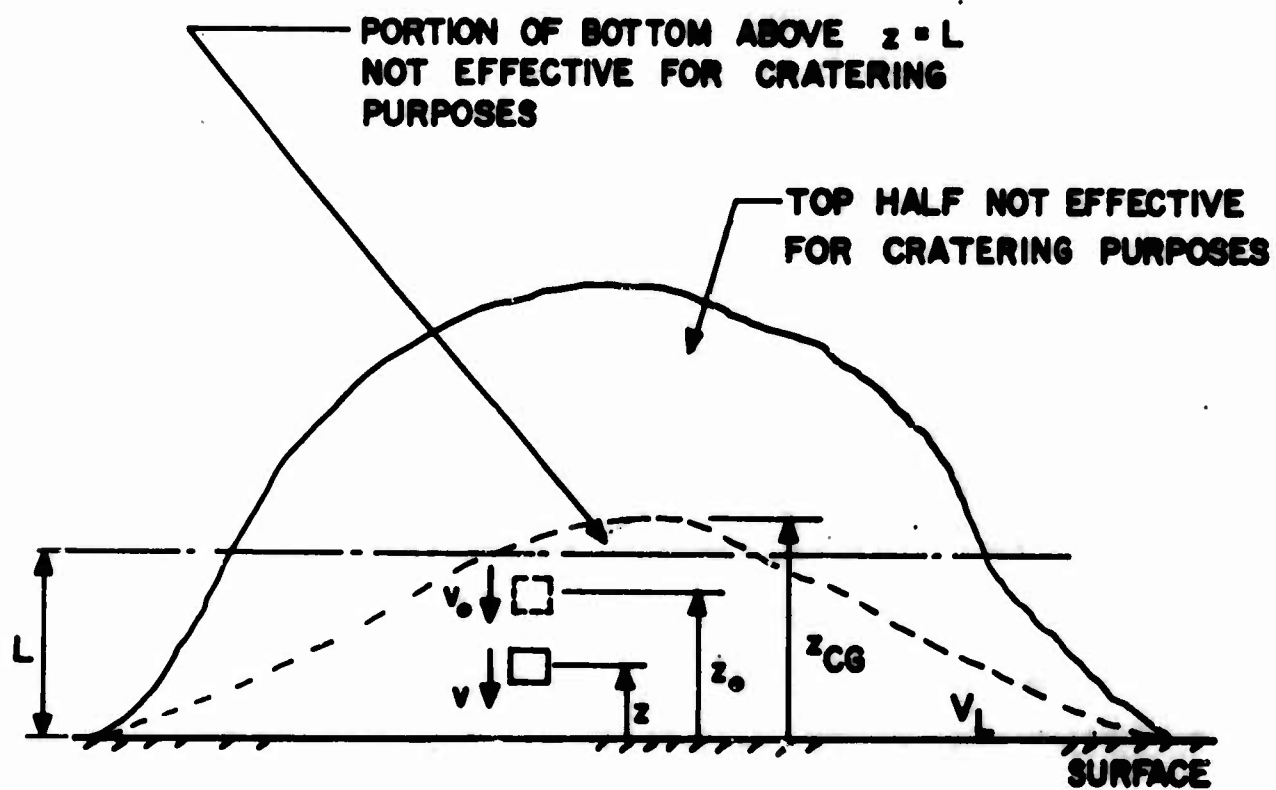


Figure 17. Notation for Typical Charge Shape

so that the velocity and position respectively become

$$v = \dot{z} = a_0 t - v_0 \quad (49a)$$

$$z = -\frac{a_0 t^2}{2} + v_0 t + z_0 \quad (49b)$$

By a series of substitutions

$$\begin{aligned} e &= \frac{1}{2}v^2 \\ &= \frac{1}{2}v_0^2 - a_0 z_0 + a_0 z \end{aligned} \quad (50)$$

and hence, e decreases as z decreases.

Secondly, if an element is initially at the critical distance L above the surface where

$$L = \frac{v_0^2}{2a_0} \quad (51)$$

then v (and hence, e) is zero when that particular element reaches the surface. In other words, all elements above the plane $z=L$ and in the bottom half of the charge will not contribute to the cratering action.

(4) Assumption 4

For the range of explosive yield considered in this report, the height of the center of gravity of the charge z_{CG} is below the plane $z=L$ so that all parts of the bottom half of the charge will contribute to cratering.

(5) Assumption 5

At the interface between the surface of the earth and the explosive, the loss of kinetic energy is negligible.

c. Cratering Factor

The energy e_s per unit mass delivered at the surface of the earth by elements originally at a distance z_0 above the surface is obtained from Equation (50):

$$\begin{aligned} e_s &\equiv e|_{z=0} \\ &= \frac{1}{2} v_0^2 \left(1 - \frac{2a_0}{v_0^2} z_0 \right) \end{aligned} \quad (52a)$$

or, after using Equation (51)

$$e_s = e_0 (1 - z_0/L) \quad (52b)$$

The total kinetic energy of the charge is

$$\begin{aligned} E_T &= \int_B e_0 \, dm \\ &= M e_0 \end{aligned} \quad (53)$$

where M denotes the total mass of the charge and B the region occupied by the total charge. On the other hand, the kinetic energy delivered to the surface of the earth is

$$\begin{aligned} E_s &= \int_{B_L} e_s \, dm \\ &= \frac{M}{2} e_0 \left(1 - \frac{z_{CG}}{2L} \right) \end{aligned} \quad (54)$$

where B_L denotes the bottom half of the charge and z_{CG} is the distance to the center of mass of the total charge.

A cratering factor C_F can be defined as the ratio of the kinetic energy reaching the earth's surface to the total kinetic energy, that is

$$\begin{aligned} C_F &\equiv E_s/E_T \\ &= \frac{1}{2} \left(1 - \frac{z_{CG}}{2L} \right) \end{aligned} \quad (55)$$

According to assumption 4, the cratering factor must lie in the range

$$\frac{1}{4} \leq C_F \leq \frac{1}{2} \quad (56)$$

Equation (55) implies that for two charges with the same total kinetic energy, the charge with the lowest center of mass will be the most effective as far as cratering is concerned.

d. Charge Shapes and Non-dimensional Variables

If W denotes the yield of an explosion in terms of an equivalent weight of TNT, then immediately after detonation, assume that the total kinetic energy of the explosive is directly proportional to W and is independent of the charge shape, that is

$$E_T = \mu W \quad (57)$$

where μ is a constant. The energy delivered to the surface is then

$$E_s = C_F \mu W \quad (58)$$

To eliminate the unknown factor μ , reference charges can be introduced. For each charge shape, let W_o denote a reference yield and define

$$E_s^o \equiv C_{Fo} \mu W_o \quad (59)$$

where

$$C_{Fo} = \frac{1}{2} \left(1 - \frac{z_{CG}^o}{L} \right) \quad (60)$$

and z_{CG}^o is the height of the center of mass of the reference charge.

If the following non-dimensional variables are introduced:

$$T = W/W_o \quad (61a)$$

$$K = E_s/E_s^o \quad (61b)$$

$$C_o^F = C_F/C_{Fo} \quad (61c)$$

then

$$K = C_o^F T \quad (62)$$


and the factor μ is not present. If z_{CG} and z_{CG}^0 are both much smaller than L , then C_0^F is approximately equal to one.

For a given class of charge shapes, the total yields can be used rather than the dimensions L , z_{CG} and z_{CG}^0 . One such set is illustrated in Figure 18 and is characterized by the fact that the volume is proportional to the cube of one dimension in each case. This restricts the group of triangular and cylindrical prisms (which includes rectangular parallelepipeds) to that for which the surface contact area A_s is proportional to the square of the height h . In effect this implies that, for example, in the case of triangular prisms, we can let the sizes change but the shapes must be similar to the reference shape.

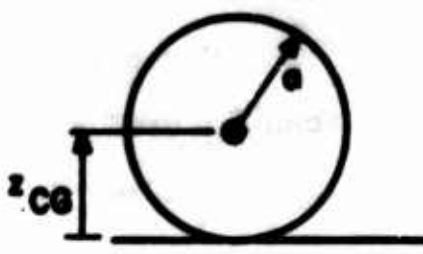
Since the yield is directly proportional to the volume, it can also be said that for this class of shapes the distance to the center of mass is proportional to the cube root of the yield. Thus, if we let

$$W_L = W \Big|_{z_{CG} = L} \quad (63)$$

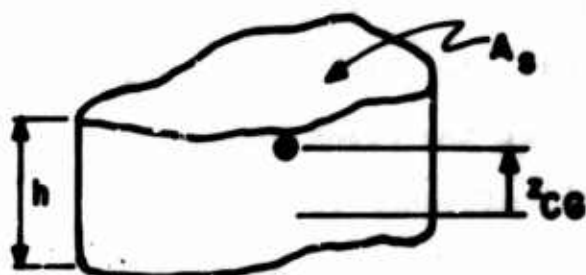
where W_L is the weapon yield for a charge shape in the same class as those in Figure 18 and whose center of mass is at a height L above the surface, then



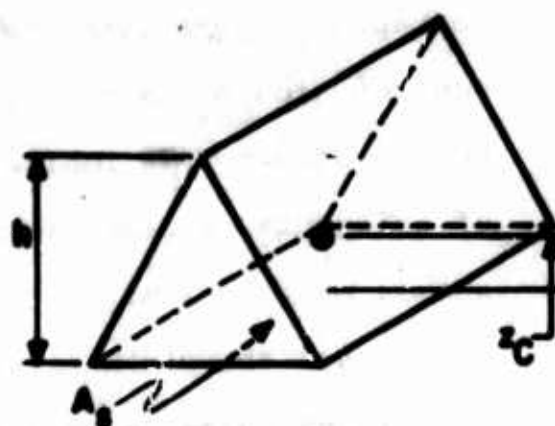
HEMISPHERE: $V = \frac{2}{3} \pi b^3$
 $z_{CG} = \frac{3}{8} b$



SPHERE: $V = \frac{4}{3} \pi a^3$
 $z_{CG} = a$



CYLINDRICAL PRISM:
 $V = A_s h$
 $z_{CG} = \frac{h}{2}$



TRIANGULAR PRISM:
 $V = \frac{1}{2} A_s h$
 $z_{CG} = \frac{h}{3}$

A_s IS PROPORTIONAL TO h^2

Figure 18. A Set of Four Charge Shapes

$$C_F = \frac{1}{4} \left[2 - \left(\frac{W}{W_L} \right)^{1/3} \right] \quad (64a)$$

$$C_{Fo} = \frac{1}{4} \left[2 - \left(\frac{W_o}{W_L} \right)^{1/3} \right] \quad (64b)$$

$$C_o^F = \frac{\left[2 - \left(\frac{W}{W_L} \right)^{1/3} \right]}{\left[2 - \left(\frac{W_o}{W_L} \right)^{1/3} \right]} \quad (64c)$$

In the absence of experimental results that would determine W_L , a value of 10^6 lbs. of TNT has been chosen for W_L for each of the charge shapes shown in Figure 18.

3. CRATER AND EJECTA FORMATIONS

a. Basic Shape Parameters

The most significant parameters associated with the description of the crater and ejecta shape are shown in Figure 19. If the origin of a cylindrical coordinate system is placed on the original surface at the center of the crater, then the crater depth is assumed to be adequately described by the parabola

$$x = a + bR + cR^2 \quad (65)$$

where a , b and c are constants and R is the distance from the origin. If D_a denotes the apparent depth of the crater at the origin, R_a the apparent radius at the original surface and if we assume that

$$\left. \frac{dx}{dR} \right|_{R=0} = 0 \quad (66)$$

then the crater depth is described by

$$x = D_a \left(1 - \frac{R^2}{R_a^2} \right) \quad 0 \leq R \leq R_a \quad (67)$$

The maximum slope of the crater, which will be of significance later in connection with energy dissipation, occurs at the intersection of the crater with the original surface and is given by

$$\left. \frac{dx}{dR} \right|_{R=R_a} = -2 \frac{D_a}{R_a} \quad (68)$$

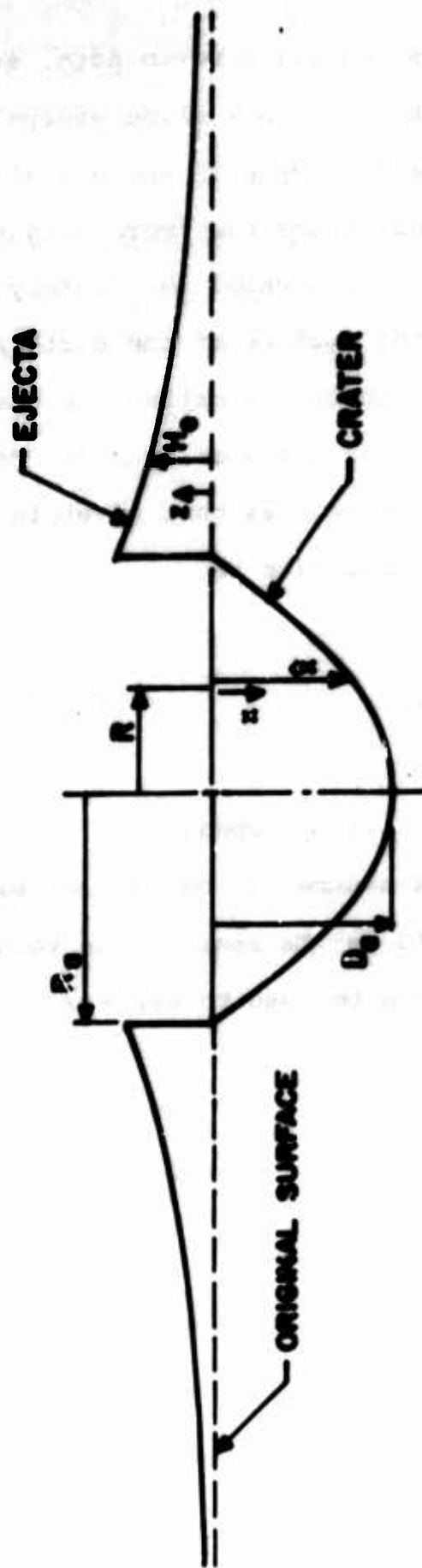


Figure 19. Idealized Crater and Ejecta Parameters

An aid in visualizing this condition is to note, as shown in Figure 20, that a cavity with this slope everywhere would be a cone with twice the depth of the actual crater.

After a detonation, particles that were originally within the boundary of the crater are located immediately beyond the top rim of the crater on the surface of the earth and this material that has been thrown out is called the ejecta. The depth of the ejecta as a function of distance from the center of the crater was assumed to be the same as that given in Reference 22 for nuclear detonations. This relation is

$$H_e = \sigma D_a \left\{ \frac{R_a}{R} \right\}^{\hat{\beta}} \quad R \geq R_a \quad (69)$$

where σ and $\hat{\beta}$ are parameters that depend on the earth media.

If the earth media is assumed to be incompressible, then the volume of the crater should be the same as the volume of the ejecta. Such a relation can be used to express σ in terms of $\hat{\beta}$:

The volume of the crater is

$$\begin{aligned} V_c &= \int_0^{R_a} \int_0^{2\pi} \int_0^x R \, dx \, d\theta \, dR \\ &= 2\pi \int_0^{R_a} D_a R \left(1 - \frac{R^2}{R_a^2} \right) dR \end{aligned}$$

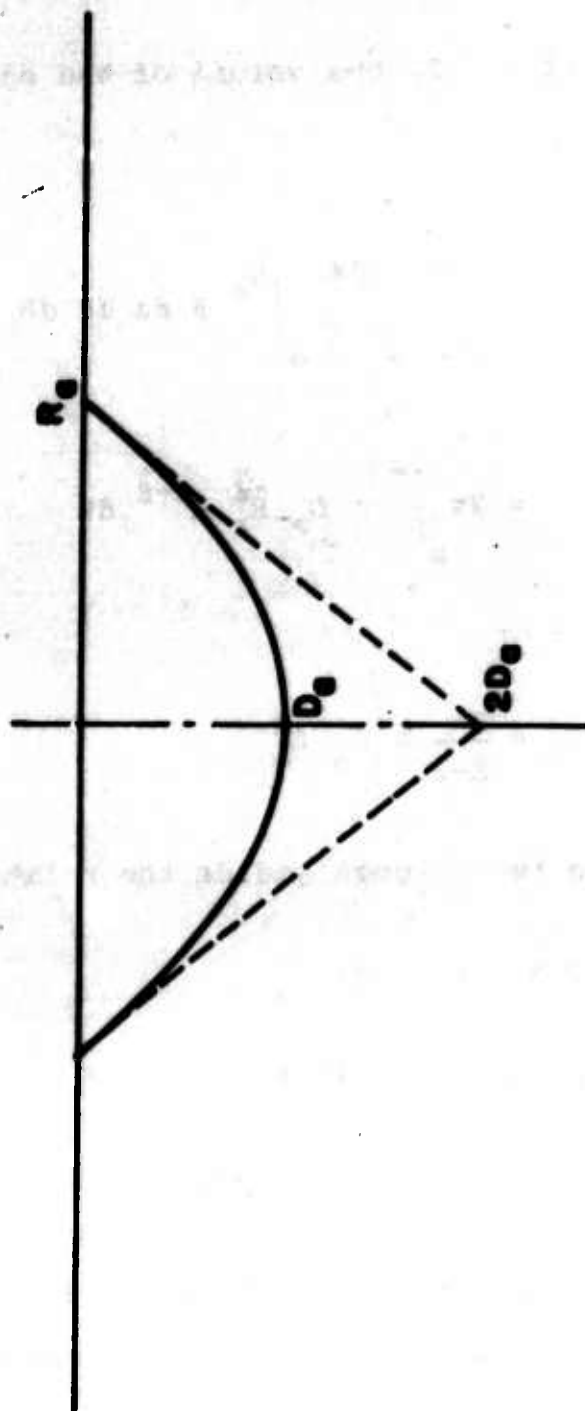


Figure 20. Maximum Crater Slope

or

$$V_c = \frac{\pi}{2} D_a R_a^2 \quad (70)$$

Similarly, if $\hat{\beta} > 2$, the volume of the ejecta V_e is given by

$$\begin{aligned} V_e &= \int_R^\infty \int_0^{2\pi} \int_0^{H_e} R \, dz \, d\theta \, dR \\ &= 2\pi \int_R^\infty \sigma D_a R_a^{\hat{\beta}} R^{1-\hat{\beta}} \, dR \end{aligned}$$

or

$$V_e = \frac{2\pi}{\hat{\beta}-2} \sigma D_a R_a^2 \quad (71)$$

Equating the two volumes yields the relation

$$\sigma = \frac{1}{4} (\hat{\beta} - 2) \quad (72)$$

so that, from Equation (69)

$$H_e = \frac{D_a}{4} (\hat{\beta} - 2) \left(\frac{R_a}{R} \right)^{\hat{\beta}} \quad (73)$$

Reference 22 suggests the values $\sigma = 0.5$ and $\hat{\beta} = 3.9$ for soil, and $\sigma = 0.3$ and $\hat{\beta} = 3.1$ for rock. However,

Equation (72) yields the value $\hat{\beta} = 4.0$ when $\sigma = 0.5$ and $\hat{\beta} = 3.2$ when $\sigma = 0.3$. Such a variation is negligible in view of the disparity in test results.

Of more significance are experimental values for the height of the crater lip. From Equation (73) the analytical expression is

$$H_e \Big|_{R=R_a} = \frac{D_a}{4} (\hat{\beta} - 2) \quad (74)$$

According to results tabulated by Vortman (Reference 16), the 100-ton Suffield Experimental Station hemispherical shot in clay yielded a crater lip height which was 27 per cent of the crater depth, which produces a value of 3.1 for $\hat{\beta}$. On the other hand, for the 500-ton Sailor Hat shot on basalt rock, the height of the crater lip was 36 per cent of the crater depth, which yields a value of 3.4 for $\hat{\beta}$.

These results imply that the values of $\hat{\beta}$ do not assume the same range of values for conventional high explosives as for nuclear explosives. Furthermore, for conventional explosives the variation in $\hat{\beta}$ may be quite small for changes in earth media.

For this project, a reference value of 3.1 was chosen for $\hat{\beta}$ for soil.

It seems plausible to assume that most of the material will move radially outward. For the next section it is necessary to know the positions of the centroids of crater

and ejecta elements that subtend a small angle $\Delta\theta$ (See Figure 21). The crater and ejecta volume elements are

$$\begin{aligned}\Delta V_c &= \Delta\theta \int_0^{R_a} \int_0^x R \, dx \, dR \\ &= \Delta\theta \frac{D_a R_a^2}{4} \\ &= \Delta V_e\end{aligned}\tag{75}$$

The coordinates to the centroids of these elements are defined as follows:

$$\Delta V_c R_c = \Delta\theta \int_0^{R_a} \int_0^x R^2 \, dx \, dR\tag{76a}$$

$$\Delta V_c x_c = \Delta\theta \int_0^{R_a} \int_0^x xR \, dx \, dR\tag{76b}$$

$$\Delta V_e R_e = \Delta\theta \int_{R_a}^{\infty} \int_0^{H_e} R^2 \, dz \, dR\tag{76c}$$

$$\Delta V_e z_e = \Delta\theta \int_{R_a}^{\infty} \int_0^{H_e} R z \, dz \, dR\tag{76d}$$

The results for $\hat{\beta} \geq 3.0$ are:

$$R_c = \frac{8}{15} R_a\tag{77a}$$

$$x_c = D_a/3\tag{77b}$$

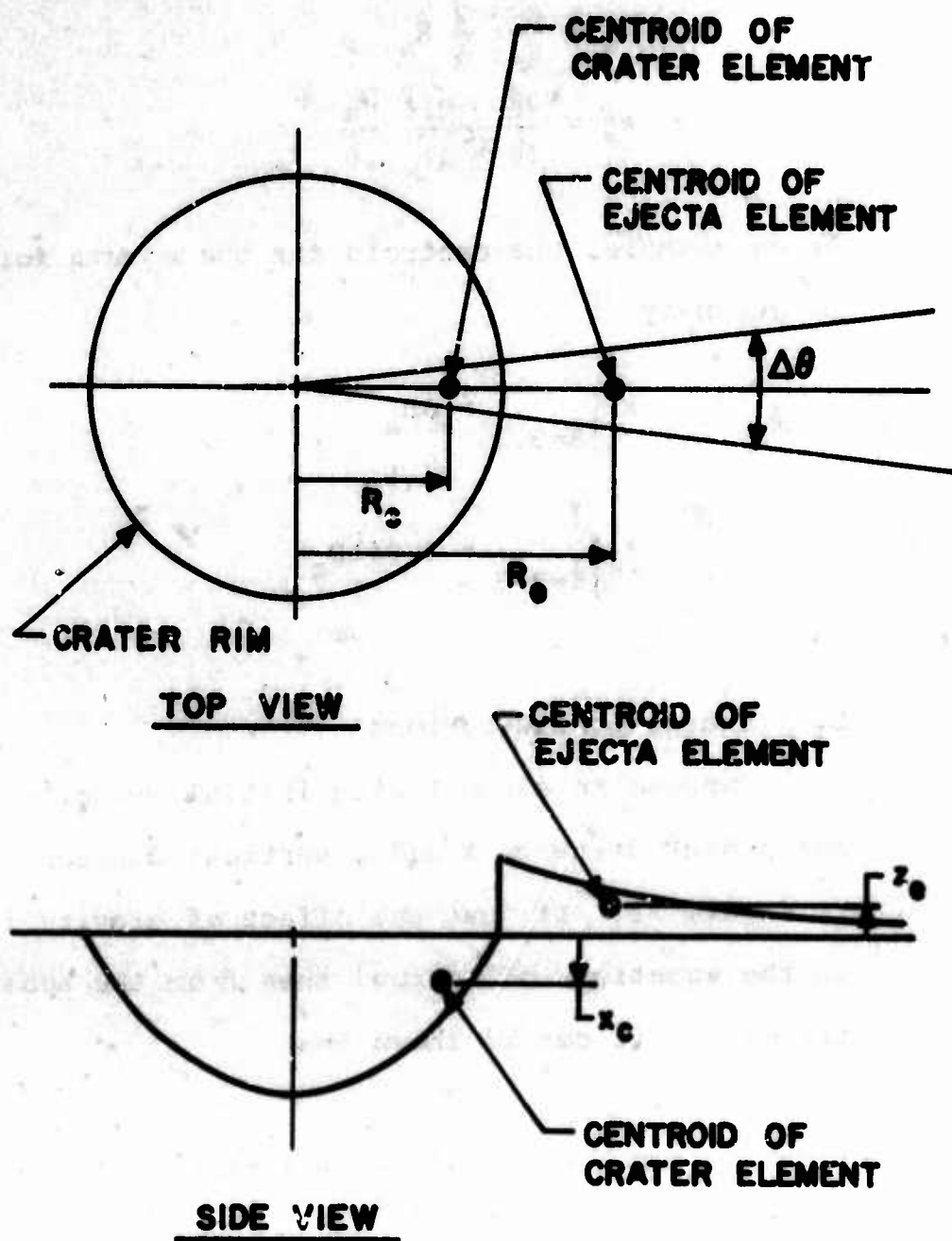


Figure 21. Centroids of Crater
and Ejecta Elements

$$R_e = \frac{\hat{\beta} - 2}{\hat{\beta} - 3} R_a \quad (77c)$$

$$z_e = \frac{(\hat{\beta} - 2)^2}{(\hat{\beta} - 1)} \frac{D_a}{16} \quad (77d)$$

As an example, the centroid for the ejecta for $\hat{\beta} = 3.2$ is given by

$$R_e \Big|_{\hat{\beta}=3.2} = 6R_a \quad (78a)$$

$$z_e \Big|_{\hat{\beta}=3.2} = 0.041D_a \quad (78b)$$

b. Energy Considerations

Suppose an element with initial velocity v_o moves a horizontal distance X and a vertical distance H as shown in Figure 22. If just the effect of gravity is considered in the equations of motion, then from the equation of the trajectory it can be shown that

$$H = - \frac{g}{2} \frac{X^2}{v_o^2 \cos^2 \beta} + X \tan \beta \quad (79)$$

For a conservative estimate on the energy requirement, choose β with H and X considered fixed such that v_o is a minimum, that is, set

$$\frac{dv_o}{d\beta} = 0 \quad (80)$$

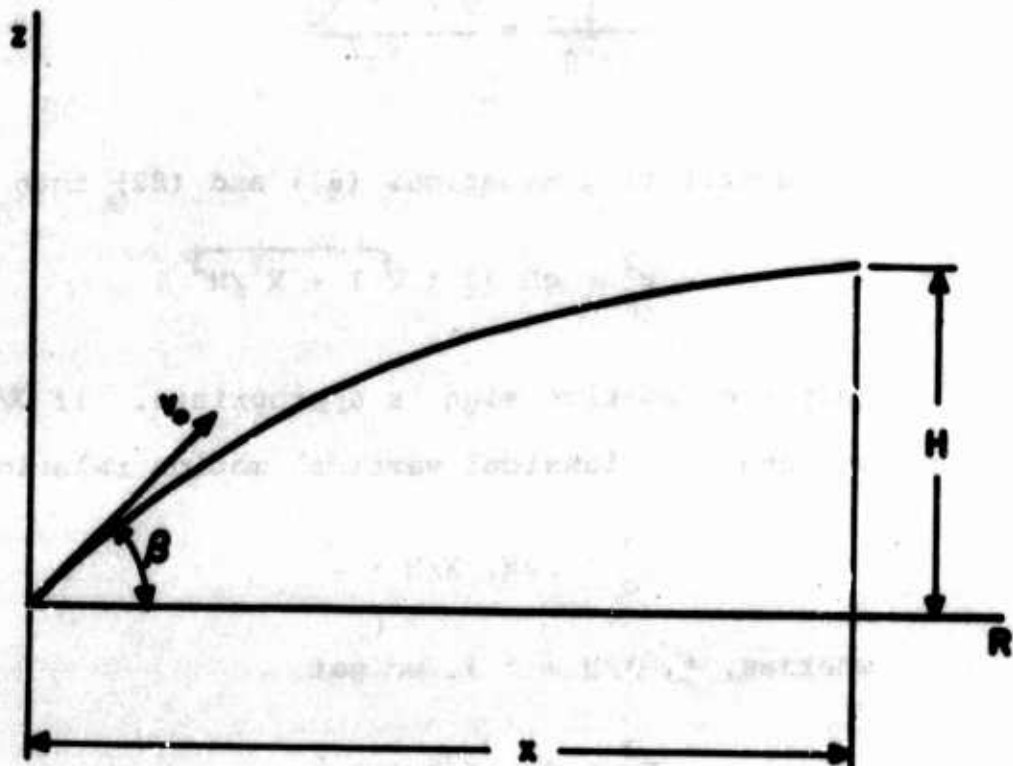


Figure 22. Trajectory of an Element

This yields

$$\tan \beta = \frac{v_o^2}{gX} \quad (81)$$

which can be written in the alternate form

$$\frac{1}{\cos^2 \beta} = \frac{g^2 X^2 + v_o^4}{g^2 X^2} \quad (82)$$

By substituting Equations (81) and (82) into (79) we get

$$v_o^2 = gH [1 \pm \sqrt{1 + X^2/H^2}] \quad (83)$$

Only the positive sign is appropriate. If $X/H \ll 1$, we have the classical vertical motion relation

$$v_o^2 = 2gH, \quad X/H \ll 1 \quad (84)$$

whereas, if $X/H \gg 1$, we get

$$v_o^2 = gX, \quad X/H \gg 1 \quad (85)$$

Suppose that on the average, an element moves from the centroid of a crater element to the centroid of an ejecta element. Then

$$\begin{aligned} X &= R_e - R_c \\ &= R_a \left(\frac{\hat{\beta} - 2}{\hat{\beta} - 3} - \frac{8}{15} \right) \end{aligned} \quad (86a)$$

$$H = x_c + z_c$$

$$= D_a \left[\frac{1}{3} + \frac{1}{16} \frac{(\hat{\beta} - 2)^2}{(\hat{\beta} - 1)} \right] \quad (86b)$$

For the range $3.1 \leq \hat{\beta} \leq 3.6$, the smallest value of X/H occurs at $\hat{\beta} = 3.6$. Hence

$$\frac{X}{H} \geq 5.5 \frac{R_a}{D_a}, \quad 3.1 \leq \hat{\beta} \leq 3.6 \quad (87)$$

For actual shots, it is generally true that the apparent radius is at least twice the apparent depth so that

$$\frac{X}{H} \geq 11 \quad (88)$$

Because of the diversity of experimental data, the inequality associated with Equation (85) can be considered satisfied and hence, with the use of Equation (86a)

$$v_o^2 = g R_a \left(\frac{\hat{\beta} - 2}{\hat{\beta} - 3} - \frac{8}{15} \right) \quad (89)$$

In order that this expression always be positive, we must have $\hat{\beta} > 3$ which is the same restriction imposed previously in connection with centroids.

If the mass density of the earth media is denoted by ρ , the total initial kinetic energy of the earth elements is approximated by

$$\begin{aligned} E_G &= \frac{1}{2} \rho V_c v_o^2 \\ &= \frac{1}{4} \rho g D_a R_a^3 \left(\frac{\hat{\beta} - 2}{\hat{\beta} - 3} - \frac{8}{15} \right) \end{aligned} \quad (90)$$

It should be emphasized that E_G is not the same as the energy input E_s since a portion of the latter will be dissipated into the ground in the form of heat.

c. Dimensional Considerations

To describe the shape of the crater it is necessary to know the ratio D_a/R_a . Postulate that this ratio primarily depends (Reference 23) on the following parameters: (1) an earth media viscosity v' , (2) mass density of the earth media ρ , (3) the kinetic energy input E_s , and (4) the apparent crater radius R_a . Such a dependence can be expressed analytically by

$$D_a/R_a = f'(\rho, E_s, v', R_a) \quad (91)$$

where f' is the unknown function. If $[M]$, $[L]$ and $[T]$ denote the fundamental dimensions of mass, length and time respectively, then the dimensions of the parameters in Equation (91) are

$$[D_a/R_a] = 1 \quad (92a)$$

$$[\rho] = [M]/[L]^3 \quad (92b)$$

$$[E_s] = [M] [L]^2/[T]^2 \quad (92c)$$

$$[R_a] = [L] \quad (92d)$$

$$[v'] = [M]/[T] [L] \quad (92e)$$

According to the Buckingham π -Theorem, the latter four variables can be combined into one non-dimensional variable which is chosen to be

$$\phi = \frac{v^2 R_a}{E_s} \quad (93)$$

where

$$v = v' / \sqrt{\rho} \quad (94)$$

can be considered a generalized viscosity. Now Equation (91) can be given as

$$\frac{D_a}{R_a} = f(\phi) \quad (95)$$

where f is a non-dimensional function of the parameter ϕ and is unknown. Since no analysis in this connection appears to be available as a guide in choosing a suitable form for f , assume a simple exponential relation of the following type:

$$D_a/R_a = k\phi^\zeta = k \left(\frac{v^2 R_a}{E_s} \right)^\zeta \quad (96)$$

where k and ζ are constants. Note that this relation will yield the maximum slope of the crater wall with the use of Equation (68).

Suppose that for one earth media, values of parameters associated with a reference charge are denoted by a superscript zero. Then, according to Equations (90) and (96)

$$E_G^0 = \frac{\pi}{4} \rho g D_a^0 (R_a^0)^3 \left(\frac{\hat{\beta} - 2}{\hat{\beta} - 3} - \frac{8}{15} \right) \quad (97a)$$

$$\frac{D_a^0}{R_a^0} = k \left(\frac{v R_a^0}{E_s^0} \right)^\zeta \quad (97b)$$

The parameters ρ , $\hat{\beta}$ and v depend only on the type of earth media and not on the size of charge. Hence, these variables do not have the superscript zero. On the other hand, it is assumed that k and ζ are independent of both earth media and charge size.

By taking appropriate ratios of the terms in Equations (90), (96) and (97) the following relations are obtained:

$$\frac{E_G}{E_G^0} = \frac{D_a}{D_a^0} \left(\frac{R_a}{R_a^0} \right)^3 \quad (98a)$$

$$\frac{D_a}{D_a^0} = \left(\frac{R_a}{R_a^0} \right)^{1+\zeta} \left(\frac{E_s^0}{E_s} \right)^\zeta \quad (98b)$$

These equations do not contain the terms that depend on the earth media; hence, they can be used for predicting

results from the knowledge of one surface detonation on a given soil or rock.

The following analysis is developed to relate the actual kinetic energy of the earth particles E_G to the kinetic energy delivered to the surface E_s .

d. Energy Dissipation

The initial kinetic energy E_G of the earth particles will differ from the kinetic energy delivered to the surface E_s by the amount of energy E_D dissipated in the form of heat:

$$E_G = E_s - E_D \quad (99)$$

From the expression in the incremental theory of plasticity (Reference 24) for energy dissipation where τ denotes stress and $\dot{\epsilon}$ strain rate

$$\tau \dot{\epsilon} = v' \dot{\epsilon}^2 \quad (100)$$

it seems appropriate to assume that E_D is linearly proportional to v' and also a function of E_s , ρ and R_a , that is

$$E_D = v' f(E_s, \rho, R_a) \quad (101)$$

Dimensional homogeneity for the equation implies that

$$E_D = b E_s \left(\frac{v'^2 R_a}{E_s} \right)^{1/2} \quad (102)$$

where b is taken to be a non-dimensional constant and v is defined by Equation (94). For a reference charge, we get

$$E_D^O = b E_s^O \left(\frac{v^2 R_a^O}{E_s^O} \right)^{1/2} \quad (103)$$

so that

$$\frac{E_D}{E_D^O} = \left(\frac{E_s}{E_s^O} \frac{R_a}{R_a^O} \right)^{1/2} \quad (104)$$

For the case of a reference charge, it is convenient to introduce a dissipation ratio

$$z_s^D = \frac{E_D^O}{E_s^O} \quad (105)$$

which is simply the ratio of the energy dissipated to the energy available at the surface. Hence E_s^D must assume a value between 0 and 1.

From Equation (99)

$$E_G = E_s \left(1 - \frac{E_O}{E_D^O} \frac{E_D^O}{E_s^O} \frac{E_s^O}{E_s} \right) \quad (106)$$

Substitute Equations (104), (105) and (61b) into (106) to get

$$\begin{aligned}
 E_G &= E_s \left[1 - \frac{E_s^D}{K} \left(K \frac{R_a}{R_a^O} \right)^{1/2} \right] \\
 &= E_s \left[1 - E_s^D \left(\frac{R_a}{K R_a^O} \right)^{1/2} \right]
 \end{aligned} \tag{107}$$

Also

$$E_G^O = E_s^O [1 - E_s^D] \tag{108}$$

so that

$$\frac{E_G}{E_G^O} = \frac{K \left[1 - E_s^D \left(\frac{R_a}{K R_a^O} \right)^{1/2} \right]}{[1 - E_s^D]} \tag{109}$$

Hence, with the use of Equation (61b), Equations (98a) and (98b) can be written in the alternate form

$$\left(\frac{R_a}{R_a^O} \right)^{4+\zeta} = \frac{K^{1+\zeta} \left[1 - E_s^D \left(\frac{R_a}{K R_a^O} \right)^{1/2} \right]}{[1 - E_s^D]} \tag{110a}$$

$$D_a/D_a^O = \left(\frac{R_a}{R_a^O} \right)^{1+\zeta} \frac{1}{K^\zeta} \quad (110b)$$

With R_a^O , D_a^O , ζ and E_s^D presumed known, these two equations give the apparent radius and depth as a function of K and hence as a function of the yield of the explosive. Then, if $\hat{\beta}$ is known, Equation (73) can be used to predict the ejecta depth.

For a given earth media (alluvium for example), ρ and $\hat{\beta}$ are assumed known. For some reference energy E_s^O , the apparent radius and depth, R_a^O and D_a^O respectively can be measured, and values for ζ and E_s^D determined experimentally. A different earth media will, in general, yield different values for these parameters which will be designated by an asterisk. For a new reference energy E_s^{*O} , R_a^{*O} and D_a^{*O} can be measured as before. The new density ρ can also be determined experimentally and it is assumed that ζ remains unchanged. The parameters $\hat{\beta}^*$ and E_s^{*D} can be determined according to the following analysis.

From Equations (103) and (105)

$$E_s^D = b \left(\frac{R_a^O}{E_s^O} \right)^{1/2} v \quad (111a)$$

$$E_s^{*D} = b \left(\frac{R_a^{*O}}{E_s^{*O}} \right)^{1/2} v^* \quad (111b)$$

or, after eliminating b

$$E_s^{*D} = E_s^D \left(\frac{R_a^{*O}}{R_a^O} \frac{E_s^O}{E_s^{*O}} \right)^{1/2} \frac{v^*}{v} \quad (112)$$

In a similar manner, Equation (97b) yields

$$\frac{D_a^{*O}}{D_a^O} = \left(\frac{R_a^{*O}}{R_a^O} \right)^{1+\zeta} \left(\frac{E_s^O}{E_s^{*O}} \right)^{\zeta} \left(\frac{v^*}{v} \right)^{2\zeta} \quad (113)$$

By eliminating v^*/v between Equations (112) and (113), we get

$$E_s^{*D} = E_s^D \left(\frac{D_a^{*O}}{D_a^O} \frac{R_a^O}{R_a^{*O}} \right)^{\frac{1}{2\zeta}} \quad (114)$$

To obtain a value for $\hat{\beta}^*$, Equations (97a) and (108) for the two media can be combined to get

$$\left(\frac{\hat{\beta}^* - 2}{\hat{\beta}^* - 3} - \frac{8}{15} \right) = \frac{E_s^{*O}}{E_s^O} \frac{(1 - E_s^{*D})}{(1 - E_s^D)} \frac{\rho}{\rho^*} \frac{D_a^O}{D_a^{*O}} \left(\frac{R_a^O}{R_a^{*O}} \right)^3 \left(\frac{\hat{\beta} - 2}{\hat{\beta} - 3} - \frac{8}{15} \right) \quad (115)$$

Equation (59) can be used to express E_s^{*O}/E_s^O in terms of reference charge yields and shapes:

$$\frac{E_s^{*O}}{E_s^O} = \frac{C_{Fo}^* W_o^*}{C_{Fo} W_o} \quad (116)$$

4. SUMMARY

For easy reference in connection with the computer program, the pertinent equations will be summarized.

For one particular earth media, W_0 denotes a reference charge for which the apparent radius R_a^0 and apparent depth D_a^0 are known. Any other yield is expressed in terms of the reference charge by means of the non-dimensional parameter

$$T = \frac{W}{W_0} \quad (117)$$

The energy E_s available at the surface is also expressed non-dimensionally by means of the factor

$$K = \frac{E_s}{E_s^0} \quad (118)$$

where

$$K = C_O^F T \quad (119)$$

and

$$C_O^F = \frac{\left[2 - \left(\frac{W}{W_L} \right)^{1/3} \right]}{\left[2 - \left(\frac{W_0}{W_L} \right)^{1/3} \right]} \quad (120)$$

For lack of a precise value, W_L is taken to be 10^6 lbs. or 500 tons of TNT.

With the dissipation ratio E_s^D for the reference charge W_0 and the particular earth media assumed known from experimental sources, the apparent radius R_a and depth D_a for charges of various values are determined from

$$\left(\frac{R_a}{R_a^0} \right)^{4+\zeta} = K^{1+\zeta} \frac{\left[1 - E_s^D \left(\frac{R_a}{KR_a^0} \right)^{1/2} \right]}{\left[1 - E_s^D \right]} \quad (121a)$$

$$\frac{D_a}{D_a^0} = \left(\frac{R_a}{R_a^0} \right)^{1+\zeta} \frac{1}{K^\zeta} \quad (121b)$$

The parameter ζ is assumed to be the same for all earth media and is chosen so that the theoretical results fit the experimental data as closely as possible.

With $\hat{\beta}$ known, the depth of ejecta is given by

$$H_e = \frac{D_a}{4} (\hat{\beta} - 2) \left(\frac{R_a}{R} \right)^{\hat{\beta}}, \quad R > R_a \quad (122)$$

One set of basic reference parameters are those associated with the 100 ton shot at the Suffield Experimental Station.

According to Reference 16, the soil, a silty clay, had a weight density of 94 lb/ft^3 and the apparent depth and radius were 21 and 70 feet respectively. As mentioned previously, an appropriate value for $\hat{\beta}$ for soil is 3.1. A value of 0.3 for both ζ and E_s^D for this reference charge and earth media appears to give reasonable results.

The above equations are also used for a different earth media. However, the new apparent depth D_a^{*O} and apparent radius R_a^{*O} must be determined experimentally for the new reference charge W_o^* . The new dissipation ratio is given by

$$E_s^{*D} = E_s^D \left(\frac{D_a^{*O}}{D_a^O} \frac{R_a^O}{R_a^{*O}} \right)^{\frac{1}{2\zeta}} \quad (123)$$

and the new ejecta parameter $\hat{\beta}^*$ can be found from

$$\left(\frac{\hat{\beta}^* - 2}{\hat{\beta}^* - 3} - \frac{8}{15} \right) = \frac{C_{Fo}^* W_o^*}{C_{Fo} W_o} \left(\frac{1 - E_s^{*D}}{1 - E_s^D} \right) \frac{\rho}{\rho^*} \frac{D_a^O}{D_a^{*O}} \left(\frac{R_a^O}{R_a^{*O}} \right)^3 \left(\frac{\hat{\beta} - 2}{\hat{\beta} - 3} - \frac{8}{15} \right) \quad (124)$$

where

$$C_{Fo} = \frac{1}{4} \left[2 - \left(\frac{W_o}{W_L} \right)^{1/3} \right] \quad (125a)$$

$$C_{Fo}^* = \frac{1}{4} \left[2 - \left(\frac{W_o^*}{W_L} \right)^{1/3} \right] \quad (125b)$$

For a discontinuous basalt rock of weight density 190 lb/ft³, Reference 16 states that a charge $W_o^* = 500$ tons of TNT yields an apparent radius $R_a^{*o} = 79$ ft. and an apparent depth $D_a^{*o} = 38$ ft. These values can be used to obtain E_s^{*D} and $\hat{\beta}^*$ for this type of rock. Then equations (121a) and (121b) with the new parameters can be used to find the dimensions of a crater for any other charge below 500 tons of TNT.

The above outline briefly describes a theory that should adequately predict the crater and ejecta shapes for a wide range of yield for conventional explosives. The effect of charge shape is included in the analysis.

For bomb stacks, the theory of this section appears to be satisfactory if only the weight of the high explosive is used. For stacks that are of the same order of magnitude as the barricade, the effect of the barricade, as far as crater and ejecta shapes are concerned, is assumed to be negligible. For cases where the bomb stack is relatively small, the situation is quite different and for most practical purposes, the crater and ejecta shapes are not too significant.

The computer program associated with the theory of this section is described in Appendix III.

SECTION V

ILLUSTRATIVE EXAMPLES

1. INTRODUCTION

In this section, a representative set of curves is presented that is based on the theory of the previous sections and the associated computer programs. Because of the large number of parameters that are present, only typical values were chosen for a graphical representation of the computer output. These curves are intended just to illustrate the type of information that can be obtained. In many instances the computer output is more detailed and can handle several possible situations which are not appropriate for a graphical display.

Some of the results of available experimental data are also plotted to indicate the degree of correlation between predicted and actual values. As stated previously, a certain amount of judgement is necessary when using these programs.

2. RESULTS FROM BLAST PRESSURE PROGRAM

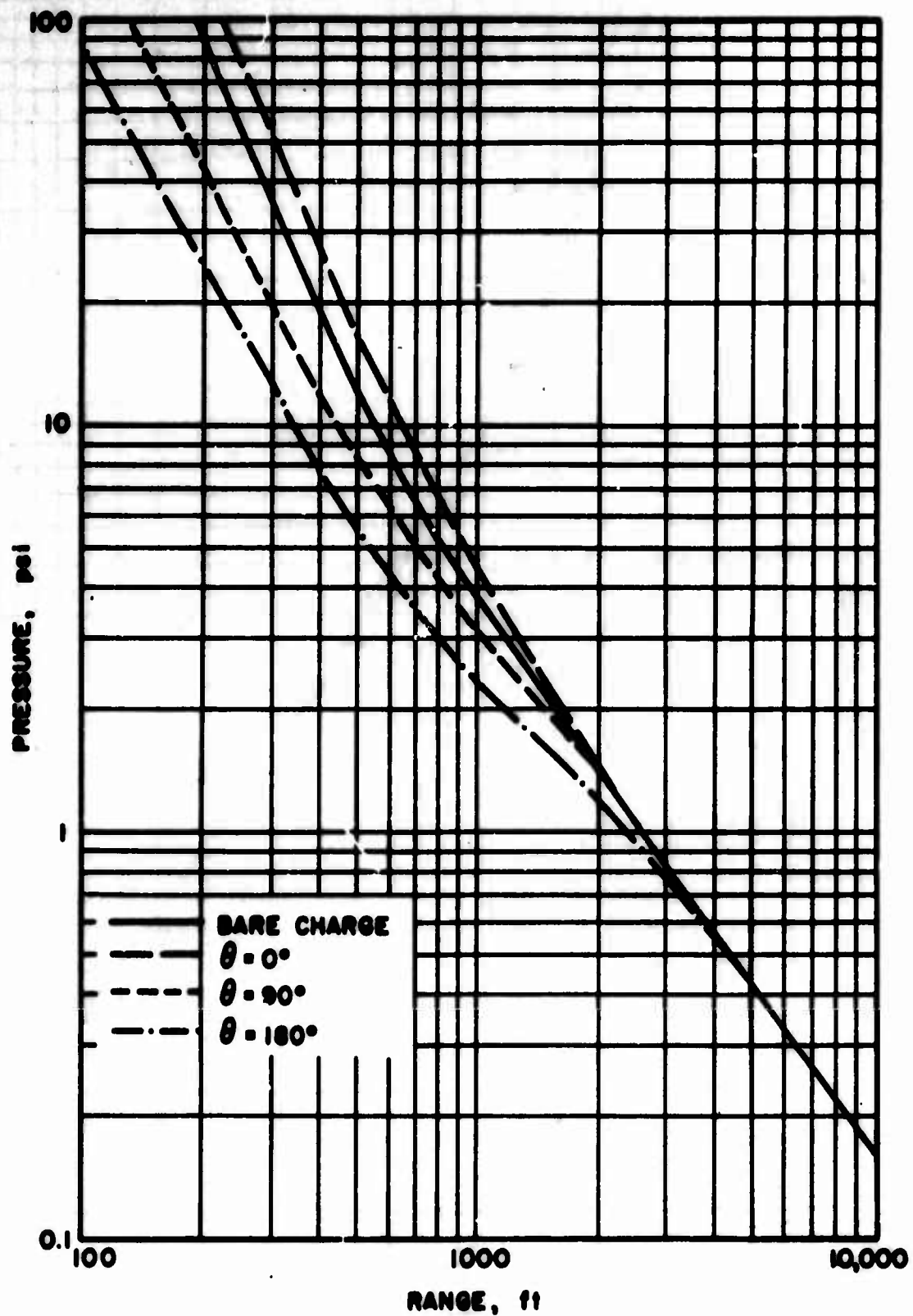
As a typical example, parameters associated with Phases I and II of the "BIG PAPA" (Reference 1) tests were used as input data for the program. The bomb stack dimensions were 30 ft. wide by 50 ft. deep by 8.83 ft. high and the corresponding barricade dimensions were 100 ft. by 70 ft. by 11 ft., respectively.

Associated with a bomb stack are several conversion factors which are listed in Reference 3. The first replaces the weight of the explosive in a bomb by an equivalent weight of TNT. According to Reference 1, which used a factor of 1.23 in converting tritonal to TNT, the bomb stacks contained an equivalent weight of 307,500 lbs. of TNT. From Reference 3, a factor of 0.6 was considered most appropriate for replacing the bomb stack by a bare charge (184,000 lbs.) that would yield the same blast pressure characteristics. A different factor must be used for impulse but since the procedure is quite analogous, impulse distributions are not given.

Pressure versus distance is plotted in Figure 23 for the following cases:

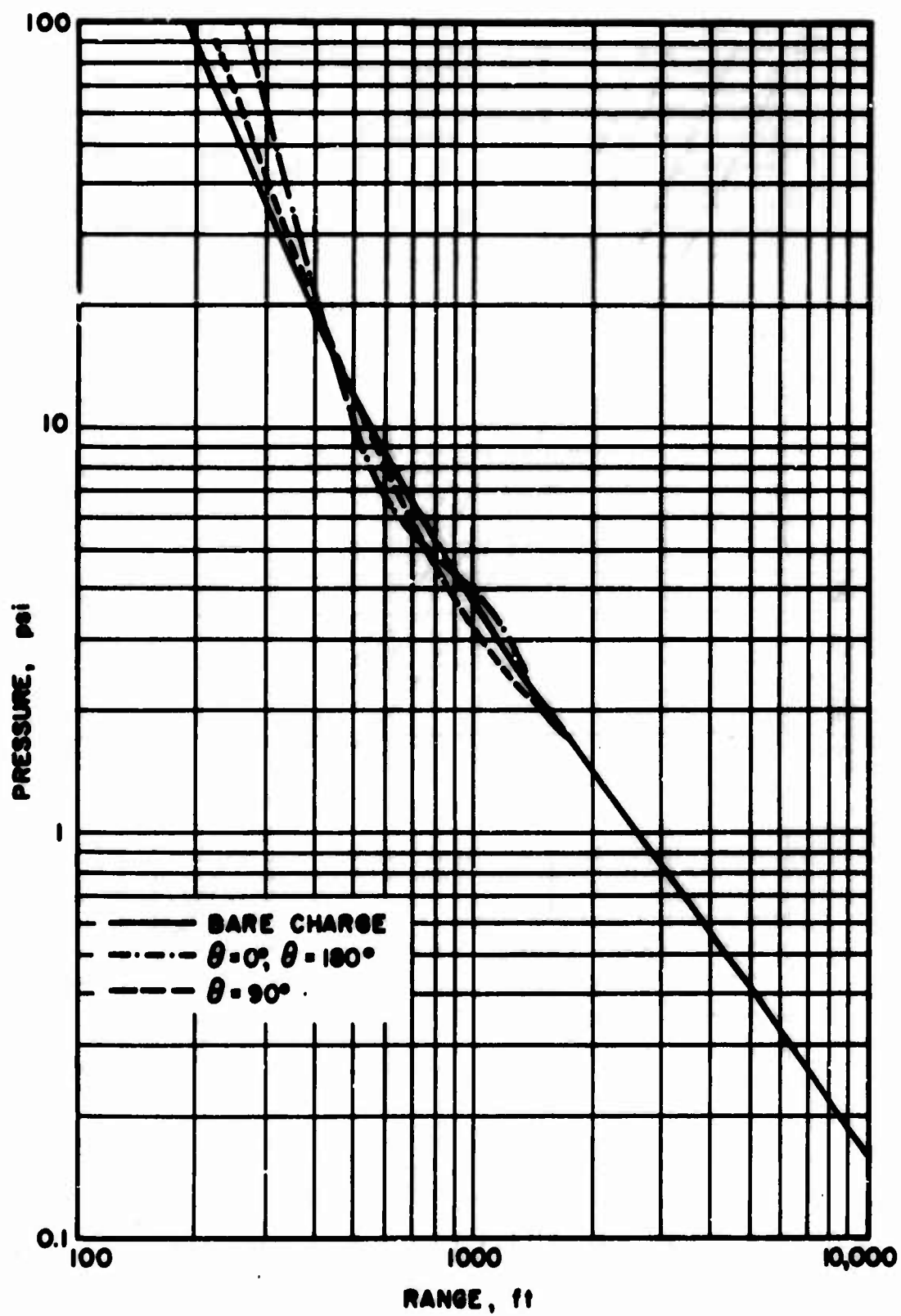
- a. Bare hemispherical unbarricaded charge,
- b. Bare hemispherical barricaded charge,
- c. Rectangular unbarricaded charge, and
- d. Rectangular barricaded charge.

Figure 23a shows rather predictable results for the effect of the barricade on the blast pressure from a hemispherical charge. For a given distance from the center of the charge, the pressure out the front or open end of the barricade is



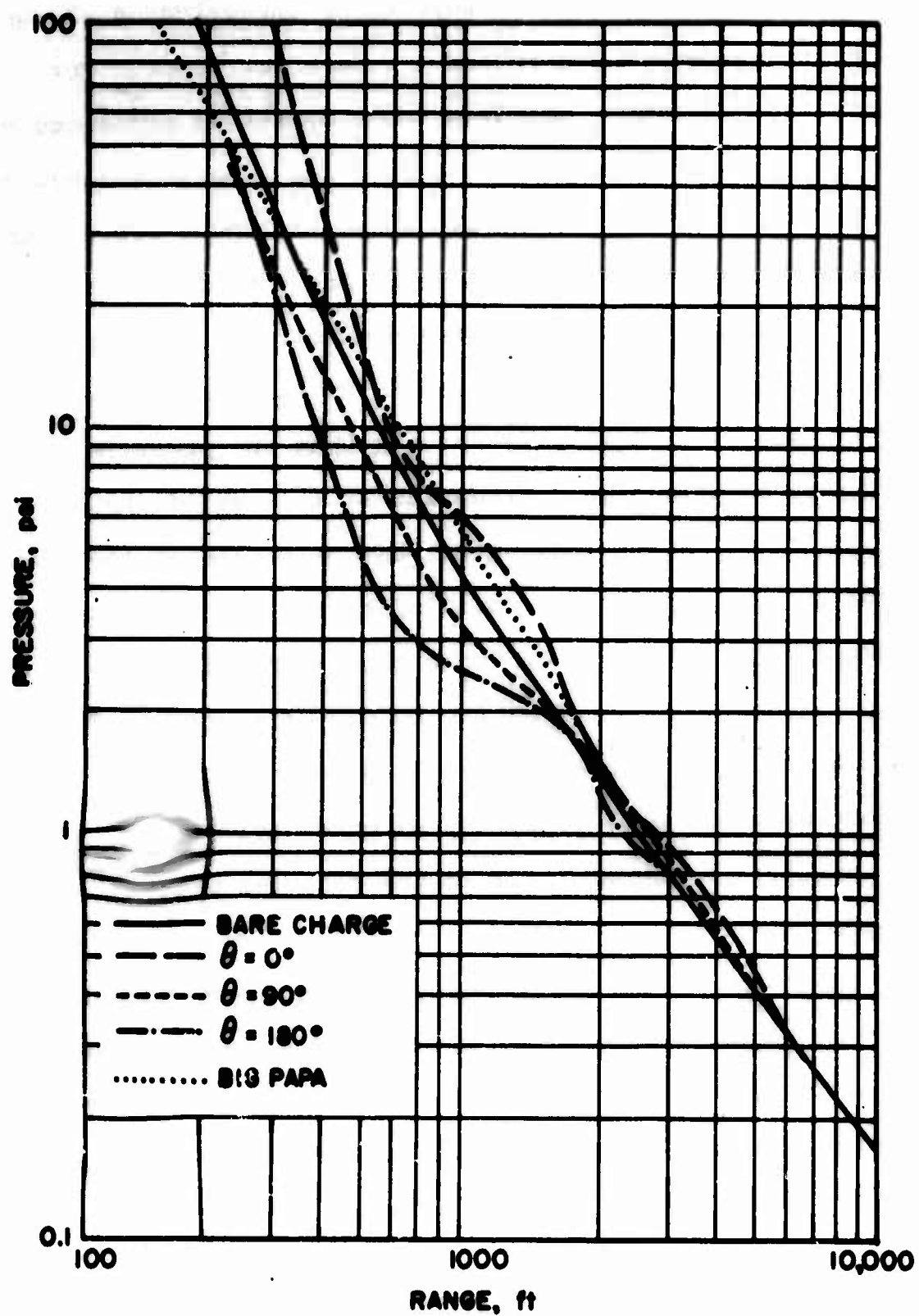
(a) Hemispherical Barricaded and Unbarricaded (Bare) Charges

Figure 23. Pressure versus Range for Various Charge and Barricade Combinations



(b) Rectangular and Hemispherical (Bare) Unbarricaded Charges

Figure 23. (Continued)



(c) Rectangular Barricaded and Hemispherical Unbarricaded (Bare) Charges

Figure 23. (Continued)

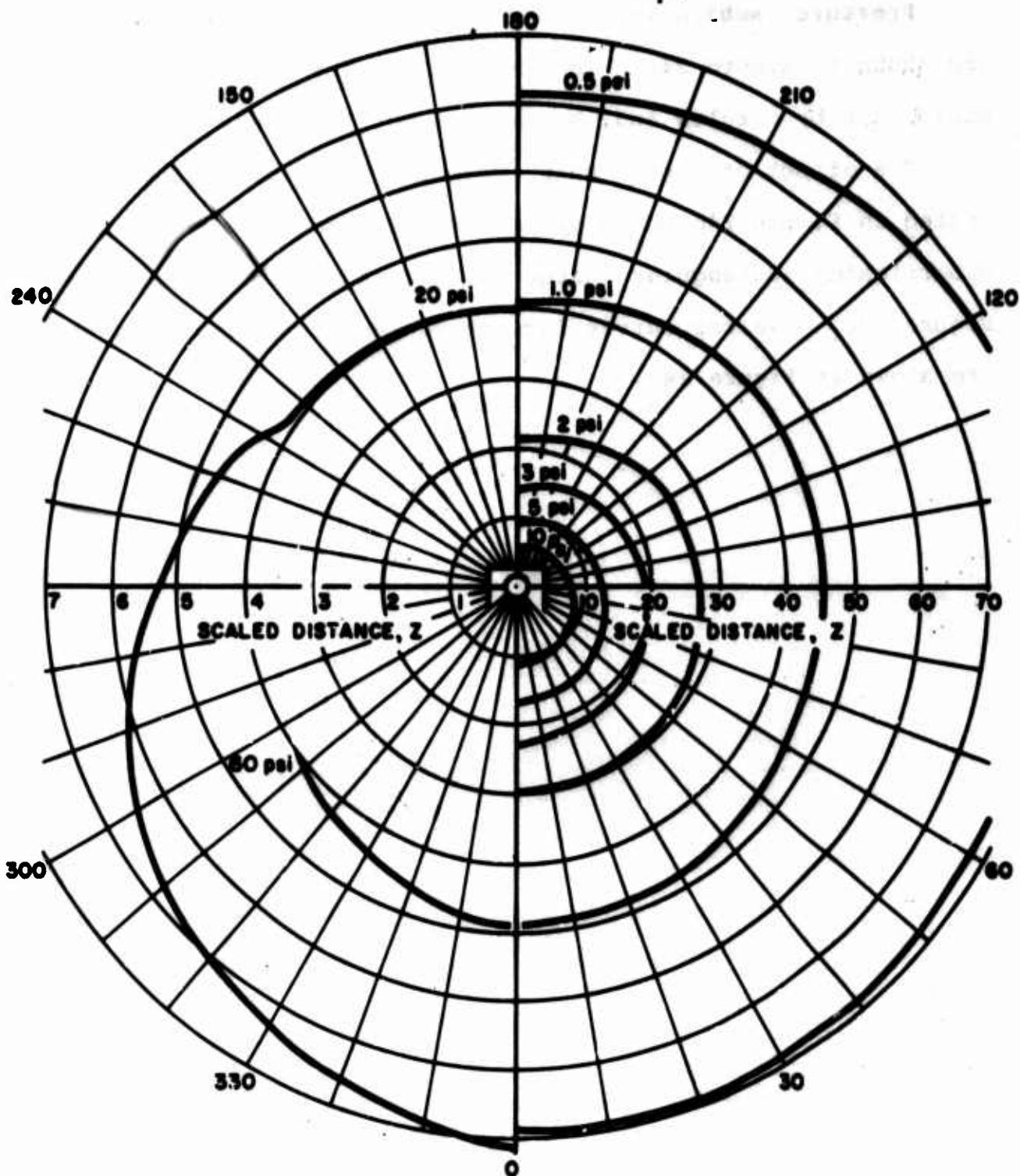
higher than that for the corresponding unbarricaded charge while the pressures out the side and the back are lower. For large ranges, the pressures approach those of the unbarricaded charge.

The pressure-distance relations for a bare rectangular charge with the same weight are shown in Figure 23b. When compared with the corresponding result for a hemispherical charge, there is a region where the pressures out the front and side of the charge decrease quite rapidly. An explanation for this is that the model initially assumes that the pressure waves propagate in directions perpendicular to each of the charge faces. Thus, rarefaction waves that originate at the corners of the charge will travel parallel to the faces as the main pressure wave travels out. When the rarefaction wave reaches the point directly out from the center of a charge face, a further decrease in pressure could be expected. However, this phenomenon needs more study and as more data become available, the appropriate coefficients in the computer program should be changed.

The combined charge geometry and barricade effects are shown in Figure 23c together with the experimental results from "BIG PAPA" as compiled in Figure 27 of Reference 1. The correlation between the "BIG PAPA" tests and the predicted pressure distribution out the back of the barricade ($\theta = 180^\circ$) is not very satisfactory. However, until test results for the effects of geometry on the pressure from large scale charges become available, the program is forced to use the data from the limited range of charge sizes used in Reference 4.

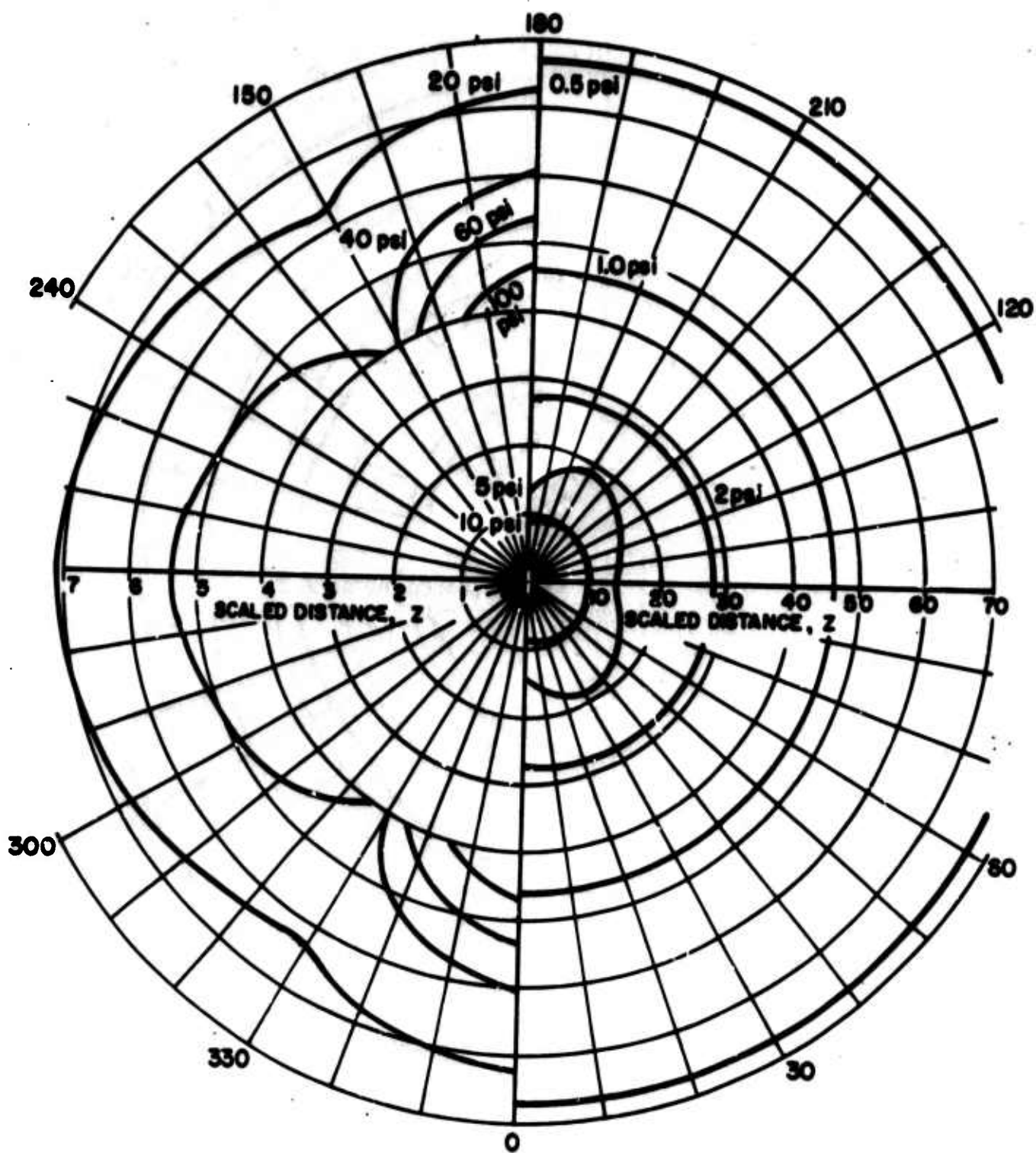
Pressure isobars for a bare hemispherical barricaded charge are shown in Figure 24a. The isobars for the unbarricaded charge would just be circles and, hence, are not included.

The effect of charge shape geometry is dramatically illustrated in Figure 24b which gives the pressure isobars for an unbarricaded rectangular charge for the same case illustrated in Figure 23b. Similar curves for the rectangular barricaded charge are shown in Figure 24c.



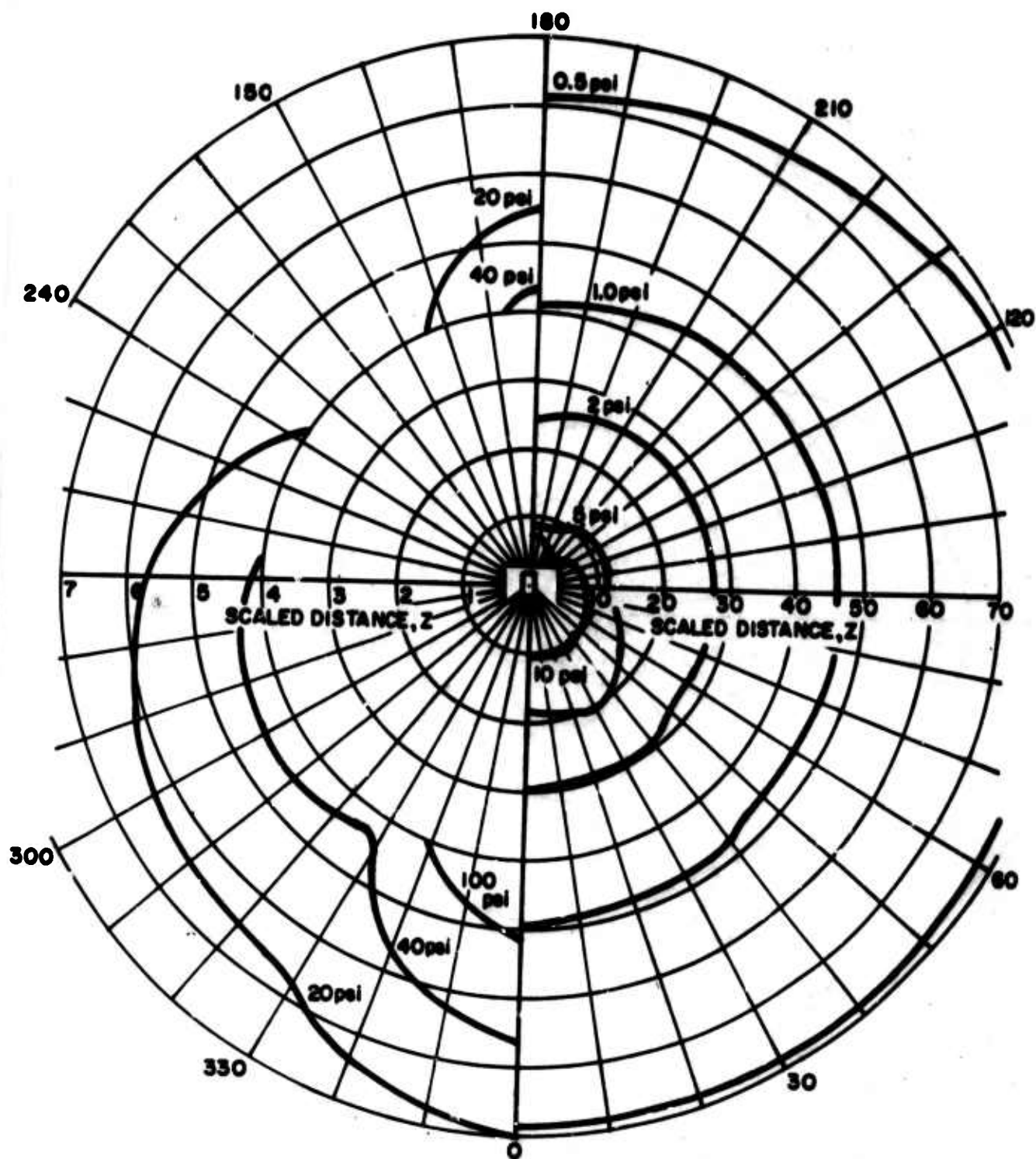
(a) Hemispherical Barricaded Charge

Figure 24. Pressure Isobars for Various Charge
and Barricade Combinations



(b) Rectangular Unbarricaded Charge

Figure 24. (Continued)



(c) Rectangular Barricaded Charge

Figure 24. (Continued)

3. FRAGMENT DISTRIBUTIONS

To illustrate the type of data that can be obtained from this portion of the program, the bomb parameters given in Figure 9 were used in conjunction with the stack of bombs considered in Part 2 of this Section. In addition, the following information was assumed:

- a. The front of the bomb was oriented at an angle of 270° counterclockwise from the front of the barricade ($\theta_B = 270^\circ$)
- b. Each bomb had a gross weight of 1500 lbs.
- c. Each bomb contained 750 lbs. of TNT
- d. There were 333 bombs in the stack, and
- e. The number of effective bombs was 266.

It should be emphasized that the bomb characteristics outlined above are purely fictional because of security reasons so that it will not be possible to compare results with experimental data.

Typical fragment trajectories associated with these bomb characteristics are shown in Figure 25. This particular set of curves was computed using a 10 degree increment for beta. These trajectories indicate that fragments ejected by the bomb for approximately $5^\circ < \beta < 50^\circ$ will impact at ranges furthest from the bomb; thus, a high density of fragments is to be expected at these impact points. However, because of air

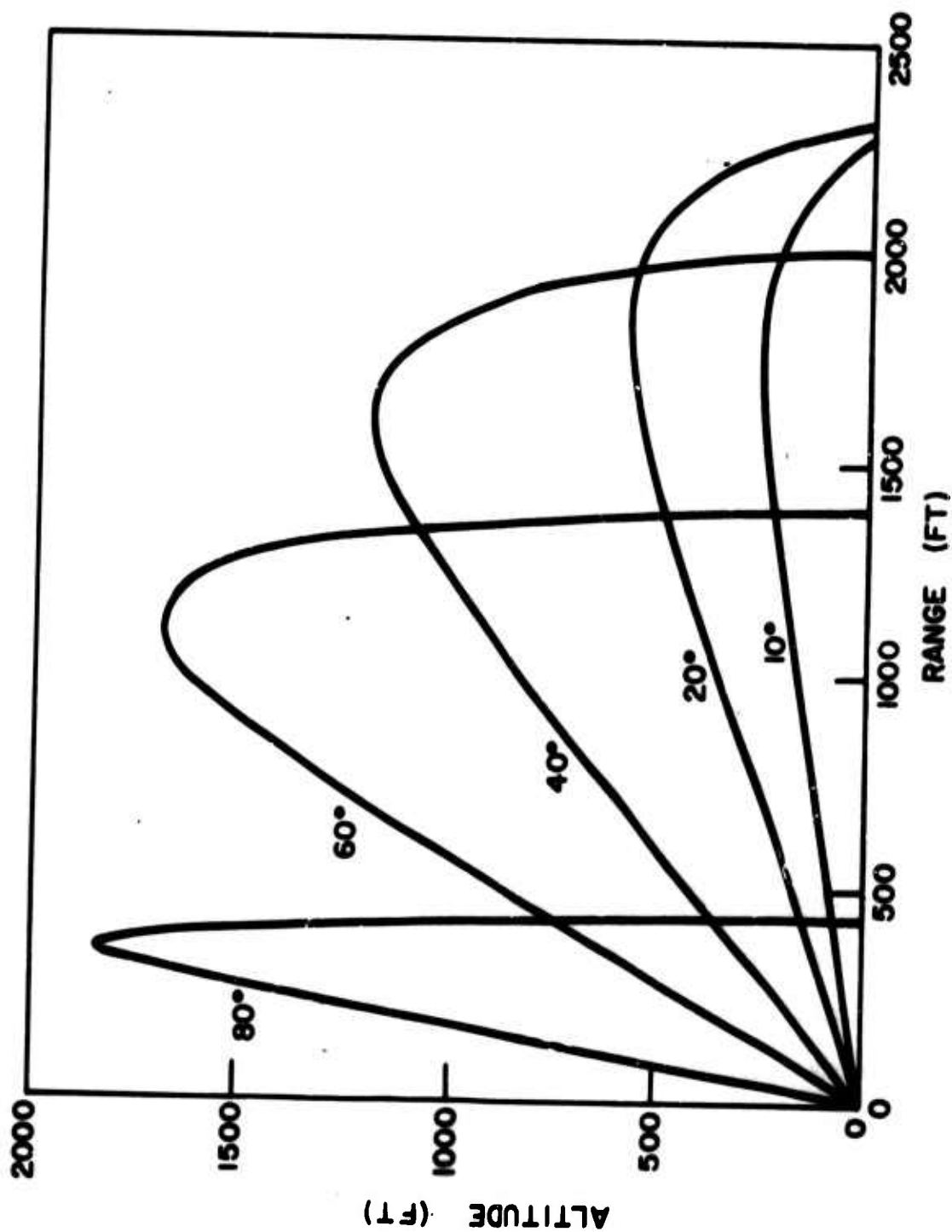


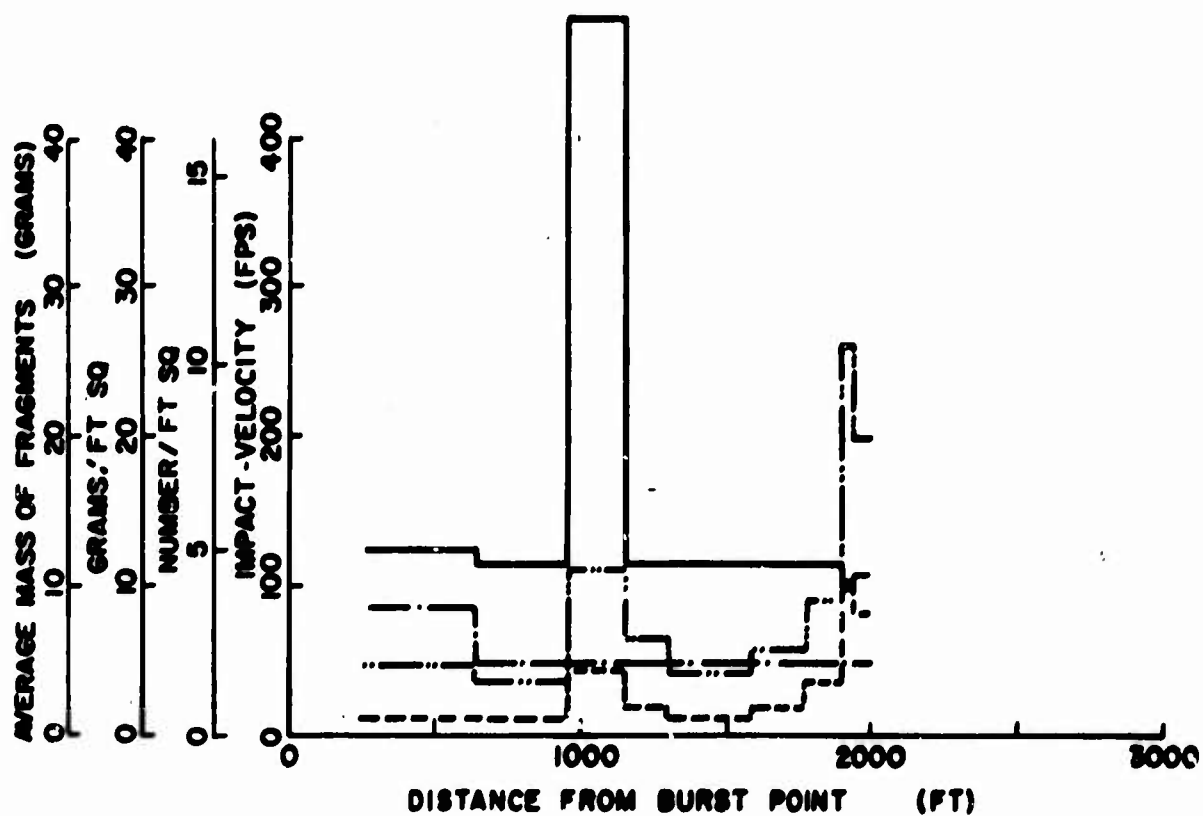
Figure 25. Typical Fragment Trajectories for a Fixed Value of Azimuth Angle and Incremental Departure Angles

friction, the impact velocity is relatively low.

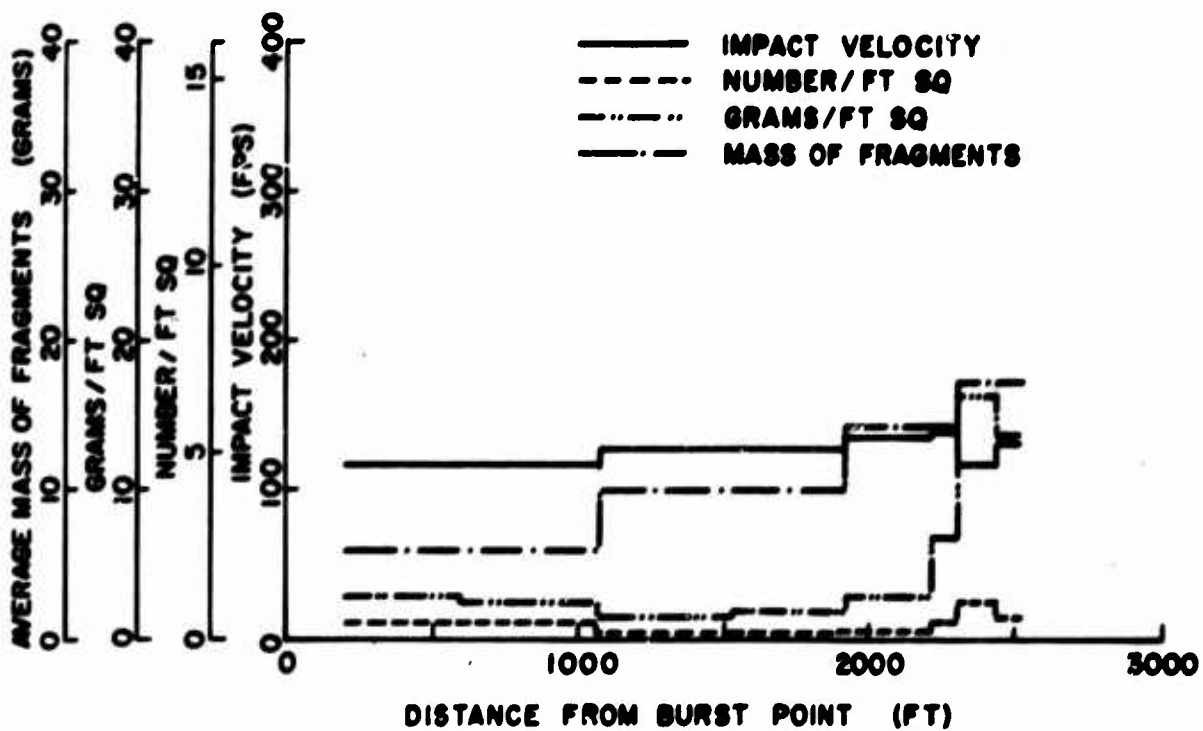
Impact conditions versus range at selected azimuth angles are shown in Figure 26. These curves appear as piece-wise lines of constant value because of the averaging techniques used in the program. By decreasing the increment in β , the changes would not be nearly as abrupt and hence, would be more realistic. All diagrams indicate a high fragment density at large ranges.

In Figure 26a, the presence of the large impact velocity is due to the absence of a barricade wall at that azimuth angle. Fragments ejected approximately parallel to the ground strike the ground much sooner than do those with a larger departure angle β and hence, these large impact velocities are to be expected.

Figures 26b, 26c, and 26d show the variation in impact conditions around the stack for representative values of the azimuth angle. For similar directions of propagation from the barricade, the impact conditions are different in Figures 26e and 26f because of the different fragmentation properties of the bomb in these directions.

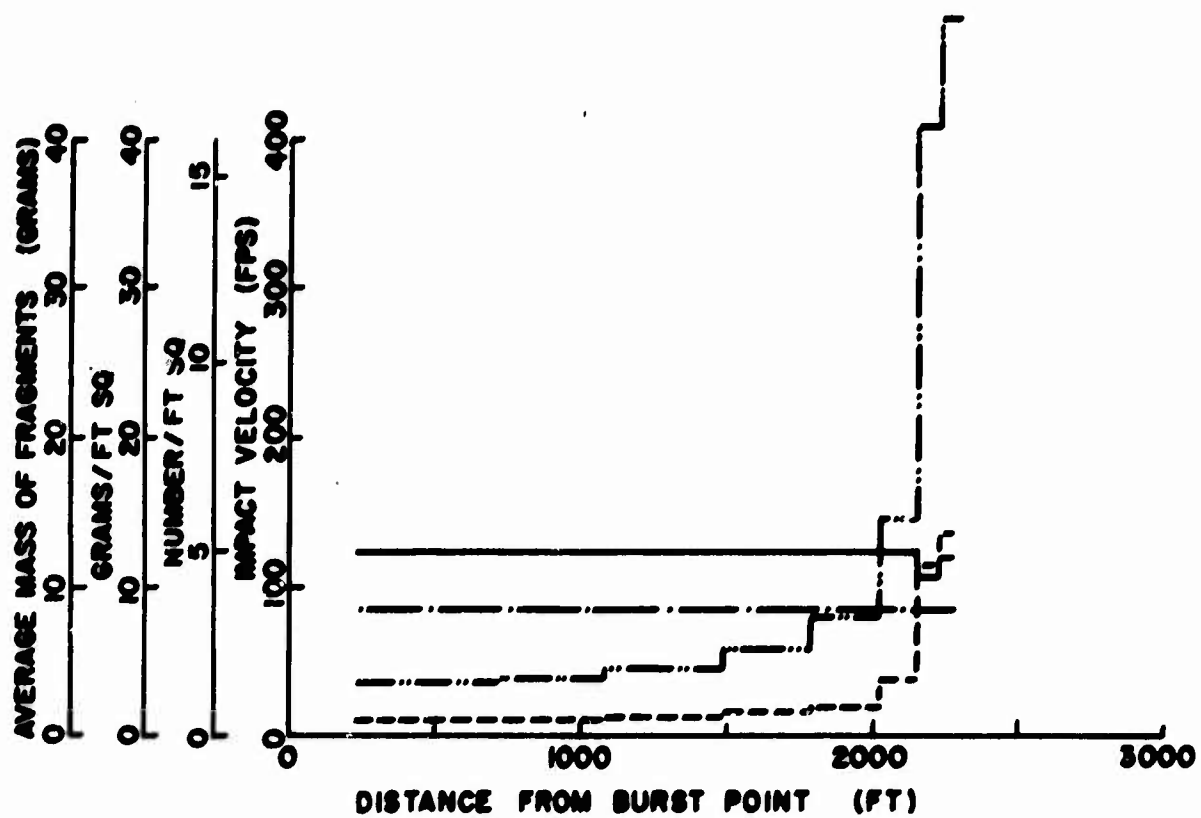


(a) AZIMUTH ANGLE = 0°

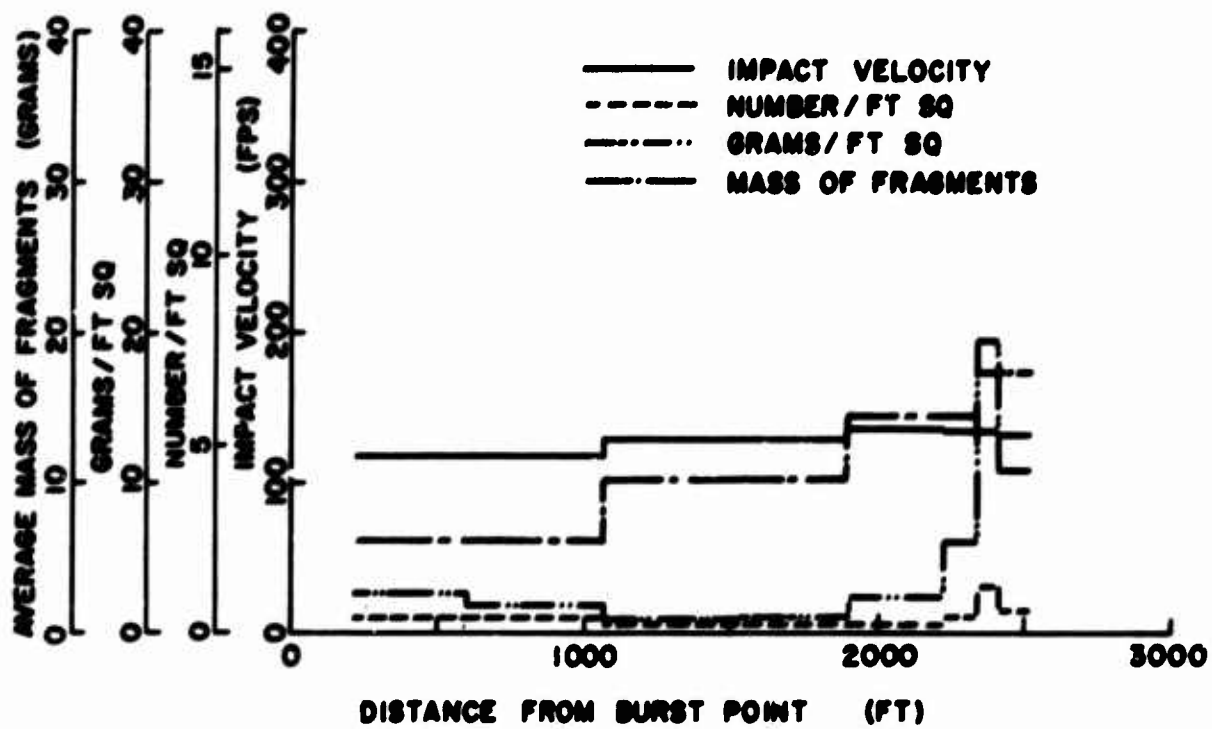


(b) AZIMUTH ANGLE = 100°

Figure 26. Impact Conditions versus Range at Selected Azimuth Angles for Sample Problem

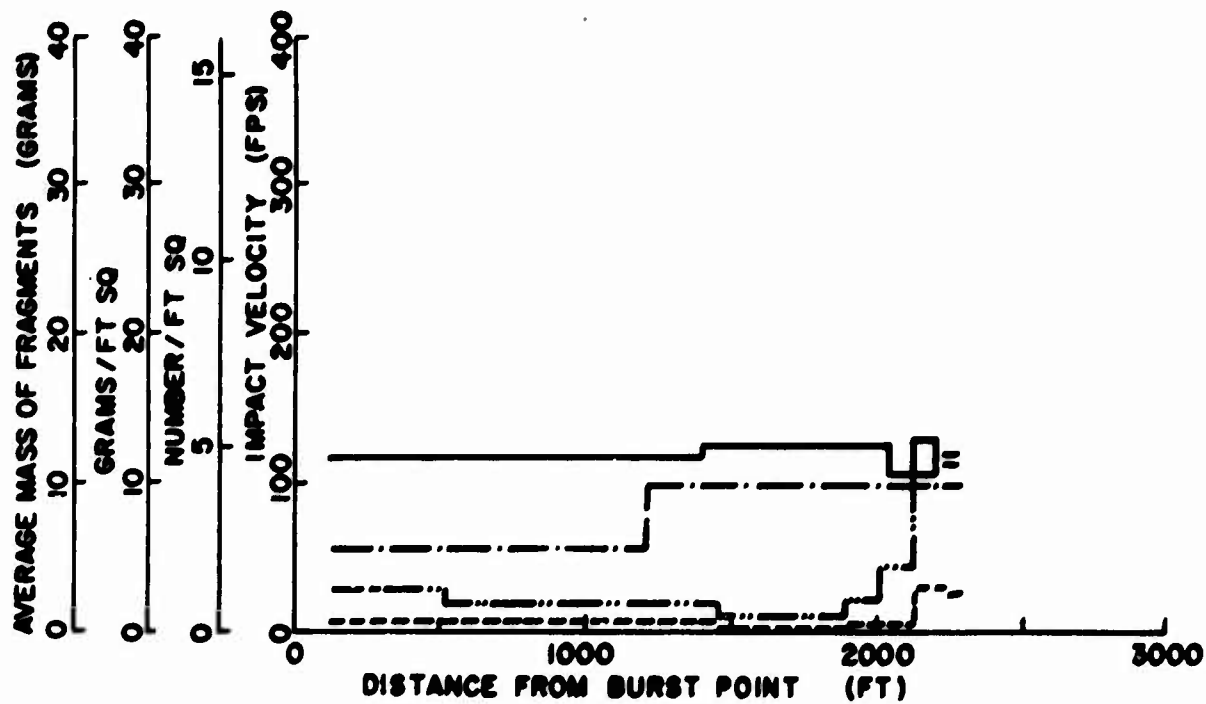


(c) AZIMUTH ANGLE = 180°

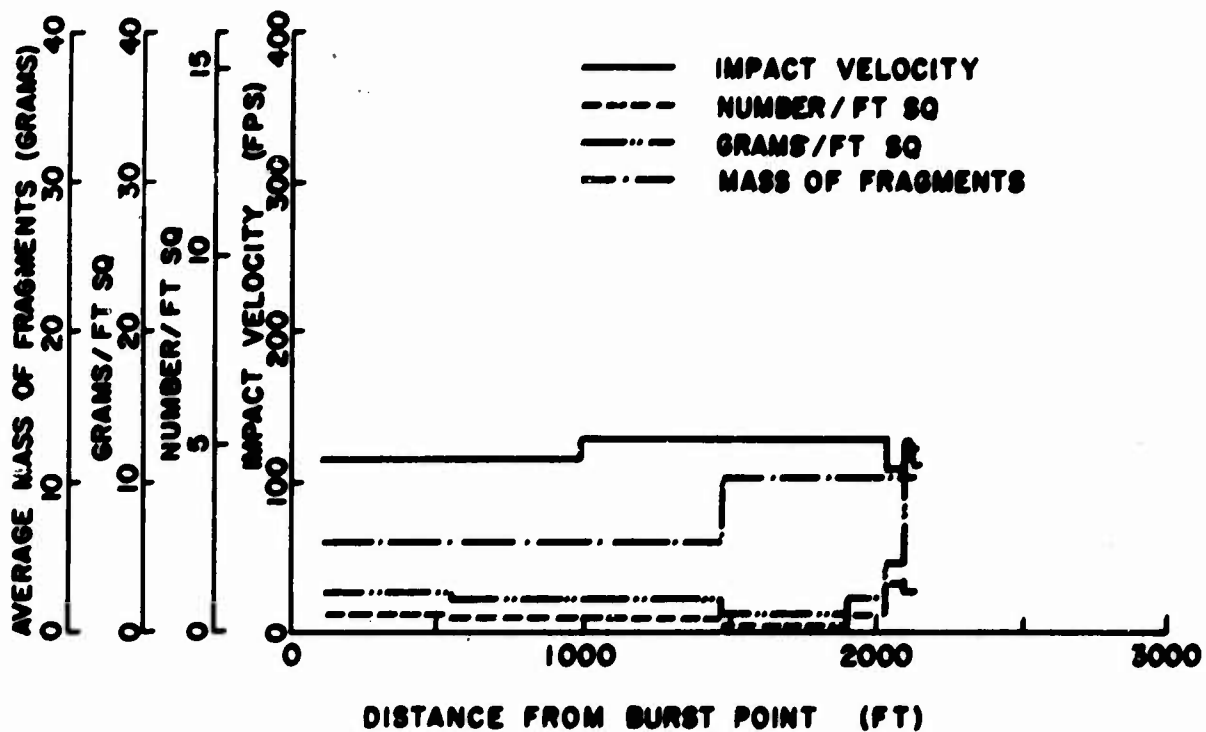


(d) AZIMUTH ANGLE = 280°

Figure 26. (Continued)



(e) AZIMUTH ANGLE = 140°



(f) AZIMUTH ANGLE = 220°

Figure 26. (Continued)

4. APPARENT CRATER AND EJECTA DIMENSIONS

The apparent radius and depth of craters in soil according to the theory of Section IV and the computer program described in Appendix III is shown in Figure 27 for a range of 10 to 500 tons of TNT. It is evident from the figure that the apparent crater radius and depth (70 ft. and 21 ft., respectively) associated with a 100 ton TNT hemispherical shot at the Suffield Experimental Station have been used as the reference parameters for this program. In addition, the following values have been assumed:

- a. The dissipation ratio $E_s^D = 0.3$,
- b. The ejecta parameter $\hat{\beta} = 3.1$, and
- c. For the range of charge sizes 10 to 500 tons of TNT,
 $\zeta = 0.3$ and $W_L = 500$ tons.

These resultant curves of Figure 27 show significant variations from scaling laws which would be represented by straight-line relationships on this plot for both apparent radius and apparent depth. Because of the attempt to include fundamental quantities in the theory, these curves should predict apparent crater dimensions more accurately than the curves associated with scaling laws. Of more importance, the parameters E_s^D and ζ can be changed if more data warrant such an adjustment. Furthermore, the effect of charge size is included in the theory and changes in shape can be accounted for by adjusting W_L .

Strictly speaking, the predicted results are applicable only for the earth media associated with the reference shot where

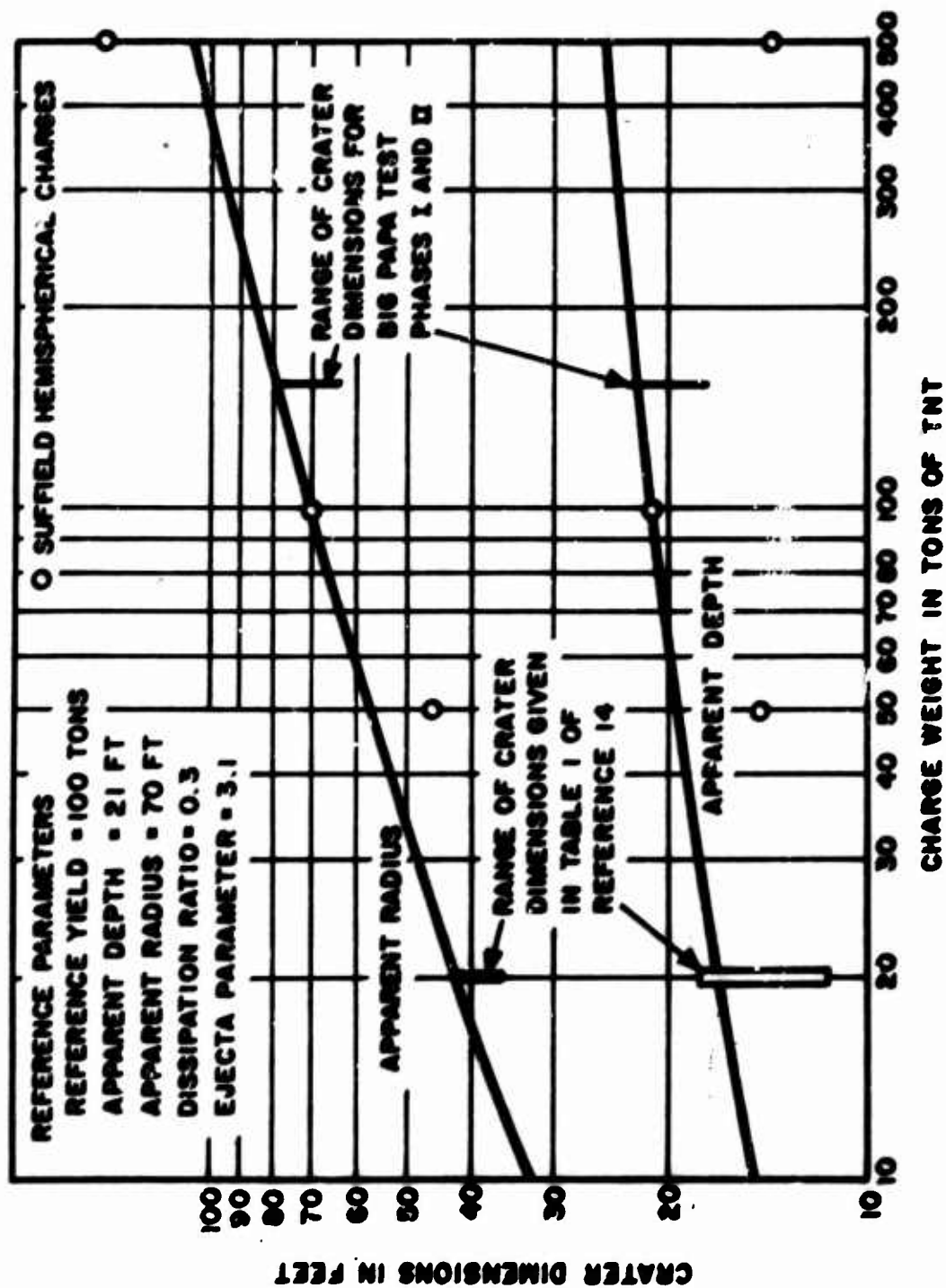


Figure 27. Apparent Crater Dimensions in Soil versus Charge Weight

the soil, a silty clay, had a weight density of 94 lb./ft.³ However, for easy reference, results from shots that may have been in a slightly different soil are also included in the figure. It is assumed that bomb stacks can be replaced by a bare charge with the equivalent amount of TNT as far as crater dimensions are concerned. Thus, some of the "BIG PAPA" test results are also included in Figure 27.

The depth of ejecta can be obtained from Figure 28 where the ejecta depth to apparent crater depth ratio is plotted as a function of the ratio of distance from the crater center (at the surface) to the apparent radius for various values of the ejecta parameter $\hat{\beta}$. Hence, to obtain the depth for a particular location, the apparent radius and depth and $\hat{\beta}$ must be known. When the earth media is soil, a value of 3.1 is used for $\hat{\beta}$.

For the type of rock encountered in the Sailor Hat test, the weight density was 190 lb./ft.³ A hemispherical charge of 500 tons of TNT produced a crater with an apparent radius of 79 ft. and an apparent depth of 38 ft. Results for hemispherical charges of other sizes are shown in Figure 29 together with the predicted values of $\hat{\beta}$ and the dissipation ratio.

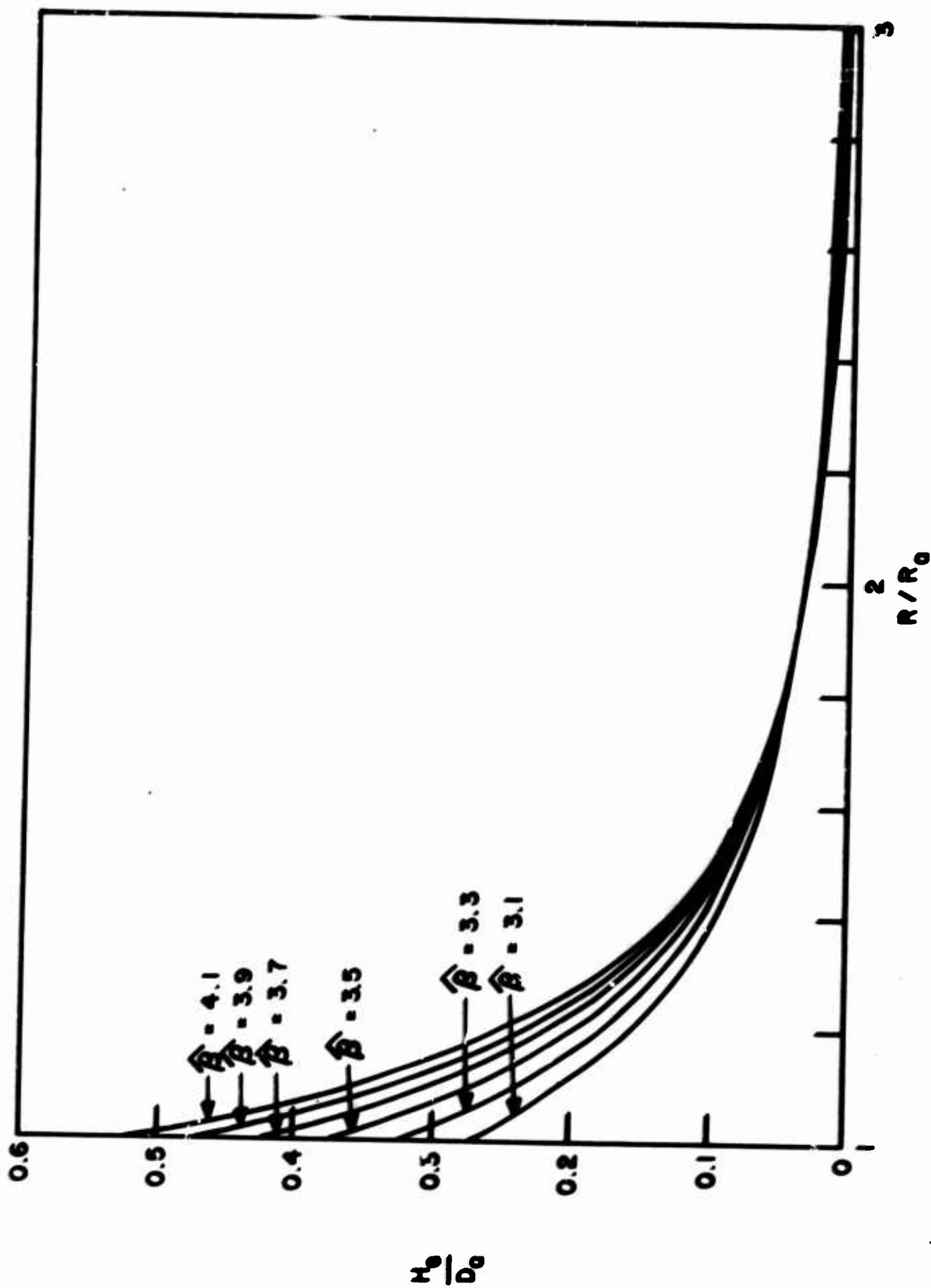


Figure 28. Non-dimensional Ejecta Shapes as a Function of Earth Media Parameter $\hat{\beta}$

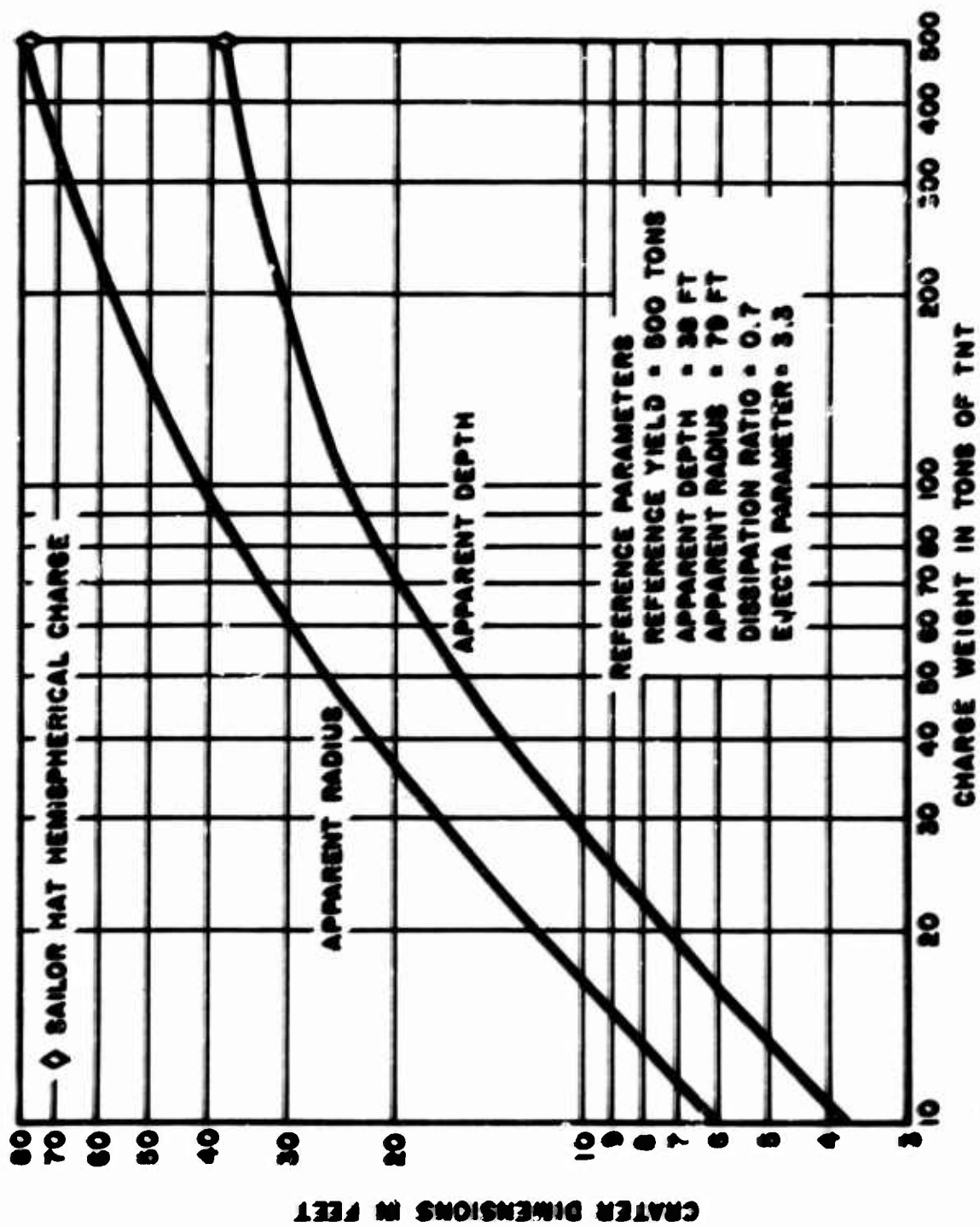


Figure 29. Apparent Crater Dimensions in Basalt Rock versus Charge Weight

5. SUMMARY

Representative sets of curves have been given based on the computer programs and the theory of the previous sections. For given charge size and shape and barricade dimensions, the programs yield the following information:

- a. Pressure versus range and impulse versus range for various azimuth angles,
- b. Pressure isobars,
- c. Impact velocity, number of fragments/ft.², average fragment mass as a function of range and azimuth angle,
- d. Apparent crater radius and depth as a function of charge yield and shape, and earth media, and
- e. Ejecta depth as a function of apparent radius and depth, and earth media.

Normally, using the computer programs for a given set of input data will be the most convenient method for design purposes. However, if a given situation occurs repeatedly, then it would be more convenient to construct a set of curves similar to those illustrated in this Section.

SECTION VI

RECOMMENDED INVESTIGATIONS

1. INTRODUCTION

During the course of this project it became apparent that a large amount of important information was not available. On the other hand, there were certain areas such as cratering in soil for which a great deal of data had been gathered. This section outlines the experimental data that would be necessary to corroborate a complete theoretical model that could be used with some degree of confidence. The requirements for data have been listed in the same order as the topics were covered in this report. It is rather obvious, however, that more than one type of data could be gathered from one test.

In addition to experimental data, the overall problem of safely storing bombs suggests a corresponding analytical study in linear programming where such factors as cost, time and safety are the limiting parameters. It is believed that such a study would be extremely useful to the Air Force and accordingly, a brief outline of the approach is given.

2. PRESSURE AND IMPULSE DATA

a. Single Bombs

Because the shape of a bomb is significantly different from that of a spherical or hemispherical charge, peak overpressure and impulse data should be obtained at various angles of azimuth and distance for bombs resting on the surface of the earth. Furthermore, the confining effect of the bomb casing should be investigated by obtaining data for bombs with the same amount of charge but with different case thicknesses. Intuitively, one might expect the initial value and the rate of decay with distance of the peak overpressure to increase as the casing thickness is increased. However, whether or not this is true, the extent of the variation should be investigated both analytically and experimentally.

b. Bomb Stacks

Similar pressure and impulse measurements should be made for bomb stacks. Tests should be conducted with the following sequences: (1) Stacks with similar shapes but with different sizes, and (2) Stacks with the same number of bombs but with different shapes.

Such a program would determine whether the confining effect of several bombs tends to increase the initial values of the peak overpressure above that expected for the amount

of explosive present or whether a slight time difference in detonation of the individual bombs results in a lowering of the expected value. Obtaining values for the unit impulse is also extremely important.

A side benefit of these results might be the preference for a particular stack shape and size based on pressure and impulse limitations rather than stacking convenience.

c. Barricades

Very little pressure and impulse data appear to be available for the region immediately outside the barricade. For a given stack size and geometry, a series of tests should be conducted for barricades with various dimensions. Significant differences could be expected close to the barricade but for regions farther away, the results should approach those of the unbarricaded stack.

3. FRAGMENT DATA

There appears to be sufficient data on the fragment sizes, number of fragments and initial velocities of fragments for individual bombs. One aspect that could be handled simultaneously with the pressure data of the previous section is the acquisition of information concerning the distribution and impact velocities of fragments from bomb stacks of various sizes and shapes. These data would yield essential information concerning interaction effects and hence, whether or not the simplified theory of Section III is adequate. If the theory associated with the fragment trajectories is fairly accurate, then the effect of barricades can be predicted quite confidently and hence a special experimental program considering barricades is not warranted in this connection.

4. CRATER DATA

A vast number of cratering programs have been conducted for bare hemispherical and spherical charges but predicting crater dimensions with the use of scaling laws is not completely satisfactory. Examples of unexpected crater sizes include 500 ton shots of the Suffield Experimental Station and of "Operation Sailor Hat". It is believed that the level of the underground water table may have affected the results of the first shot mentioned above. The variation from the normal crater shape of the latter shot may be due to the type of rock at that particular location.

In light of the large amount of crater data available it does not seem advisable at this point to conduct more tests of the same type until there exists a better understanding of the effects of the various parameters that describe the earth media. However, in connection with this program, a number of tests do seem advisable.

One of these is concerned with the effect of charge shape on the crater dimensions. For example, for the same earth media and the same charge weight, a series of shots should be conducted in which the charge shape is varied. Typical examples would be rectangular, cubical, and triangular shapes.

Another series could involve the use of stacked bombs, again for one earth media. Such tests would illustrate the interaction effects of bombs and the effect of stack size and

shape. Furthermore, tests of this kind could lead to comparisons with the results of bare charges of the type mentioned above. According to the theory developed in Section IV the shape with the lowest center of mass will produce the largest crater and the basic hypothesis behind this theory should be checked.

Also of considerable interest is the effect of barricade size on crater dimensions. Experimental data in this area would be very useful for both theoretical and immediate practical use.

5. OPTIMIZATION OF STORAGE AREAS

In developing a munitions storage area, several factors must be taken into consideration. These include the cost and availability of land, possible methods of stacking bombs and building barricades, degree of safety in connection with fragments, cratering, peak overpressure and impulse, the time available to stack the bombs, and so on. With the experimental and theoretical methods available it appears that it might be possible to develop a computer program that would optimize a given parameter under a given set of circumstances.

One example could be the following: Suppose that a particular amount of munitions had to be stored on a given area and the safety requirement was primarily one of ensuring that no fragments landed outside this area. The problem would then entail finding the appropriate combination of munition stack shapes, dimensions and distributions of the stacks together with barricade shapes and dimensions that would satisfy this requirement. If more than one combination was adequate, then additional factors such as cost and time could be included in the program.

Another possibility would be to determine the "safest" possible arrangement that could be developed in a given amount of time. To determine the safety aspect, degrees of importance would have to be attached to each of the hazardous factors associated with a munitions dump. Likewise, the parameters

describing the time to stack the bombs would be included and by using the principles of linear programming, the optimum configuration would be predicted.

Since there are a large number of possibilities that could be of interest to the Air Force, it would seem that the possibility of developing a program that could predict optimal arrangements should be considered. The results could be significant improvements in safety, time and cost.

SECTION VII

CONCLUSIONS

Analytical models and subsequent computer codes have been developed for typical large quantity high-explosive detonations of those types of conventional munitions stored by the Air Force in aboveground barricaded modules. The parameters that are predicted from these codes include peak overpressure, unit impulse, distributions of fragment impact coordinates and velocities, crater dimensions and depth of ejecta. The geometries of the bomb stack and the barricade are taken into account as well as the type of earth media. Results of large-scale tests had indicated that the burning time of detonation and the point of initiation of a bomb stack were not too significant and, hence, these parameters are not considered.

Because of the lack of wide-scale, definitive experimental data, it was considered more appropriate to use a combination of analysis and empirical curve fitting in connection with the models. Accordingly, some engineering judgement must be used with the computer codes since there may be some disparity in the values of parameters for an actual problem and the values that are used in the model.

Every effort was made to use the latest experimental and theoretical results. However, there are several areas in which

vital gaps in fundamental knowledge exist. A limited program of testing is necessary to obtain this information and the types of tests that should be run are listed in this report.

Of more immediate benefit to the Air Force is the development of computer codes which would optimize a base layout under a given set of conditions. Such codes could produce the safest possible combination of munition modules for a given area or, alternatively, the cost and amount of time required to construct a safe munitions storage area could be minimized.

The codes that have been developed should be extremely helpful in predicting the danger zone for a munitions storage area. In selecting models that yield governing parameters with respect to the safety of a base, a conservative approach has been adopted. Thus, as better technical information becomes available, these codes can be adjusted and better use of available ground space for storing munitions can be made.

APPENDIX I
BLAST EFFECT PROGRAM

1. FORTRAN PROGRAM DESCRIPTION

The computer code described in this Appendix follows the development of Section II on Blast Effects. The computations are performed in the same order as outlined in the development of the analytical model whenever possible. A flow chart for the computer code is included in Appendix I-2. A printout of the computer code is included in Appendix I-4.

The first section of the computer code establishes (a) the coefficients for the various polynomials needed during the computations, (b) overpressures to be solved in isobar option, and (c) degrees of different polynomials required in computations, and (d) lists format statements.

Each problem to be run requires a control card to be read. If more data are to be read, the control card indicates the amount to be read and the variables that are to be reassigned. The control card also sets the parameters describing bomb stack and barricade and indicates azimuth angles for which the pressure and impulse are desired. After the control card is read, the heading on the output is printed to record the parameters of the problem for future reference.

The solution is obtained by computing the pressure and positive impulse for a bare hemispherical charge of TNT at the

scaled distances $Z = 4.0, 4.1, 4.2, \dots, 480, 490, 500$. The incremental steps of Z are as follows:

$$\Delta Z = 0.10 \text{ for } 4.0 \leq Z < 5.0$$

$$\Delta Z = 0.20 \text{ for } 5.0 \leq Z < 10.0$$

$$\Delta Z = 1.0 \text{ for } 10.0 \leq Z < 50.0$$

$$\Delta Z = 2.0 \text{ for } 50.0 \leq Z < 100.0$$

$$\Delta Z = 10.0 \text{ for } 100.0 \leq Z < 500.0$$

Pressure and impulse are evaluated from the polynomials previously fitted to the $\ln P - \ln Z$ and $\ln I - \ln Z$ representations of Figure 8. If a scaled distance Z falls within the confine of the barricade the pressure and impulse are not computed. This evaluation of pressure and impulse for a bare hemispherical charge is completed previous to statement number 335 in the code.

If the charge of TNT is rectangular rather than hemispherical, the effects of the change in geometry are evaluated according to the theory of Section II-4. The evaluation of effect of charge geometry on pressure and impulse distributions is performed between statements 335 and 460 in the computer code. The procedure used is to evaluate the pressure ratio and positive impulse ratio perpendicular to the faces of the rectangle and along a line through the center of mass of the charge and the corner where the faces of the rectangle meet. The values of pressure ratio and positive impulse ratio for angles other than those perpendicular to the faces and through the corners are obtained by linear interpolation between the

two known values that span the angle. Later in the program the pressure ratio and positive impulse ratio will be used to multiply the corresponding values of pressure and positive impulse at a distance Z for a bare hemispherical charge to obtain pressure and positive impulse for the rectangular charge being modeled.

If a barricade is present around a stack of TNT, its shape is assumed to be rectangular with the center of mass of the stack of TNT very nearly corresponding to the geometric center of the barricade in the plan view. The walls of the barricade are assumed to be parallel to the sides of the stack of TNT.

The effect of the presence of a barricade is evaluated according to the theory of Section II-5 between statement numbers 465 and 555 in the computer code. The pressure and positive impulse ratios (BP and BI), that will be multiplied by the pressure and positive impulse for a bare hemispherical charge at the corresponding distances, can be evaluated directly for directions perpendicular to the walls of the barricade and out the rear corner of the barricade by interpolation from the input data. The ratios for angles not equal to those just mentioned are obtained by a linear interpolation scheme from the values obtained for direction perpendicular to the walls and out the rear corner of the barricade. It is only necessary to determine which two known directions the angle θ lies between to choose the proper data for interpolation.

This concludes the evaluation of the pressure and positive impulse ratios that are needed to estimate the effective change

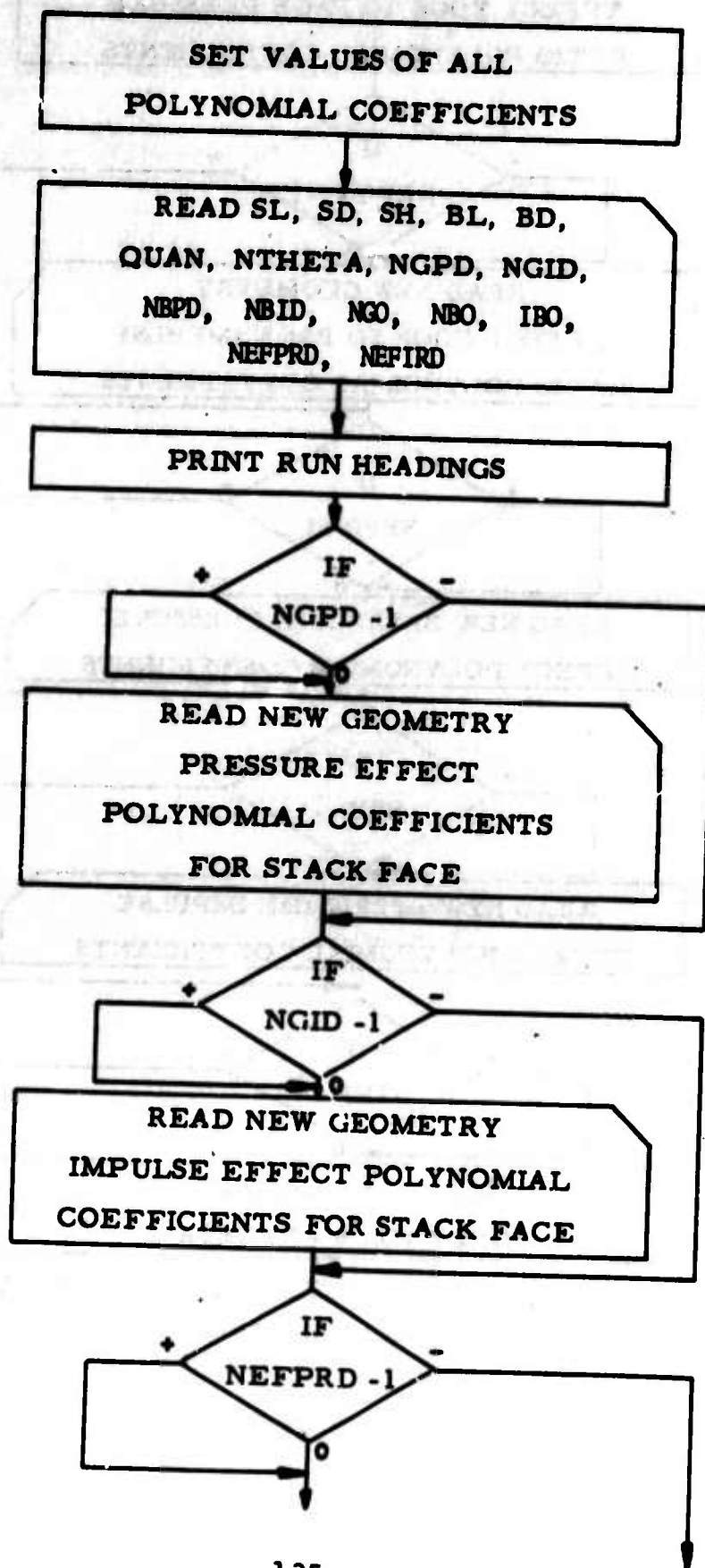
in pressure and impulse distribution produced by the change in charge geometry from a hemispherical to a rectangular shape and the presence of a barricade around the charge.

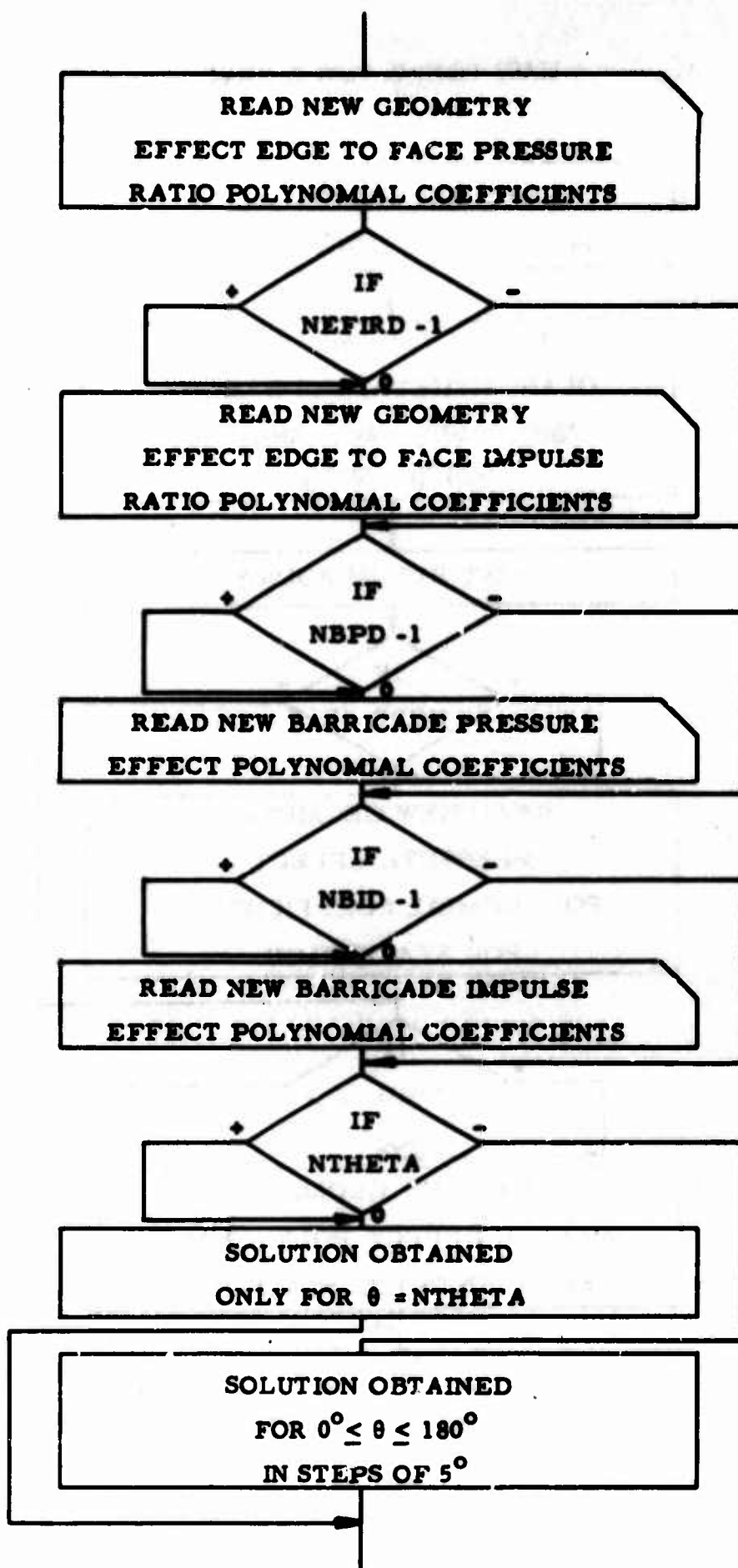
To obtain the estimated pressure and positive impulse distributions, it is only necessary to multiply the pressure and positive impulse distributions for the bare hemispherical charge by the appropriate pressure and impulse ratios as derived above. These computations are performed and printed out in the computer code between statements 560 and 565.

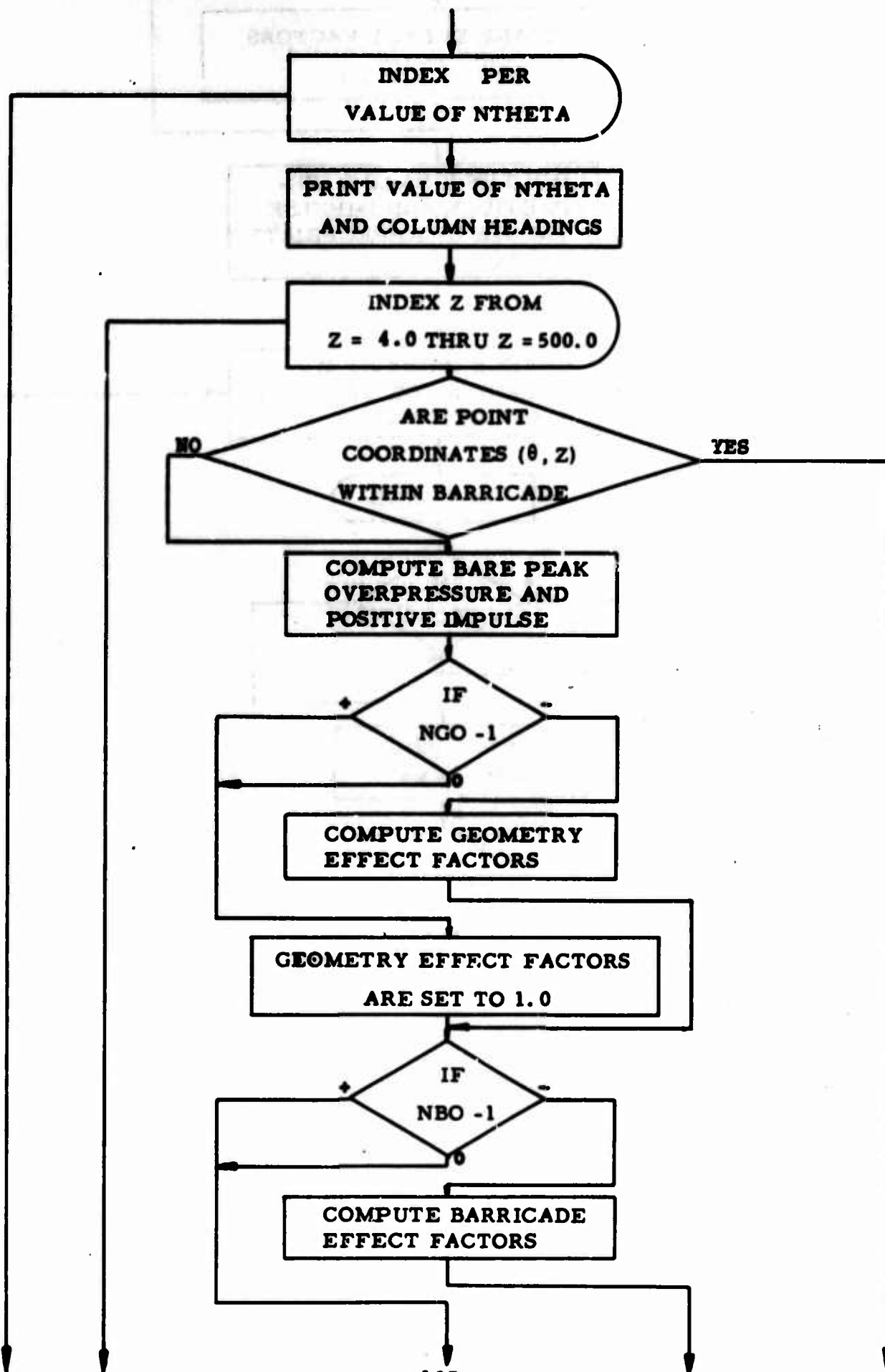
If isobar plots are desired to indicate distance to lines of constant pressure the statements 630 through 680 are executed by setting IBO = 0, otherwise IBO = 1. The distances to points of equal pressure along lines separated by 5° increments are evaluated by starting at the extreme distance ($Z = 500$) and comparing expected pressure to isobar pressure for decreasing values of Z until expected pressure is greater than the isobar pressure. When the points on either side of the distance where isobar pressure equals expected pressure are found, the distance to the isobar pressure is found by linear interpolation. If the expected pressure along a direction of propagation does not attain the isobar pressure, the symbol PNR is printed instead of the distance. This indicates that the isobar pressure is not reached along that direction. This method of evaluation continues until all the distances to the isobar pressures have been evaluated along the directions indicated.

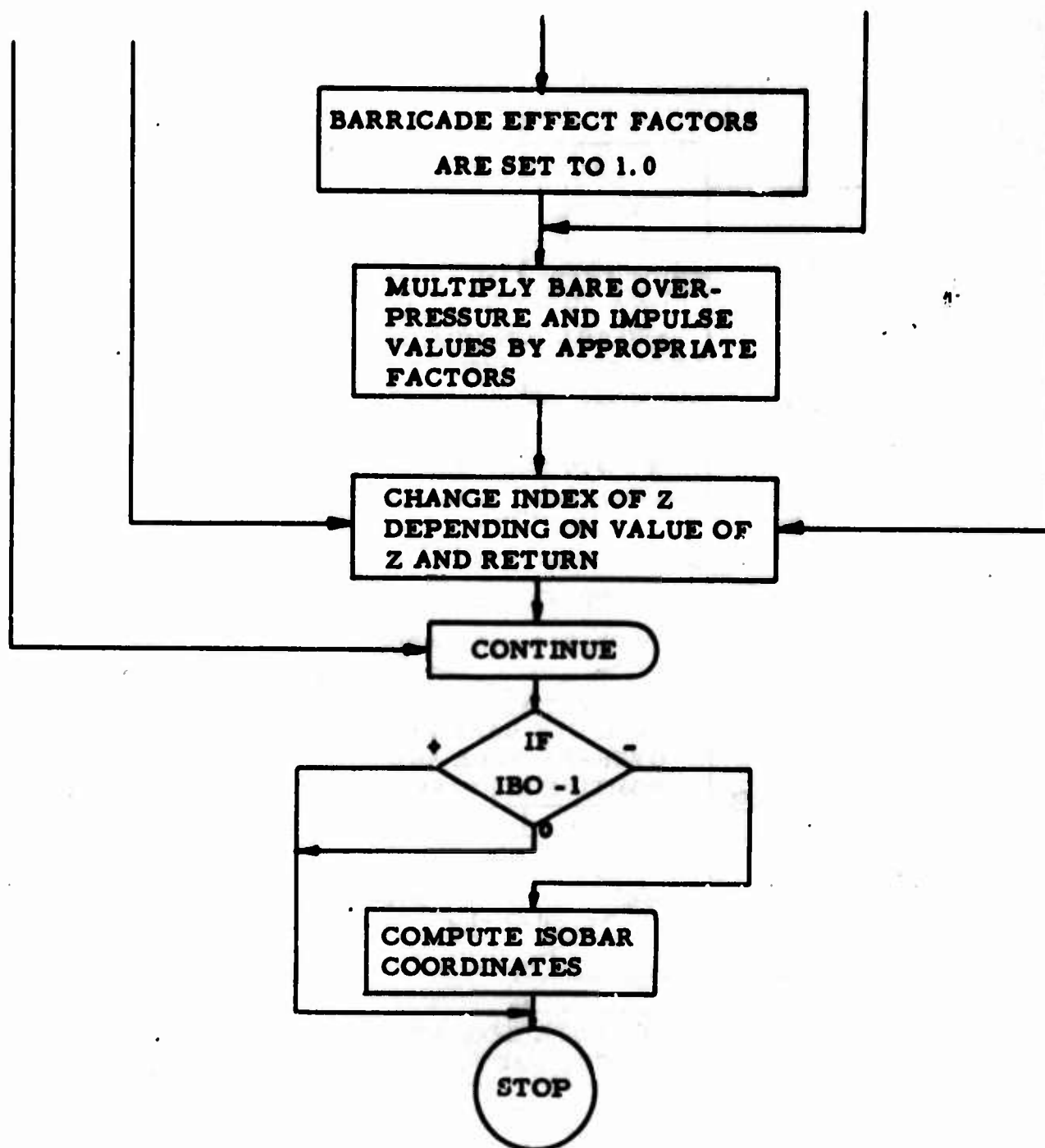
2.

BLAST PROGRAM FLOW DIAGRAM









3. LIST OF VARIABLES TO COMPUTER PROGRAM FOR ANALYTICAL
BLAST EFFECT MODEL

A(I,J)	Polynomial Coefficients to determine rectangular charge face pressure to spherical charge pressure ratio.
AFPR	Average pressure at a distance Z perpendicular to faces of charge.
AFSIR	Average impulse at a distance Z perpendicular to faces of charge.
ARD	Face/Area ratio from front of bomb stack.
ARL	Face/Area ratio from side of bomb stack.
A1, A2, A3	Polynomial to evaluate pressure out from faces of stack at a distance Z from the blast.
B(I,J)	Polynomial Coefficients to determine rectangular charge face impulse to spherical charge pressure.
BD	Barricade depth, ft.
BI	Factor to multiply by bare hemispherical charge impulse to include effect of barricade.
BIE(I,J)	Polynomial coefficients to determine effect of a barricade on blast impulse distribution.
BL	Barricade length, ft.
BOP(I)	Overpressure from a bare hemispherical unbarricaded charge.
BP	Factor to multiply by bare hemispherical charge pressure to include effect of barricade.
BPE(I,J)	Polynomial coefficients to determine effect of a barricade on blast pressure distribution.

BPHI1	Angle whose tangent is (BL/BD) .
BPHI2	Angle whose tangent is $(BL/-BD)$.
BSOPI(I)	Impulse from a bare hemispherical unbarricaded charge.
BTHETA	Angle through corner of barricade.
B1, B2, B3	Polynomial to evaluate impulse out from faces of stack at a distance Z from the blast.
C	Polynomial for pressure from a bare hemispherical charge evaluated at a distance Z.
CRQ	Cube root of charge yield, $\text{lbs.}^{1/3}$.
D	Polynomial for impulse from a bare hemispherical charge evaluated at a distance Z.
EFIR(I)	Polynomial coefficients to determine edge to average face impulse ratio versus Z.
EFPR(I)	Polynomial coefficients to determine edge to average face pressure ratio versus Z.
FG	Factor to multiply by bare hemispherical charge pressure to include effect of rectangular charge.
POP(I,J)	Pressure expected due to changes in geometry and (OR) barricade.
FSOPI(I,J)	Impulse expected due to changes in geometry and (OR) barricade.
GI	Factor to multiply by bare hemispherical charge impulse to include effect of rectangular charge.
GTHETA	Complementary angle of NTHETA.
IBO	Isobar Option, IBO = 0 solves for isobars, IBO = 1 no isobars computed.
M	Number of increments of Z within a certain range of Z values.

NBID	Number of cards to be read containing new barricade impulse data.
NBO	Barricade option, NBO = 0 rectangular barricade is included, NBO = 1 solves for no barricade.
NBPD	Number of cards to be read containing new barricade pressure data.
NDBIE	Degree of polynomial for estimating barricade impulse effect.
NDBPE	Degree of polynomial for estimating barricade pressure effect.
NDEFIR	Degree of polynomial for estimating edge/face impulse ratio.
NDEFPR	Degree of polynomial for estimating edge/face pressure ratio.
NDEG	Integer number of 5-degree increments in NTHETA.
NDGID	Degree of polynomial for rectangular charge face impulse to spherical charge impulse.
NDGPD	Degree of polynomial for rectangular charge face pressure ratio to spherical charge pressure.
NDOP	Degree of polynomial for pressure versus z for a spherical charge.
NDSOPI	Degree of polynomial for impulse versus z for a spherical charge.
NEFIRD	Number of cards to be read containing new edge/face impulse ratio data.
NEFPRD	Number of cards to be read containing new edge/face pressure ratio data.
NGID	Number of cards to be read containing new geometry impulse data.
NGO	Geometry option, NGO = 1 solves for hemispherical charge, NGO = 0 solves for rectangular charge.

NGPD	Number of cards to be read containing new geometry pressure data.
NTHETA	Angle at which pressure and impulse desired, degrees.
NUM	Indexing variable.
OP(I)	Polynomial coefficients to determine pressure versus Z for a hemispherical charge.
P(I)	Isobar pressures to be solved, psi.
PP	Isobar pressure to be solved, psi.
PRE	Polynomial to evaluate pressure out from corner of stack at a distance Z from the blast.
P2, P1	Known pressures at distances Z2, Z1, psi.
QUAN	Equivalent amount of TNT in stack, lbs.
RAD	Number degrees per radian.
RD(I,J)	Distance from blast, ft.
RR	Converts fixed point variable to floating point.
S	Size of increments of Z within a certain range of Z' values, $\text{ft}/(\text{lbs.}^{1/3})$.
SD	Stack depth, ft.
SH	Stack height, ft.
SIRE	Polynomial to evaluate impulse out from corner of stack at a distance Z from the blast.
SL	Stack length, ft.
SOPI(I)	Polynomial coefficients to determine impulse versus Z for a hemispherical charge.
TB	Same angle as NTHETA.
TBI	Temporary barricade impulse ratio.

TBC	Temporary barricade pressure ratio.
THETA	Degrees, Angle NETHETA in degrees.
THETAE	Angle measured from front of bomb stack to corner of bomb stack.
TN	NTHETA - 90°.
TR	NTHETA /90.
X	Log Z.
Z	Scaled distance from blast, $\text{ft}/(\text{lbs.}^{1/3})$.
ZC	Absolute value of $Z \cos(\text{theta})$, $\text{ft}/(\text{lbs.}^{1/3})$.
ZI(J,N)	Scaled distance to isobar pressure PP, $\text{ft}/(\text{lbs.}^{1/3})$.
ZQ	Value of $Z \sin(\text{theat})$, $\text{ft}/(\text{lbs.}^{1/3})$.
ZR(I,J)	Scaled distance at a particular angle and range.
Z2, Z1	Known distances that span distance to isobar pressure, $\text{ft}/(\text{lbs.}^{1/3})$.

4. PRINTOUT OF PROGRAM FOR ANALYTICAL BLAST EFFECT MODEL

```

PROGRAM BLAST (INPUT,OUTPUT)
000041 DIMENSION SOP(195),SSOP(195),POP(37,195),PSOP(37,195),A(3,9),P(3
1,9),OP(11),SOPI(11),OPE(4,11),OIE(4,11),PO(37,195),ZR(37,195),P(22
2),ZI(37,22),WZ(37),EPFR(9),EFIR(9)

C
C ISOBAR PRESSURES TO BE SOUGHT IN ISOBAR OPTION
000041 DATA P(1),P(2),P(3),P(4),P(5),P(6),P(7),P(8),P(9),P(10),P(11),P(12
1),P(13),P(14),P(15),P(16),P(17),P(18),P(19),P(20),P(21),P(22)/1000
2.,000.,400.,400.,200.,100.,60.,60.,40.,20.,10.,9.,8.,7.,6.,5.,4.,3
3.,2.,1.,0.5,0.10/

C
C COEFFICIENTS OF CONSTANTS A,B,C VS Z TO DETERMINE RECTANGULAR
C CHARGE FACE PRESSURE TO SPHERICAL CHARGE PRESSURE RATIO
000041 DATA AT(1,1),AT(1,2),AT(1,3),AT(1,4),AT(1,5),AT(1,6),AT(2,1),AT(2,2),AT(2,3
1),AT(2,4),AT(2,5),AT(2,6),AT(3,1),AT(3,2),AT(3,3),AT(3,4),AT(3,5),AT(3,6)/
219.91981,-5.492211,0.564339,-0.026578, 0.971890E-03,-0.461177E-05,
3-161.9033,47.41294,-4.988612,0.233948,-0.510784E-02,0.414069E-04,
4272.6186,-77.46474,0.204485,-0.324434,0.046964E-02,-0.690800E-04/

C
C COEFFICIENTS OF CONSTANTS D,E,F VS Z TO DETERMINE RECTANGULAR
C CHARGE FACE IMPULSE TO SPHERICAL CHARGE IMPULSE RATIO
000041 DATA DT(1,1),DT(1,2),DT(1,3),DT(1,4),DT(1,5),DT(1,6),DT(2,1),DT(2,2),DT(2,3
1),DT(2,4),DT(2,5),DT(2,6),DT(3,1),DT(3,2),DT(3,3),DT(3,4),DT(3,5),DT(3,6)/
25.90688,-1.71385,0.21629,-0.1166E-01,0.274063E-03,-0.83524E-05,
3-1.30157,4.67308,-0.99579,0.64936E-01,-0.10676E-02,0.15110E-04,
4-0.16859,-4.92241,1.43765,-.99908E-01,0.26624E-02,-0.24519E-04/

C
C COEFFICIENTS TO DETERMINE EDGE TO AVERAGE FACE PRESSURE RATIO VS Z
000041 DATA EFPR(1),EFPR(2),EFPR(3),EFPR(4),EFPR(5),EFPR(6),EFPR(7)/-0.94
142047E-01,-0.3279577E-02,0.3172664E-01,-0.2700099E-02,0.0060014E-0
26,-0.1294399E-05,0.7819624E-08/

C
C COEFFICIENTS TO DETERMINE EDGE TO AVERAGE FACE IMPULSE RATIO VS Z
000041 DATA EFIR(1),EFIR(2),EFIR(3),EFIR(4),EFIR(5)/-0.3879756E+00,0.2953
176E+00,-0.1519496E-01,0.2943603E-03,-0.1946049E-05/

C
C NUMBER OFC PER RADIAN, DEGREE OF POLYNOMIALS FOR - (A,B,C), (D,E,F),
C PRESSURE VS Z, IMPULSE VS Z, BARRICADE PRESSURE EFFPOT, BARRICADE
C IMPULSE EFFECT, EDGE/FACE PRESSURE RATIO, EDGE/FACE IMPULSE RATIO
000041 DATA RAD,NOCP,NOCTD,NOOP,NOSOP,NOAPE,NOAIE,NOEFPR,NOEFIR/57.2957
1795,6,6,10,9,5,5,7,5/

C
C COEFFICIENTS TO DETERMINE PRESSURE VS Z FOR HEMISPHERICAL CHARGE
000041 DATA OP(1),OP(2),OP(3),OP(4),OP(5),OP(7),OP(6),OP(8),OP(9),OP(10)/
10.7036810E+01,-1.1653724E+01,-0.2916401E+00,-0.1137714E+00,0.30104
205E-01,-0.2796470E-01,0.5035194E-01,0.5957960E-02,-0.5100014E-03,0
3.1795565E-04/

C
C COEFFICIENTS TO DETERMINE SCALED IMPULSE VS Z FOR HEMISPHERICAL CHARGE
000041 DATA SOPI(1),SOPI(2),SOPI(3),SOPI(4),SOPI(5),SOPI(6),SOPI(7),SOPI(
18)/0.3129244E+01,-0.1295979E+00,0.4112452E+00,-0.7687394E+00,0.496
29224E+00,-1.1804197E+00,0.2805658E-01,-0.1791242E-02/

C
C COEFFICIENTS TO DETERMINE BARRICADE EFFECT ON BLAST PRESSURE

```



```

C          PRESSURE RATIO DATA
C          NEFIRD = NUMBER OF CARDS TO BE READ IN CONTAINING NEW EDGE/FACE
C          IMPULSE RATIO DATA
C
000044      199 READ 18 , SL,SD,SH,SL,SD,QUAN,NTHETA,NGPD,NGID,NBPD,NBID,NGO,MRO,
          1 180,NEFPRD,NEFIRD
C
C          PRINT HEADING ON OUTPUT
C
000107      IF ( NGO - 1 ) 200,203,203
000112      200 PRINT 134
000115      PRINT 130 , SL,SD
000126      GO TO 206
000129      203 PRINT 138
000130      206 IF (NBO - 1 ) 209,212,212
000133      209 PRINT 137
000136      PRINT 131 , SL, SD
000145      GO TO 215
000146      212 PRINT 139
000151      215 PRINT 4 , QUAN
000156      CRQ = QUAN ** 0.3333333
C
C----- THETA IS THE ANGLE MEASURED FROM FRONT OF BOMB STACK TO CORNER
C          OF BOMB STACK.  THETA = ATAN2(SL,SD)*RAD
C
000161      THETA = ATAN2(SL,SD) * RAD
C
C          NEW GEOMETRY PRESSURE DATA OPTION, NGPD IS THE NUMBER OF CARDS
C          TO BE READ CONTAINING NEW DATA
C
000164      IF (NGPD - 1) 221,218,218
000167      218 NGPD = NGPD + 1
000171      READ 13 , (A(1,I),A(2,I),A(3,I), I = 1,NGPD)
000212      NNGPD = NGPD
C
C          NEW GEOMETRY IMPULSE DATA OPTION, NGID IS THE NUMBER OF CARDS TO BE
C          READ CONTAINING NEW DATA
C
000214      221 IF (NGID - 1) 227,224,224
000217      224 NGID = NGID + 1
000221      READ 13 , (B(1,I),B(2,I),B(3,I), I = 1,NGID)
000242      NNGID = NGID
C
C          NEW EDGE/FACE PRESSURE RATIO DATA OPTION, NEFPRD IS THE NUMBER OF
C          CARDS TO BE READ CONTAINING NEW DATA
C
000244      227 IF (NEFPRD - 1) 233,230,230
000247      230 NEFPRD = NEFPRD + 1
000251      READ 31 , (EFPR(I), I = 1,NEFPRD)
000263      NDEFPR = NEFPRD
C
C          NEW EDGE/FACE IMPULSE RATIO DATA OPTION, NEFIRD IS THE NUMBER OF
C          CARDS TO BE READ CONTAINING NEW DATA
C
000265      233 IF (NEFIRD - 1) 239,236,236
000270      236 NEFIRD = NEFIRD + 1
000272      READ 31 , (EFIR(I), I = 1,NEFIRD)
000304      NDEFIR = NEFIRD
C
C          NEW BARRICADE PRESSURE DATA OPTION, NBPD IS THE NUMBER OF CARDS TO
C          BE READ CONTAINING NEW DATA
C
000306      239 IF (NBPD - 1) 245,242,242
000311      242 NBPD = NBPD + 1

```



```

000313      READ 10 , (BPE(1,I),BPF(2,I),BPE(3,I),BPE(4,I),I=1,NB)
000337      NOBPE = NBPD
000341      265 00 250 J=1,NOBPE
000343      00 250 I=1,4
000351      250 BPE(I,J) = BPE(I,J)
C
C      NEW BARRICADE IMPULSE DATA OPTION, NBID IS THE NUMBER OF CARDS
C      TO BE READ CONTAINING NEW DATA
C
000356      IF (NBID - 1) 260,255,255
000360      255 NBID = NBID + 1
000362      READ 10 , (BIE(1,I),BIE(2,I),BIE(3,I),BIE(4,I),I=1,NBID)
000406      NOBIE = NBID
000410      260 IF (NTHETA) 265,270,270
000412      265 MNM = 181
000413      JN = 1
000414      GO TO 275
000415      270 MNM = NTHETA + 2
000417      JN = NTHETA + 1
C
C      MAJOR LOOP- INDEXES THETA FROM 0-180 IF NTHETA READ IN IS -1
C      WHEN NTHETA IS POS. PROGRAM SOLVES ONLY FOR ANGLE NTHETA
C      THETA IS TO BE READ INTO PROGRAM IN DEGREES BETWEEN 0 AND 180
C
C      TO REDUCE THE AMOUNT OF PRINTOUT WHEN SOLVING FOR PRESSURE ISOGARS
C      SUPPRESS PRINT OF PRESSURES AND IMPULSES VS.DIST.FOR ANGLES
C      COMPUTED BY MAKING STMTS.280,295,299,563, AND 620 INTO
C      NONEXECUTABLE COMMENTS AND ADD A CARD 620 CONTINUE
C
000421      275 00 625 MN = JN,MNM,5
000423      NTHETA = MN - 1
C
C      SET FIRST INCREMENT OF DISTANCE
C
000424      Z = 3.9
000426      280 PRINT 100 , NTHETA
C
C      PRINT OUTPUT COLUMN HEADINGS
C
000433      285 PRINT 102
000436      290 PRINT 103
C
C----- ESTABLISH CONSTANTS FOR PROBLEM PARAMETERS
C
000441      M = 11
000442      S = 0.10
000444      BPHI1=ATAN2(BL,90)* RAD
000447      BPHI2=ATAN2(BL,-90)* RAD
000455      NUM = 0
000455      RR = NTHETA
000457      THETA = RR / RAD
000460      NDEG = NTHETA / 5 + 1
C
C      SECOND MAJOR LOOP - INDEXES Z FROM 4 - 500
C
000464      300 DO 565 K=1,M
C
000470      NUM = NUM + 1
000471      BP = 0.0
000471      FG = 0.0
000472      GI = 0.0
000472      AI = 0.0
000473      SOP(NUM) = 0.0
000473      SSOPI(NUM) = 0.0

```

```

000474      FOP(NDEG,NUM) = 0.0
000475      FSOPI(NDEG,NUM) = 0.0
      C
000477      Z = Z + S
000501      ZR(NDEG,NUM) = Z
000504      ZC = Z * COS(THETA)
000506      ZQ = Z * SIN(THETA)
000510      ZQ = Z * SIN(THETA)
      C
000513      IF (OPHI1 - NYHETA) 309,315,315
000517      309 IF (OPHI2 - NYHETA) 315,315,315
000522      315 IF (ZQ - ((R1/2.0)/CRQ)) 565,320,320
000527      315 IF (ZC - ((R1/2.0)/CRQ)) 565,320,320
      C
000533      320 X = ALOG(Z)
000535      C = 0.0
      C
      C      BARE PRESSURE VS Z
      C
000537      DO 325 J = 1,NOOP
000543      N = J - 1
000546      325 C = C + OP(J) * (X ** N)
000553      SOP(NUM) = EXP(C)
000556      D = 0.0
      C
      C      BARE IMPULSE VS Z
      C
000557      DO 330 J = 1,NOFOPI
000563      N = J - 1
000566      330 D = D + SOPI(J) * (X ** N)
000573      FSOPI(NUM) = EXP(D) * CRQ
      C
      C      BEGINNING OF GEOMETRY OPTION - IF DESIRED, THIS SECTION SOLVES FOR
      C      TWO FACTORS PG AND GI WHICH ARE TO BE MULTIPLIED BY BARE PRESSURE
      C      AND BARE IMPULSE TO INCLUDE RECTANGULAR CHARGE GEOMETRY EFFECT
      C
000577      IF (NGO - 1) 335,460,460
000602      335 IF (Z - 50.0) 340,460,460
      C
000607      340 ARL = 1.0/((SO/SH) + 2.0 + 2.0*(SO/SL))
000614      ARD = 1.0/((SL/SH) + 2.0 + 2.0*(SL/SO))
000621      A1 = 0.0
000622      A2 = 0.0
000623      A3 = 0.0
      C
000624      B1 = 0.0
000624      B2 = 0.0
000625      B3 = 0.0
      C
000625      PRE = 0.0
000626      SIDE = 0.0
      C
      C----- EVALUATE POLYNOMIALS A1, A2, A3, AT Z
      C
000627      DO 400 L = 1,NOGPD
000640      J = L - 1
      C
000641      A1 = A(1,L) * (Z ** J) + A1
000646      A2 = A(2,L) * (Z ** J) + A2
000653      400 A3 = A(3,L) * (Z ** J) + A3
      C
000662      IF (Z.LE.26.0) GO TO 405

```

```

C
000664      A1 = 1.0
000665      A2 = 0.
000666      A3 = 0.
C
C
C----- EVALUATE PRESSURE RATIO AT Z PERPENDICULAR TO WIDTH OF STACK
C              AND PERPENDICULAR TO DEPTH OF STACK
C
000667      405 PRL = A1 + A2 * ARL + A3*(ARL** 2)
000674      PRD = A1 + A2 * ARD + A3*(ARD** 2)
C
C----- EVALUATE POLYNOMIAL COEFFICIENTS Q1,Q2,AND Q3 AT Z
C
000701      DO 410 L = 1,NDGID
000712      J = L - 1
000713      Q1 = Q(1,L) *(Z ** J) + Q1
000720      Q2 = Q(2,L) *(Z ** J) + Q2
000725      410 Q3 = Q(3,L) *(Z ** J) + Q3
C
000734      IF(Z.LE.26.0) GO TO 415
C
000736      Q1 = 1.0
000737      Q2 = 0.
000740      Q3 = 0.
C
C----- EVALUATE IMPULSE RATIO AT DIST. Z PERPENDICULAR TO DEPTH AND
C              LENGTH OF STACK
C
000741      415 S1RL = Q1 + Q2 * ARL + Q3 *(ARL ** 2)
000746      S1RD = Q1 + Q2 * ARD + Q3 *(ARD ** 2)
C
C----- AVERAGE PRESSURE RATIO
C
000752      AFPR = (PRL + PRD) / 2.0
C
C----- AVERAGE IMPULSE RATIO
C
000755      AFSIR = (S1RL + S1RD) / 2.0
C
C----- SOLVE FOR PRESSURE AND IMPULSE RATIO OUT CORNER OF STACK
C
000760      DO 420 L = 1,NDFFPR
000767      J = L - 1
000770      420 PRE = PRE + EFPR(L) *(Z ** J)
C
000775      IF ( PRE. LT. 0.0 ) PRE = 0.0
000777      IF ( Z. GT. 29.0 ) PRE = 1.0
C
C----- PRESSURE OUT CORNER AT DIST. Z = PRESSURE RATIO*AVG.PRESSURE
C              FROM FACES
C
001003      PRE = PRE * AFPR
C
001005      DO 425 L = 1,NDFFIR
001013      J = L - 1
001014      425 S1RE = S1RE + EFIR(L) *(Z ** J)
C
001021      IF ( S1RE. LT. 0.0 ) S1RE = 0.0
001023      IF ( Z. GT. 37.0 ) S1RE = 1.0
C
C----- IMPULSE OUT CORNER AT DIST. Z = IMPULSE RATIO * AVG IMPULSE
C              FROM FACES
C

```



```

001027      SIRE = SIRE * AFSIR
001030      IF (NTHETA - 90) 435,435,435
001033      430 GTHETA = 180 - NTHETA
001036      60 TO 440
001038      435 GTHETA = NTHETA
C
C----- IF THE ANGLES WHERE THE PRESS. AND IMPULSE ARE DESIRED DO NOT
C      EQUAL THE ANGLE THROUGH THE CORNER OF THE CHARGE, CHOOSE
C      THE PROPER FORMULAE TO INTERPOLATE FOR THE PRESS. AND
C      IMPULSE RATIOS (PG AND PI.)
C
001040      440 IF (GTHETA - THETA) 450,445,455
001043      445 GI = SIRE
001045      PG = PRE
001048      60 TO 465
001051      450 PG = ((GTHETA/THETA) * (PRE - PRL)) + PRL
001054      GI = ((GTHETA/THETA) * (SIRE - SIRL)) + SIRL
001060      60 TO 465
001063      455 PG = (((GTHETA - THETA)/(90.0 - THETA)) * (PRD - PRE)) + PRE
001067      GI = (((GTHETA - THETA)/(90.0 - THETA)) * (SIRD - SIRE)) + SIRE
001072      60 TO 465
001073      460 PG = 1.0
001074      GI = 1.0
C
C      BEGINNING OF BARRICADE OPTION - IF DESIRED, THIS SECTION SOLVES FOR
C      TWO FACTORS BP AND BI WHICH ARE TO BE MULTIPLIED BY BARE PRESSURE
C      AND BARE IMPULSE TO INCLUDE BARRICADE EFFECTS
C
001076      465 IF (NBO - 1) 470,555,555
001101      470 IF (Z - 100.00) 475,555,555
001104      475 IF (NTHETA - 90) 480,480,520
001107      480 THE = NTHETA
001110      TR = THE / 90.0
C
C----- INTERPOLATE BETWEEN KNOWN CURVES FOR THE APPROPRIATE VALUES OF
C      BARRICADE PRESS. EFFECT (BPE) TO EVALUATE THE POLYNOMIAL
C      FOR BARRICADE PRESSURE RATIO (BP)
C
001112      DO 500 J = 1, NBP
001124      L = J - 1
001125      PE = (TR) * (BPE(2,J) - BPE(1,J)) + BPE(1,J)
001130      500 BP = BP + PE * (Z ** L)
C
C----- INTERPOLATE BETWEEN KNOWN CURVES FOR THE APPROPRIATE VALUES OF
C      BARRICADE IMPULSE EFFECT (BIE) TO EVALUATE THE POLYNOMIAL
C      FOR BARRICADE IMPULSE RATIO (BI).
C
001136      DO 505 J = 1, NBI
001147      L = J - 1
001150      EI = (TR) * (BIE(2,J) - BIE(1,J)) + BIE(1,J)
001153      505 BI = BI + EI * (Z ** L)
C
C----- TO INSURE REASONABLE RESULTS GUARANTEE THAT FOR A BARRICADED
C      CHARGE THE RESULTS APPROACH THOSE FOR A UNBARRICADED
C      CHARGE ASYMPTOTICALLY
C
001161      IF (Z.LE.4.5) 510,515
001166      510 TRI = PI
001167      TRP = RP
C
001171      515 IF (TRI.GT.1.0.AND.BI.LT.1.0) BI = 1.0
001202      IF (TRI.LT.1.0.AND.BI.GT.1.0) BI = 1.0
001212      IF (TRP.GT.1.0.AND.BP.LT.1.0) BP = 1.0
001222      IF (TRP.LT.1.0.AND.BP.GT.1.0) BP = 1.0

```



```

001231      C      GO TO 560
      C
      C----- FOLLOWING STATEMENTS TO 555 APPLY FOR THETA GREATER THAN PI/2
001232      520 BTHETA = ATAN(BD/BL) * RAD + 90.
001241      TB = BTHETA
      C
      C----- CHECK LOCATION OF THETA WITH RESPECT TO ANGLE THROUGH CORNER
      C      OF BARRICADE TO DETERMINE APPROPRIATE SET OF EQUATIONS
      C      TO INTERPOLATE FOR EFFECT OF BARRICADE ON PRESS. AND
      C      IMPULSE RATIOS ( BP AND BI )
001242      IF (TB - BTHETA) 525,525,540
      C
001245      525 DO 530 J = 1,NDBPE
001263      L = J - 1
001264      TN = BTHETA - 90
001265      PE = ((TN)/(BTHETA-90.))* (BPE(3,J)-BPE(2,J)) + BPE(2,J)
001271      530 BP = BP + PE * (Z ** L)
      C
001277      DO 535 J = 1,NDBIE
001313      L = J - 1
001314      EI = ((TN)/(BTHETA - 90.))* (BIE(3,J)-BIE(2,J)) + BIE(2,J)
001317      535 BI = BI + EI * (Z ** L)
      C
001325      IF(BI.GE.1.0) BI = 1.0
001330      IF(BP.GE.1.0) BP = 1.0
001333      GO TO 560
      C
001334      540 DO 545 J = 1, NDBPE
001352      L = J - 1
001353      PE = ((TB - BTHETA)/(180. - BTHETA))* (BPE(4,J) - BPE(3,J)) + BPE(
13,J)
001356      545 BP = BP + PE * (Z ** L)
      C
001364      DO 550 J = 1,NDBIE
001401      L = J - 1
001402      EI = ((TB - BTHETA)/(180. - BTHETA))* (BIE(4,J)-BIE(3,J)) + BIE(3,J)
001405      550 BI = BI + EI * (Z ** L)
      C
001413      IF(BI.GE.1.0) BI = 1.0
001416      IF(BP.GE.1.0) BP = 1.0
001421      GO TO 560
      C
001422      555 BI = 1.0
001423      BP = 1.0
      C
      C----- MULTIPLY OVER PRESSURE FOR A BARE HEMISPHERICAL CHARGE BY EFFECTS
      C      OF GEOMETRY (FG) AND BARRICADE (BP) TO OBTAIN THE
      C      PREDICTED VALUE FOR PRESSURE AT DISTANCE Z AND ANGLE
      C      THETA
001431      560 FOP(NDEG,NUM) = BOP(NUM) * BP * FG
      C
      C----- MULTIPLY IMPULSE FOR A BARE HEMISPHERICAL CHARGE BY EFFECTS
      C      OF GEOMETRY (GI) AND BARRICADE (BI) TO OBTAIN THE
      C      PREDICTED VALUE FOR IMPULSE AT DISTANCE Z AND ANGLE
      C      THETA
001433      FSOPI(NDEG,NUM) = BSOPI(NUM) * BI * GI
      C
      C----- CONVERT Z TO FEET
      C

```

```

001436      RD(NDEG,NUM) = ZR(NDEG,NUM) * CRQ
001440      563 PRINT 101, ZR(NDEG,NUM),RDP(NUM),FOP(NDEG,NUM),GSOPI(NUM),FSOPI(NDEG,NUM),RD(NDEG,NUM)
001473      565 CONTINUE
001476      IF (Z - 4.9) 570,575,575
001500      570 N = 40
001501      S = 0.10
001503      GO TO 300
001503      575 IF (Z - 9.9) 580,585,585
001506      580 N = 25
001507      S = 0.20
001511      GO TO 300
001511      585 IF (Z - 49.9) 590,600,610
001514      590 N = 40
001515      S = 1.0
001517      GO TO 300
001517      600 IF (Z - 99.9) 605,610,610
001522      605 N = 25
001523      S = 2.0
001525      GO TO 300
001525      610 IF (Z - 499.9) 615,620,620
001530      615 N = 40
001531      S = 10.0
001533      GO TO 300
001533      620 PRINT 123
001536      625 CONTINUE

```

C
C ISOBAR COORDINATE OPTION - THIS SECTION SOLVES FOR THE Z AT THE
C ANGLES 0 - 180 FOR THE PRESSURES INPUT AS P(N) IN THE DATA
C

```

001541      IF (180 - 1) 630,645,645

```

```

C
001543      630 DO 680 N = 1,22
001545      PP = P(N)
001547      PRINT 155, PP
001554      PRINT 159
001557      PRINT 158

```

```

C
001562      DO 680 J = 1,37
001564      MN = (J - 1) * 5
001566      LL = 142
001567      DO 670 L = 1, 141
001571      LL = LL - 1
001572      IF ( FOP(J,LL) - PP ) 670, 660, 645
001607      645 LLL = LL + 1
001610      Z2 = ZR(J,LLL)
001613      Z1 = ZR(J,LL)
001615      P2 = FOP(J,LLL)
001616      P1 = FOP(J,LL)
001620      ZI(J,N) = ((Z2-Z1) * (P1 - PP)) / (P1-P2) + Z1
001626      GO TO 675
001627      660 ZI(J,N) = ZR(J,L)
001636      GO TO 675
001637      670 CONTINUE
001641      PRINT 156, MN
001644      GO TO 680
001647      675 PRINT 157, MN, ZI(J,N)
001661      680 CONTINUE

```

C
C TO RUN A SINGLE PROBLEM THE FOLLOWING TWO CARDS SHOULD BE
C 645 CALL EXIT
C END
C TO RUN A SERIES OF PROBLEMS THE FOLLOWING THREE CARDS SHOULD BE
C 645 GO TO 199

	C	CALL EXIT
	C	END
001615	605	GO TO 199
001666		CALL EXIT
001667		END

5. INPUT FORMAT

The input to the Blast Program normally is one card (See Figure 30) consisting of the following parameters and control options in their respective order on the input card:

a. SL - F6.2 Format--stack length in feet, measured parallel to the open end of the barricade, or perpendicular to the line for theta (θ) equal to zero degrees (See Figure 31).

b. SD - F6.2 Format--stack depth in feet, measured perpendicular to the open end of the barricade or parallel to the line for theta (θ) equal to zero degrees (See Figure 31).

c. SH - F6.2 Format--stack height in feet.

d. BL - F6.2 Format--barricade length in feet, measured parallel to the open end of the barricade (See Figure 31).

e. BD - F6.2 Format--barricade depth in feet, measured perpendicular to the barricade open end (See Figure 31).

f. QUAN - F8.0 Format--quantity of explosives in explosive stack in equivalent pounds of TNT. The value of QUAN is to be determined by converting the weight of explosives in the stack to its equivalent weight of TNT and multiplying by the appropriate bomb factor.

g. NTHETA - I4 Format--for $0 \leq \text{NTHETA} \leq 180$ the computer code will solve for peak overpressures and positive impulses at selected values of scaled distance Z ($4.0 \leq Z \leq 500.0$) only along the angle specified (See Figure 31). For NTHETA = -1 the computer code will solve for peak overpressure and positive impulse

COLUMN NUMBER

5	10	15	20	25	30	35	40	45	50	55	60	65	70	75	80
↓	↓	↓	↓	↓	↓	↓	↓	↓	↓	↓	↓	↓	↓	↓	↓
30.00	50.00	8.83	92.00	71.00	307500.	-1	0	0	0	0	0	1	0	0	0

Figure 30. Typical Input Data Card for Program BLAST

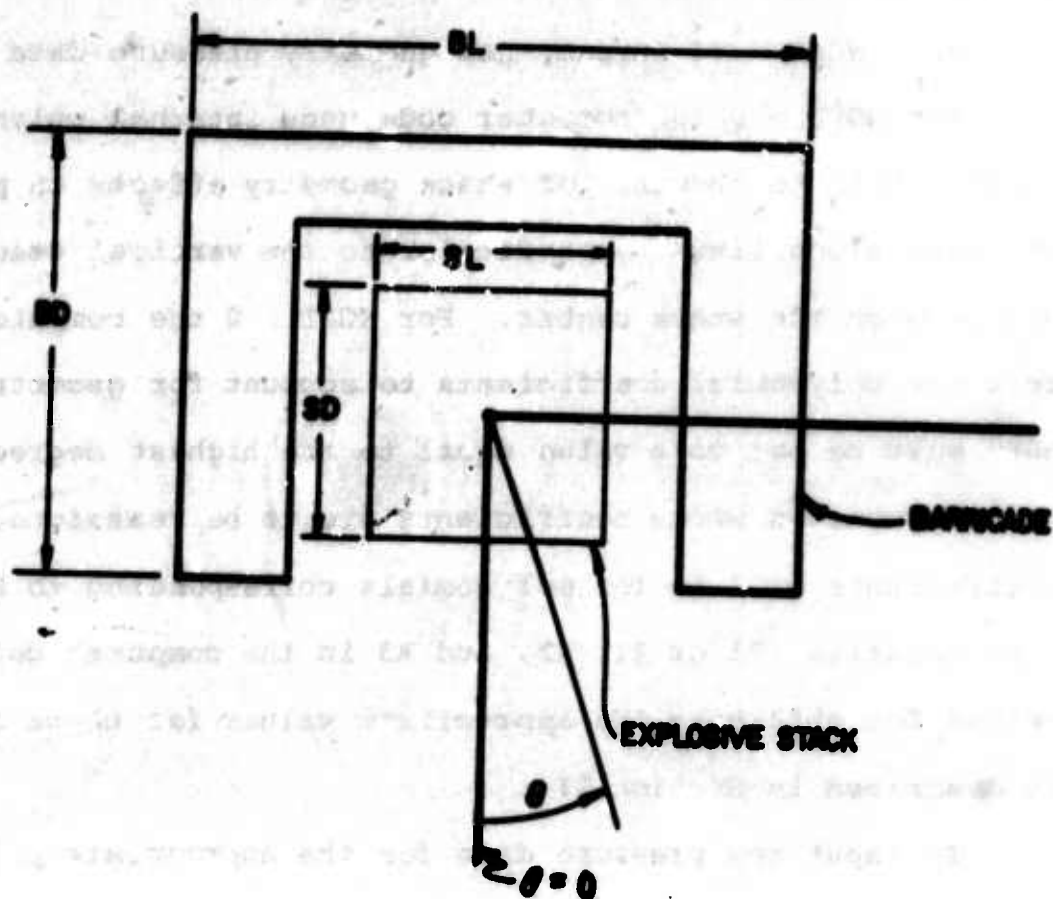


Figure 31. Stack and Barricade Geometry Parameters

at selected values of scaled distance Z ($4.0 \leq Z \leq 500.0$) along lines from theta θ equal to zero degrees through theta θ equal to 180 degrees in increments of 5 degrees.

h. NGPD - I4 Format--new geometry pressure data option.

For NGPD = 0 the computer code uses internal polynomial coefficients to account for stack geometry effects on peak overpressure along lines perpendicular to the vertical stack faces and through the stack center. For NGPD > 0 the computer code will read new polynomial coefficients to account for geometric effects. NGPD must be set to a value equal to the highest degree of the new polynomials whose coefficients are to be reassigned. These coefficients will be for polynomials corresponding to B, C, and D in Equation (7) or A1, A2, and A3 in the computer code. The method for obtaining the appropriate values for these coefficients is described in Section II.

To input new pressure data for the appropriate polynomial coefficients a total of NGPD + 1 data cards are required for polynomials of maximum order equal to NGPD. Each data card will contain one coefficient for each polynomial B, C, and D in a 3E14.7 Format. The first card will contain the zeroth order coefficients for B, C, and D respectively. The second card will contain the first order coefficients for B, C, and D respectively, etc. The final card in this data set will contain the NGPDth order coefficients for B, C, and D respectively.

i. NGID - I4 Format--new geometry impulse data option.

For NGID = 0 the computer code uses internal polynomial coefficients to account for stack geometry effect on impulse along a line perpendicular to the vertical stack faces and through the stack center. For NGID > 0 the computer code will read new polynomial coefficients to account for geometric effects. The number of coefficients, number of data cards, and the values for the coefficients can be determined as in h above. The variations from part h is that the coefficients will be for polynomials F, G, and H in Equation (7) or B1, B2, B3 in the computer code.

j. NBPD - I4 Format--new barricade pressure data option.

For NBPD = 0 the computer code uses internal polynomial coefficients to account for barricade geometry effects on peak overpressure along lines perpendicular to the barricade walls and through the barricade center, and along lines through the corner where the barricade walls meet and the barricade center. For NBPD > 0 the computer code will read new polynomial coefficients as in h above. These new coefficients will be for polynomials to define pressure ratios in directions A, B, C, and D in Figure 8. The number of coefficients, number of data cards, and values of coefficients can be determined in a manner similar to part h above. Each data card will contain one coefficient for each polynomial. The data card Format will be 4E14.7.

k. NBID - I4 Format--New barricade impulse data option.

For NBID = 0 the computer code uses internal polynomial coefficients to account for barricade geometry effects on impulse

ratios in directions A, B, C, and D in Figure 8. The number of coefficients, number of data cards, and values of coefficients can be determined in a manner similar to part h above. Each data card will contain one coefficient for each polynomial. The data card Format will be 4E14.7.

l. NGO - I4 Format--no geometry option. For NGO = 0, the program solves the problem according to the model development and includes explosive stack geometry effects. For NGO = 1, the program solution excludes explosive stack geometry effects.

m. NBO - I4 Format--no barricade option. For NBO = 0, the program solves the problem according to the model development and includes barricade effects. For NBO = 1, the program solution excludes barricade effects.

n. IBO - I4 Format --isobar option. For IBO = 1, the program computations exclude the isobar option. For IBO = 0, the computations include the isobar option which also requires that NTHETA = -1 (See part g above).

o. NEFPRD - I4 Format--new edge to face pressure ratio data option. For NEFPRD = 0, the computer code uses internal polynomial coefficients to account for stack geometry effect on the ratio of pressure along a line through the corner where the vertical faces of the bomb stack meet and the center of the bomb stack to pressure along a line perpendicular to the vertical faces and through the stack center. For NEFPRD > 0, the computer code will read new polynomial coefficients as in h above. The number of coefficients, number of data cards, and values of

coefficients can be determined in a manner similar to part h above. Each data card will contain one coefficient in an E14.7 Format.

p. NEFIRD - I4 Format--new edge to face impulse ratio data option. For NEFIRD = 0, the computer code uses internal polynomial coefficients to account for stack geometry effect on the ratio of impulse along a line through the corner where the vertical faces of the bomb stack meet and the center of the bomb stack to impulse along a line perpendicular to the vertical faces and through the stack center. For NEFIRD > 0, the computer code will read new polynomial coefficients as in h above. The number of coefficients, number of data cards, and values of coefficients can be determined in a manner similar to part h above. Each data card will contain one coefficient in an E14.7 Format.

6. OUTPUT FORMAT

The output from the Blast Program depends on the options that are chosen on the input control card. The output will be as follows:

a. Geometry effect

- (1) If the geometric effects of the stack $SL \times SD$ are to be considered, the program will print out

GEOMETRY OPTION USED

STACK LENGTH = SL STACK DEPTH = SD

- (2) If the geometric effect of the stack is not considered, the program will solve the remainder of the problem for a bare hemispherical charge and print out

GEOMETRY OPTION NOT USED

b. Barricade effect

- (1) If the effect of the presence of a barricade $BL \times BD$ around the stack is to be considered, the program will print out

BARRICADE OPTION USED

BARRICADE LENGTH = BL BARRICADE DEPTH = BD

- (2) If the problem is to be solved without a barricade, the program will print out

BARRICADE OPTION NOT USED

c. Charge Weight

The equivalent amount of TNT (i.e., m lbs.) that is represented in the stack of bombs is printed out as
QUANTITY OF EXPLOSIVES IN STACK = m LBS OF TNT

d. Pressure and Impulse Distributions

(1) The azimuth angle θ is first printed

AT THETA = θ DEGREES

(2) The following headings are then listed:

	BARE Z OVERPRESSURE	MODIFIED OVERPRESSURE	BARE IMPULSE	MODIFIED IMPULSE	RADIUS
--	------------------------	--------------------------	-----------------	---------------------	--------

(3) Under these titles, the following computed values are printed: (a) scaled distance, (b) pressure from a bare hemispherical charge, (c) estimated pressure from the actual charge (shaped and/or barricaded), (d) positive impulse from a bare hemispherical charge, (e) estimated impulse from the actual charge, and (f) distance in feet.

e. Pressure Isobars

(1) If the isobar option has been used the program computes the scaled distance to the isobar pressures in increments of 5 degrees between the azimuth angles of 0 and 180 degrees. Scaled distance will be solved for isobar pressures of 1000, 800, 600, 400, 200, 100, 80, 60, 40, 20, 10, 9, 8, 7, 6, 5, 4, 3, 2, 1, 0.5, and 0.1 psi.

The first line to be printed under this option is
THE ISOBAR COORDINATES FOR AN OVERPRESSURE OF 1000 ARE

(2) The next line

(PNR = PRESSURE NOT REACHED)

defines the symbol which is used instead of the radius when
the pressure given in Part (1) is not attained.

(3) The following headings are then listed:

THETA

Z

(4) Under these titles, computed values of the azimuth
angle and scaled distance for the prescribed pressure are
printed.. If the prescribed pressure is higher than any of
the computed values for the particular line of propagation,
then the symbol PNR is printed under Z.

The sequence of output given by Parts (1) to (4) is
repeated for each of the pressures listed in Part (1).

APPENDIX II

FRAGMENTATION PROGRAM

1. FORTRAN PROGRAM DESCRIPTION

This computer code corresponds to the analytical model described in Section III.

The first step is to define the problem. A control card is read to instruct the computer to retain previous sets of data for barricade, fragment, or fragment dispersion on multiple runs or to read in new data for barricade, fragment, or fragment dispersion. The control card also instructs the computer to (a) solve the problem with or without a barricade, (b) sets the increments of theta (azimuth angle) and beta (angle of departure), (c) solve for a certain angular orientation of bombs in the barricade, and (d) sets the height of the center of the bomb stack.

When the barricade data are read into the code, the input is converted to radius to barricade, $R3(J)$, and height of barricade, $ZW(J)$, for each angle of θ , $\theta(J)$. J is an integer where $1 \leq J \leq (360/ITH)+1$. ITH is the increment of theta.

Initial conditions for the fragments are read into the program in terms of polar angle measured from the nose of the

bomb. The input increments of polar angle must correspond to the increments of azimuth angle for the barricade (cylindrical) coordinates (i.e., if $\Delta\theta_{\text{output}} = 20^\circ$, values of fragment mass, initial velocity, and number of fragments must be read for values between 0° and 180° at the angles $0^\circ, 20^\circ, 40^\circ \dots, 180^\circ$).

To include the effect of a multiple number of bombs existing in the stack, a correction factor is included. This factor has been named "EFNB" for "Effective Number of Single Bombs in Stack." EFNB must be determined experimentally such that the fragment dispersion pattern for the "Effective Number of Bombs" is the same as for the detonated stack.

If the current problem being solved has experimental results to compare with the computer output, a permanent record can be printed with the output by using Table 4--Experimental Fragment Dispersion Data. To use this option, NCD4 is given a number on the Control Card corresponding to the number of data cards that are to be read into Table 4. The input format will be discussed in Appendix II-5. No computations are performed using these data. The information is read in and immediately printed out to establish a permanent record.

So far in this section the emphasis has been to organize the available information in a usable form for the subroutine

TRAJ3. The subroutine in this program computes the trajectory for the fragment "launched" at the azimuth angle, θ , and departure angle, β ; considers properties of the fragment and forces acting on it; estimates the range, velocity, number of fragments, and fragment mass at the impact point, Table 5; and estimates the distribution along the directions of propagation, Table 6.

To produce the distribution pattern, the differences in angle for the directions of propagation are established by the value of ITH read from the control card. The program is designed to solve for the distribution 360° around the bomb stack in increments of ITH. TTA is the name given to the angle measured from the center of the open side of a three-sided barricade to the radial direction of the trajectory. TTA will take on the values $0^\circ \leq \text{TTA} \leq 360^\circ$ and will increase in increments of ITH. NOTE: This convention for TTA is established as a standard. Actually, barricades of any shape that can be approximated by one or more broken lines of finitely many linear segments can be handled by reading in the angles and distances to the ends and the height of the segments. The format for reading in the barricade data will be described in Appendix II-5. In general, the origin for measuring theta can be placed in any

position, but the standard has been chosen to produce computer results that can be easily compared.

The computer code will solve for the increments of TTA just described when the DO statement on the major loop of TRAJ3 is as follows:

```
DO 1800 J = 1, JTMM1
```

JTMM1 is the integer value of 360° divided by increment Theta, ITH, where any resulting decimals are dropped.

$$JTMM1 = \frac{360^\circ}{ITH}$$

Example 1. If the radial directions of the trajectory are described in 20° increments, $ITH = 20$, the program must go through the DO loop $360/20$ or 18 times.

Example 2. For $ITH = 14^\circ$ the program must go through the DO loop $360/14 = 25.7$ or 25 times.

If the distribution pattern is desired in a specific direction $\tilde{\theta}$ it is necessary to compute the number of increments of ITH in $\tilde{\theta}$, rounding the result to the nearest integer value.

For future discussion, call this integer L. The Do statement in the major loop of TRAJ3 would be

DO 1800 J = L, L

Example 3. If the radial distribution is desired for the direction

$$\tilde{\theta} = 120^\circ \text{ and } ITH = 20^\circ$$

$$120^\circ / 20^\circ = 6$$

OR

$$L = 6$$

Example 4. If $\tilde{\theta} = 131^\circ$ and $ITH = 20^\circ$

$$131^\circ / 20^\circ = 6.55$$

OR

$$L = 7$$

This means that the computer would solve the problem for $\tilde{\theta} = 140^\circ$ instead of the angle 131° desired. To avoid this difference, it would be necessary to change the increment of theta to a more suitable value to produce an angle exactly equal or very near to the desired angle. Note that when the distribution in a direction $\tilde{\theta}$ is computed, the area effected by the fragments in that trajectory is between the angles $\tilde{\theta} - ITH/2$ and $\tilde{\theta} + ITH/2$.

For each azimuth angle TTA to be used the program will solve for a series of departure angles from the barricade, BETA. The values of BETA will be between the angles -89° and $+89^\circ$ since $+90^\circ$ and -90° are of no interest and cause problems with some of the trigometric functions. The distinct values of BETA will be determined by the increment of beta, IB, on the control card. A large value for IB will produce coarse approximations, but require fewer computations than a small value for IB.

Example 5. For $IB = 20^\circ$ the program will compute JBMX trajectories for each angle TTA. JBMX is computed in the program as follows:

- 1) The number of increments of IB in 89° dropping any resulting decimal values is NB.

$$NB = 89^\circ / 20^\circ = 4$$

- 2) The maximum number of increments of BETA that will be solved between -89° and $+89^\circ$ is JBMX.

$$JBMX = 2 \times NB + 1$$

$$= 9$$

For each value of TTA the trajectory will be computed for BETA = -80° , -60° , -40° , -20° , 0° , 20° , 40° , 60° and 80° .

Example 6. For $IB = 10^\circ$

$$1) \quad NB = 89^\circ / 10 = 8$$

$$2) \quad JBMX = 2 \times 8 + 1 \\ = 17$$

For each value of TTA the trajectory will be computed for

BETA = -85° , -80° , -75° , ..., $+80^\circ$, and $+85^\circ$.

To change the program to compute trajectories for BETA from 0° to 89° would require the following card changes

Statement No.

1640-12 $JBMX = NB + 1$

1640-1 $BETA = 0.$

Increments of beta, IB, would remain as previously discussed.

To compute a trajectory the governing parameters for the fragment must be set. Since the fragment parameters are in terms of polar bomb coordinates, the angle between the initial direction of the fragment and the bomb centerline out the nose of the bomb must be computed. This angle has been named GAMMA and will be a function of TTA, BETA, and the angle to the centerline out the nose of the bomb, ANGD. This computation appears in the program as statement 1640 + 17.

1640 + 17 GAMMA = (ASIN((SBS + CBS * SNS) **.5)) *57.3

where

$$SBS = \sin^2 (\text{BETA})$$

$$CBS = \cos^2 (\text{BETA})$$

$$SNS = \sin^2 (\text{THETA-ANGD})$$

Since GAMMA can take on any value between 0° and 180° and the fragment parameters are read in at discrete angles, the values at the discrete angle nearest to GAMMA are applied as the conditions at GAMMA.

Each trajectory is computed as a broken line of finitely many linear segments as indicated by Equations (26a) to (26c).

The initial conditions at the beginning of each linear segment are the initial conditions at the bomb stack or are the end conditions from the previous segment.

The difference in angle α between adjacent segments is DEL. The value of DEL is computed in the program as a function of position, velocity, and direction of fragment velocity.

The initial value of DEL is computed so that the horizontal distance that the fragment has traveled after the first step is slightly beyond the barricade wall. This appears in the program at Statement No. 1640 + 21 as

1640 + 21 DEL = G*1.01 *DISTB/(VZER*VZER)

where

G = gravity constant

DISTB = distance to barricade

VZER = intial velocity at bomb stack

Succeeding values of DEL are computed in such a way that either the increase in range or change in height is 50 ft. depending on whether or not BETA is less than or greater than 45° respectively. In the computer program the statements appear as follows: To increment the range in 50 foot increments statement 1752 is used

1752 DEL = G * 50./VSQ

Check if absolute value of BETA is greater than 45°, if it is, DEL is changed by the two statements following 1725:

1725 + 1 VAL1 = ABS(ALPH1)

1725 + 2 (VAL1.GE.0.7853) DEL = ABS(DEL*COSAL1)/SINAL1

where

ALPH1 = the angle the segment of the trajectory being considered makes with the horizontal.

COSAL1 = COS(ALPH1)

SINAL1 = SIN(ALPH1)

Two exceptions exist that cause DEL to take on different values than just described. The first exception occurs when the value of DEL that is computed as above is used in Statement No. 1646+4 and the resulting velocity, V2, is negative. V2 is the predicted velocity at the end of the linear segment being considered. In this case DEL is repeatedly cut in half and the

velocity recalculated until V2 remains positive. This check and modification is done with Statement Numbers 1649-3 to 1649-1.

```
1649-3    IF(V2.GT.0.)  GO TO 1649
1649-2    DEL = DEL/2.
1649-1    GO TO 1646
```

The second exception occurs near the top of the trajectory when the speed of the fragment is less than 100 feet/second. The value of DEL should be much less than one. Since DEL is a function of one divided by speed squared, small speeds can produce values for DEL on the order of one hundred. To avoid this possibility, set DEL equal to 0.1 for speeds less than 100 fps to establish the proper order of magnitude and let the routine in the preceding paragraph make any further modifications that may be required. This adjustment to the program variable DEL is checked and modified with statements 1725-3 to 1725-1 as follows:

```
1725-3    IF(V1.GT.100.) GO TO 1725
1725-2    DEL = .1
1725-1    GO TO 1645
```

The last bit of information required before computing the trajectory is the Ballistic Coefficient C which is a function of the fragment mass and hence it must be calculated for each

trajectory since fragment mass varies with the direction of "launch". C is computed in statement 1645-1.

$$1645-1 \quad C = RHP * CD / (FM(K) ** .33333)$$

where

RHP = a combined set of constants for a fragment

CD = drag coefficient

FM(K) = fragment mass in the direction of launch

To indicate if the top of the barricade has been cleared or not cleared, a dummy variable, NBCL, is used. Initially the value of NBCL is -1 indicating that the barricade has not been cleared. If there is no barricade in the radial direction of the trajectory or if the fragment clears the top of the barricade, NBCL is set equal to +1 and the trajectory of the fragment is computed.

The trajectory of the fragment is approximated by a broken line of finitely many linear segments where the angle between the segment and a horizontal line is continuously decreasing. The initial conditions for each segment are known from the terminal conditions of the previous segment or the initial conditions at the bomb. The initial conditions for a segment include range, X1, altitude, Y1, velocity, V1, and angle between the trajectory segment and a horizontal line, ALPH1. The terminal conditions include range, X2, altitude, Y2, velocity, V2 and direction of terminal velocity, ALPH2. The terminal conditions

for each segment are computed as the trajectory is mapped until the fragment strikes the ground inside the barricade, strikes the barricade wall, or clears the barricade and impacts the ground at some distance. The printed output from the program, discussed in detail in Appendix II-6, will include information to indicate that the fragments do not clear the barricade or will record the impact range and velocity for each combination of launch angles TTA and BETA.

The number of fragments landing at each impact point is assumed to be the same as the number initially launched in the trajectories by a single bomb multiplied by the number of effective bombs, EFNB. The number of fragments, NUM(K), in a trajectory will be dependent on the angles TTA and BETA and the increments of each of these angles ITH and IB. NUM(K) can be approximated using equation III-36. In the program this appears as statement 1645-10.

1645-10 NUM(K)=FPS(IGAMA)*RITH*(SIN(RBTA2))- SIN(RBTA1))*EFNB

where

K - indicates the angle of departure, BETA

IGAMA - indicates the angle GAMMA

FPS() - fragments per steradian

RITH - increment of theta, TTA, in radians

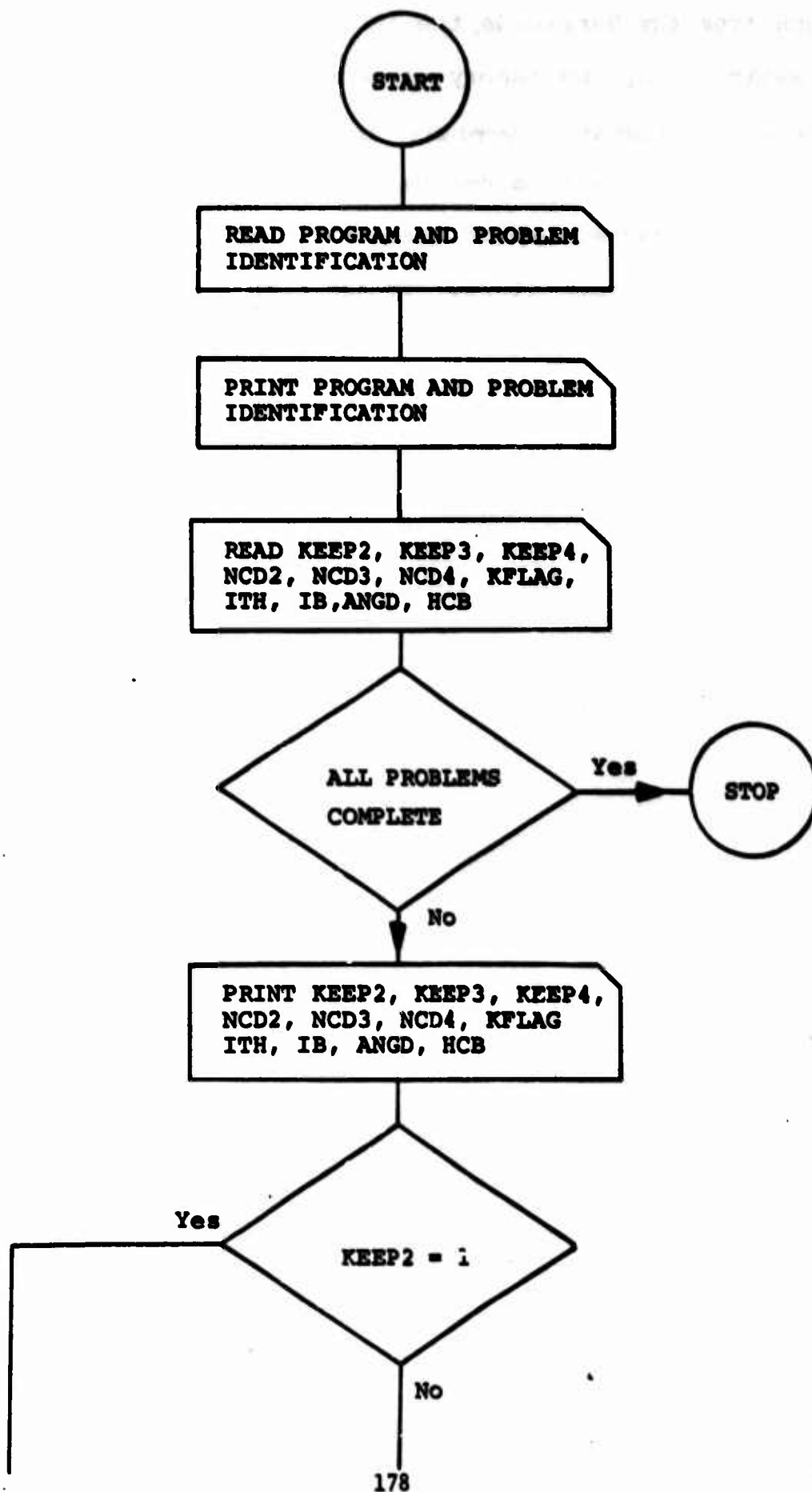
RBTA2 - radians to angle BETA + IB/2

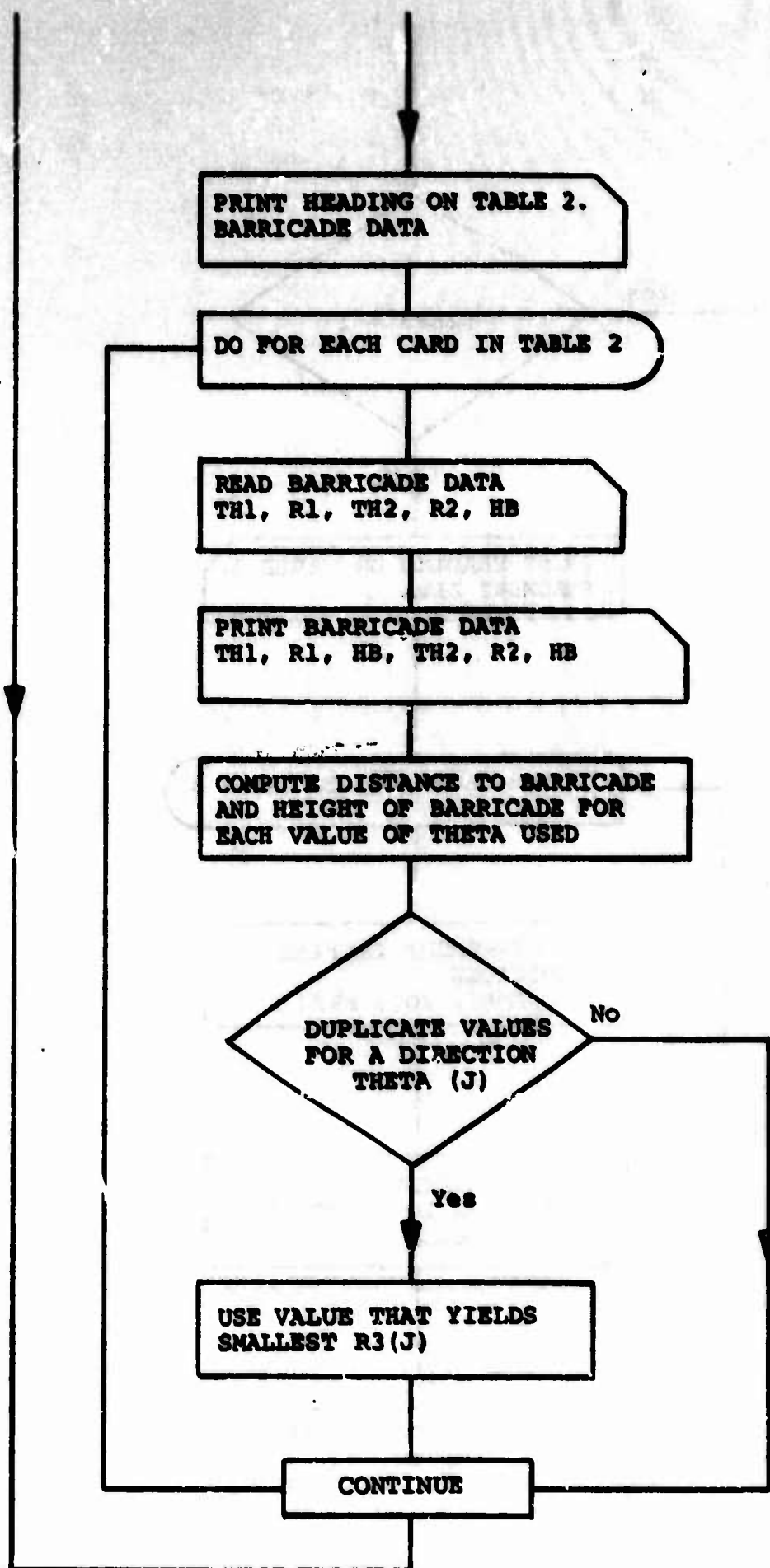
RBTA1 - radians to angle BETA - IB/2

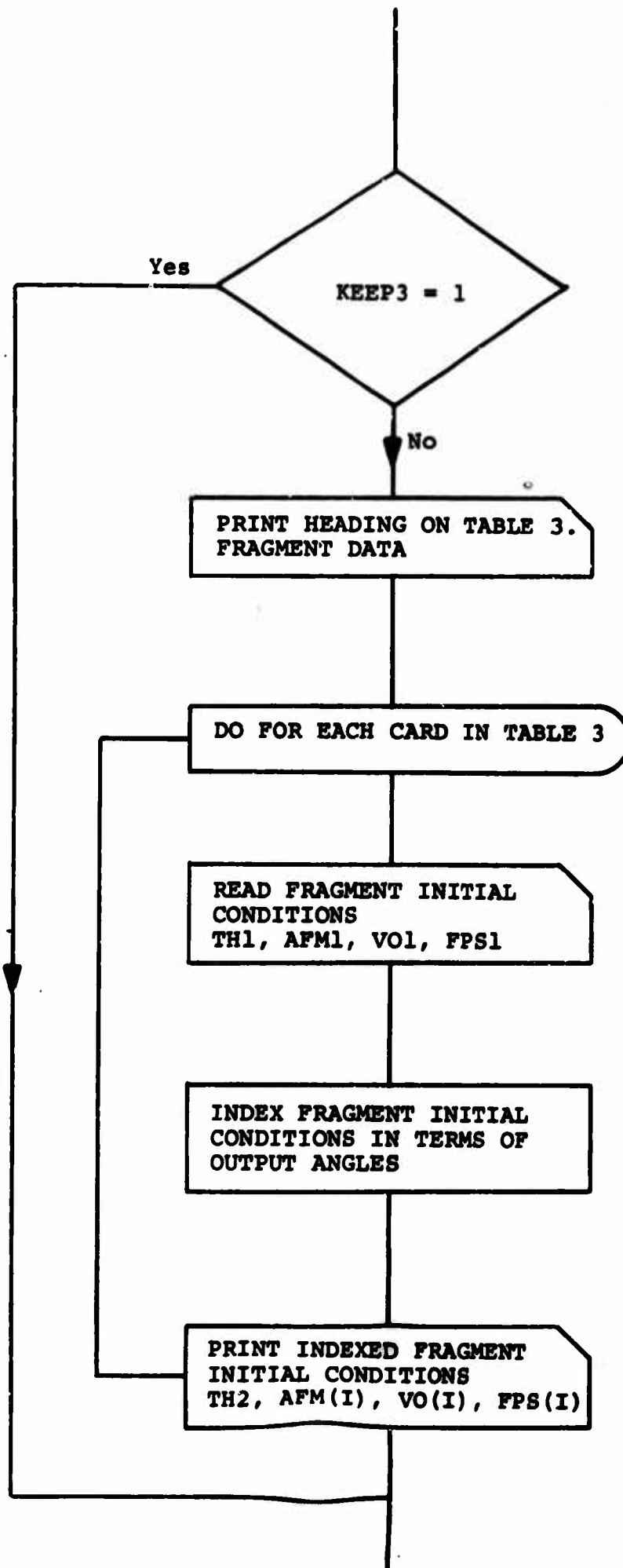
EFNB - effective number of bombs in stack

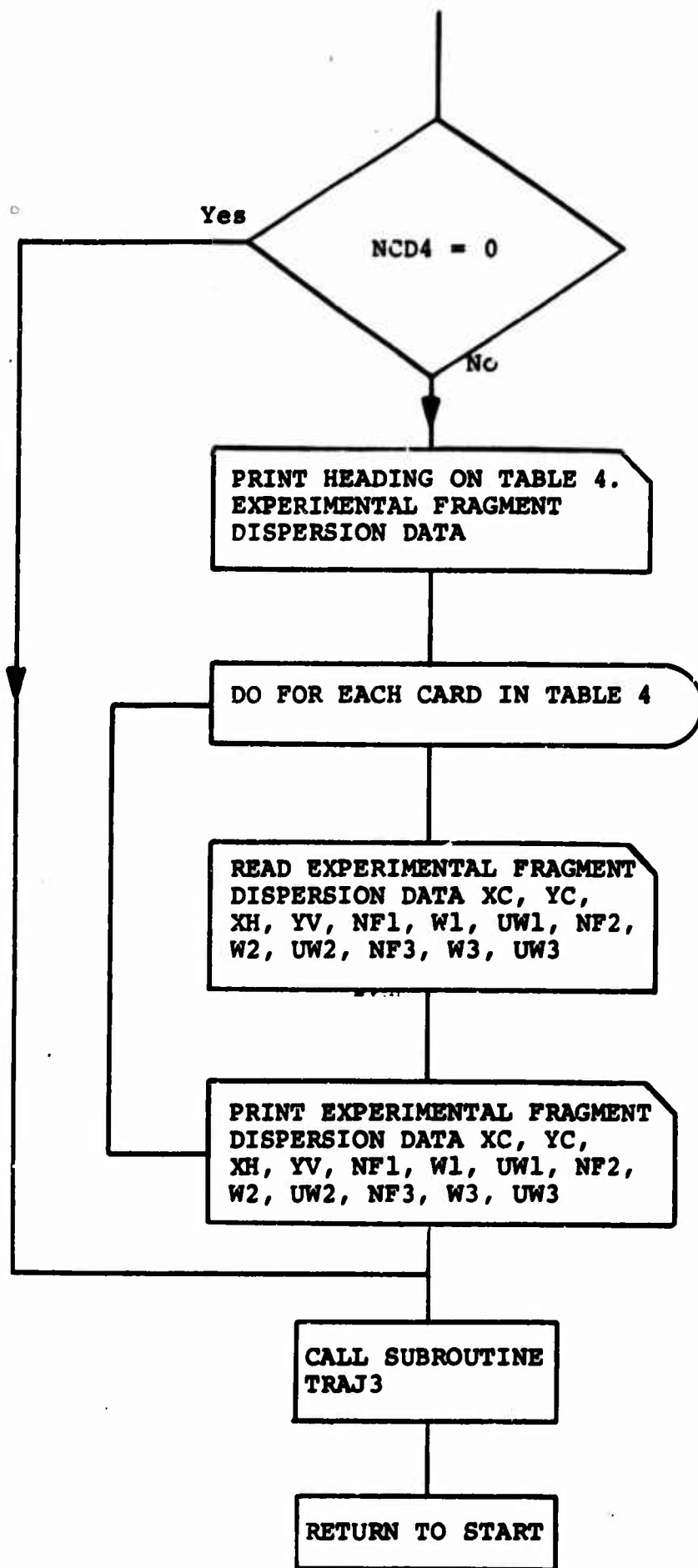
With the impact conditions known along the radial directions from the barricade, the average distribution/sq. ft. can be estimated by the theory of Section III.4f. The data along a radial direction are ordered according to the increasing magnitude of impact ranges using statements 1740 + 1 through 1790. The assumed impact area, the number of fragments/sq. ft. and weight of fragments/sq. ft are computed and then printed as Table 6.

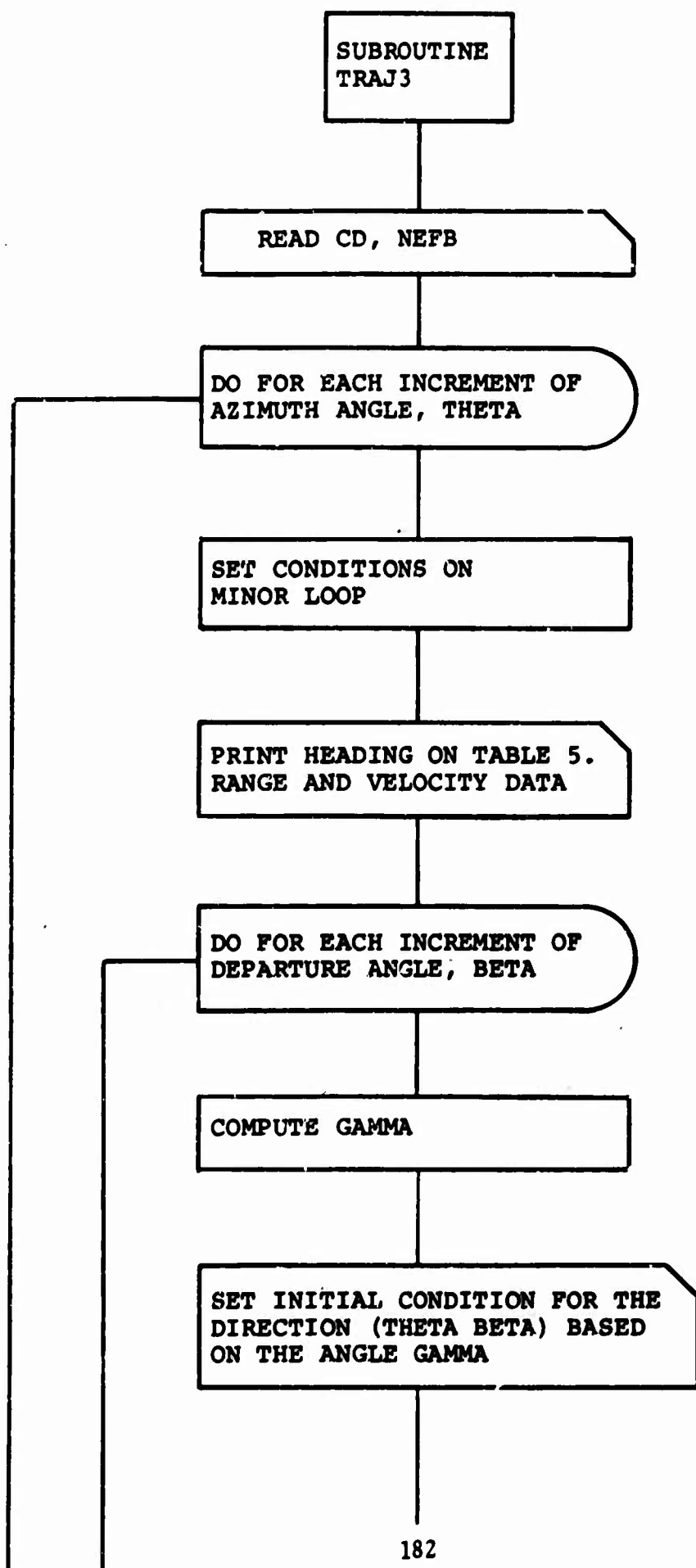
2.0 FRAGMENTATION PROGRAM FLOW DIAGRAM

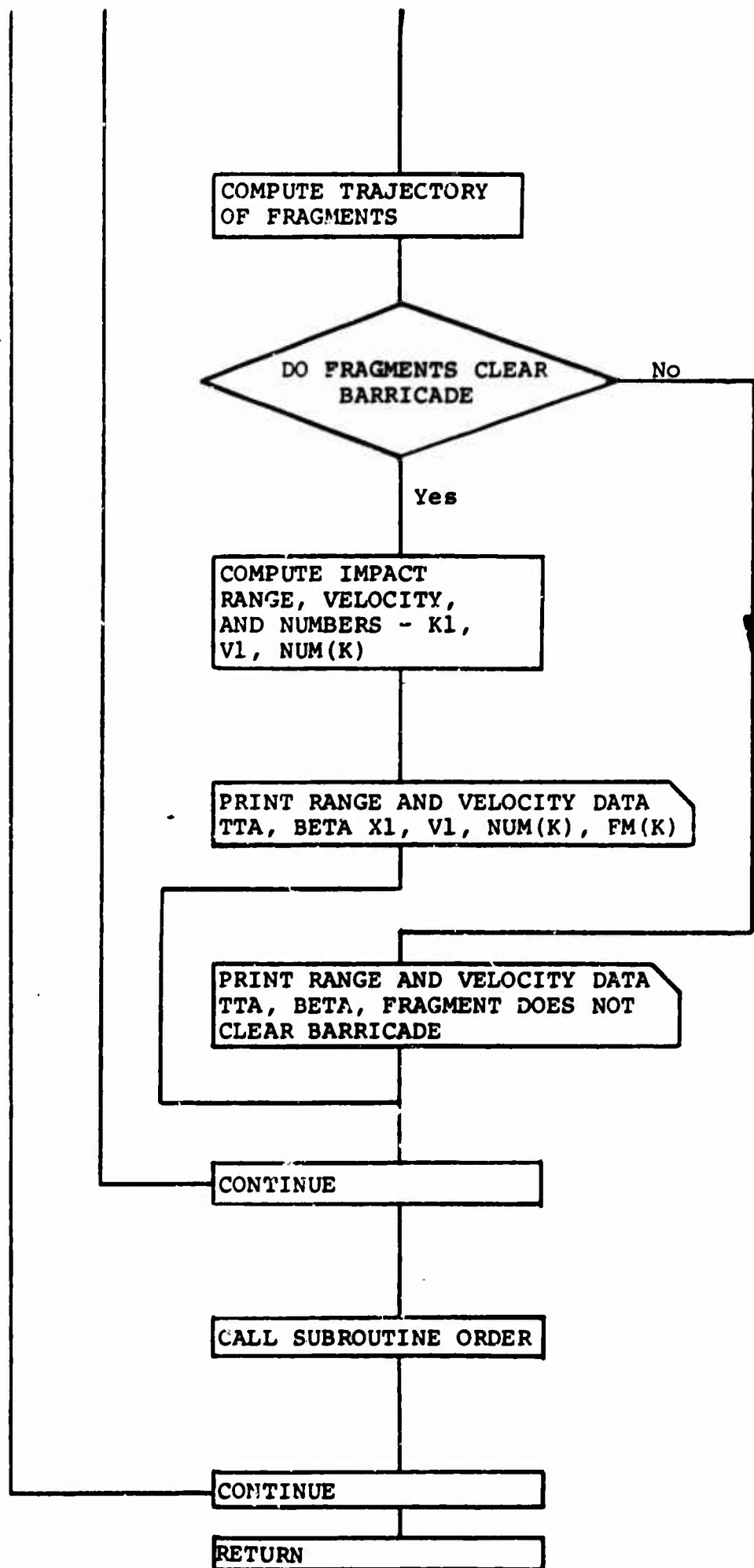


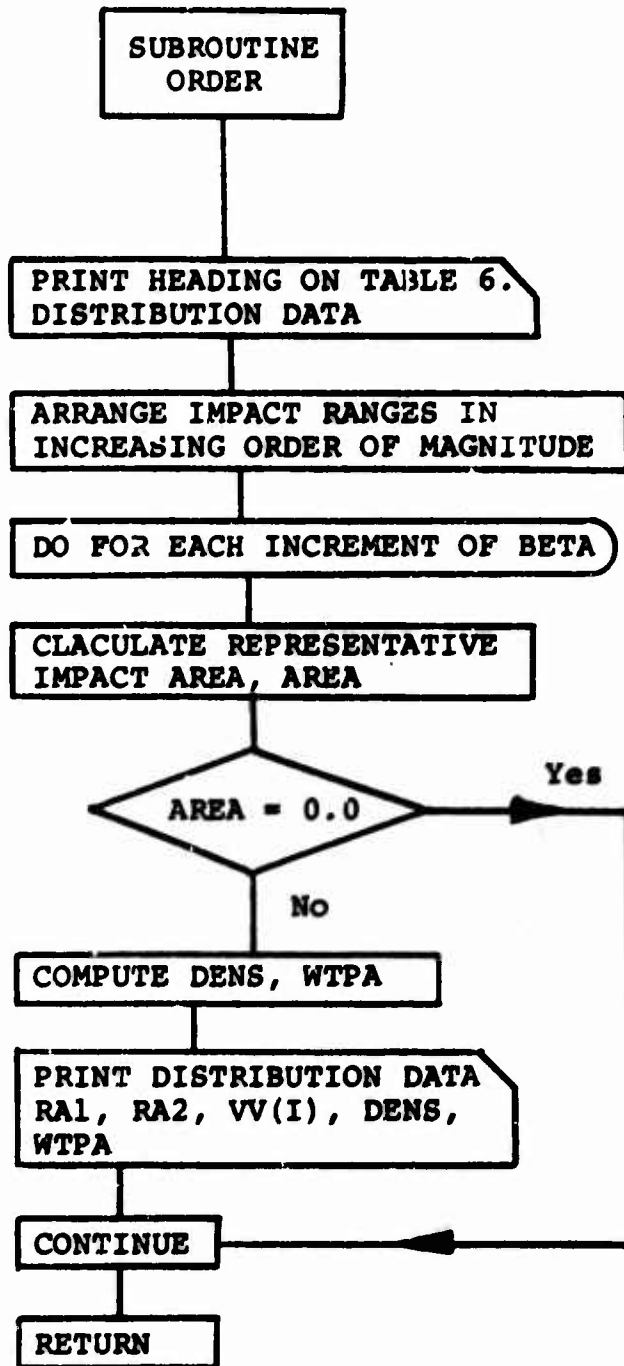












3. LIST OF VARIABLES TO COMPUTER PROGRAM FOR ANALYTICAL FRAGMENTATION MODEL

AFM(J)	Average fragment mass emitted by bomb at an angle GAMMA
ALPH1	Direction of fragment velocity at start of a segment of trajectory.
ALPH2	Direction of fragment velocity at end of a segment of trajectory
ANG	Number of radians in TH1.
ANGD	Equal to θ_B in Section III
AREA	Representative area of impact zone for a trajectory.
BETA	Angle between horizontal and initial velocity of fragment.
BETA1, etc.	Angles defining region containing trajectory, used to calculate number of steradians.
C	Ballistic coefficient
CBETA	$\cos(\text{BETA})$
CBS	$\cos^2(\text{BETA})$
CD	Drag coefficient
COSAL1, etc.	$\cos(\text{ALPH1}), \text{etc.}$
D	Distance along barricade
DB	Increment BETA divided by 2.
DELDG	DEL/G
DELTA	Angle between R3 and barricade wall.
DENS	Number of fragments/sq.ft. in impact zone
DISTB	Distance to barricade from center of bomb stack.

DTH	Angle between ends of barricade segment.
DTHB2	Increment of THETA divided by 2.
D1	Intermediate value to solve for SII and ALPHA.
EFNB	Number of single bombs to produce same distribution as bomb stack.
ETA	Difference between barricade and bomb coordinates.
FITH	Floating point increment of THETA.
FL1, etc.	Floating-point number of TH1, etc.
FM	Fragment mass.
FPS(J)	Average fragment/staradian in direction GAMMA, bomb coordinates.
G	Gravitational constant.
GAMMA	Angle between VO and bomb centerline.
HB	Height of barricade for segment defined by TH1-TH2.
HCB	Height of center of bomb stack about ground.
HEITB	Height of barricade.
IB	Increment of departure angle BETA.
IGAMA	Integer number of increments of THETA in GAMMA.
ITH	Increment of azimuth angle THETA.
JBMX	Number of increments of BETA (IB) between -89° and 89°.
JTHMX	Number of integer values of ITH in 360°.
KANG	Integer value for ANG.
KEEP2	IF 1, Hold Table 2 Data from previous run.
KEEP3	IF 1, Hold Table 3 Data from previous run.

KEEP4	IF 1, hold Table 4 Data from previous run.
KFLAG	Indicator to initialize R3 and ZW to zero.
KNG1	Integer number of increments ITH between barricade and bomb coordinates.
KTH1	Integer degrees to start of barricade segment.
KTH2	Integer degrees to end of barricade segment.
NB	Max. number of increments of BETA in 89°.
NBCL	Index to indicate when barricade has been cleared.
NCD2	Number of cards to be read for Table 2.
NCD3	Number of cards to be read for Table 3.
NCD4	Number of cards to be read for Table 4.
NF1, etc.	Number of fragments in impact area 1, etc.
NTH1	Nearest integer number of increments of ITH in TH1.
NTH2	Nearest integer number of increments of ITH in TH2.
NUM(K)	Number of fragments in a given trajectory.
PHI	Angle between barricade and R2.
RA1	Radius to inner bound of representative impact area.
RA2	Radius to outer bound of representative impact area.
RBETA	Number of radians in BETA.
RBTA1, etc.	Number of radians in BETA1, etc.
RETA	Number of radians in ETA.
RHP	Constants for computing drag force.

RIB	Number of radians in increment BETA.
RITH	Number of radians in ITH.
RKTH1, etc.	Number of radians in TH1, etc.
RTH1	Radians in TH1.
RTH2	Radians in TH2.
R1	Radius to beginning of barricade segment being defined.
R2	Radius to end of barricade segment being defined.
R3(J)	Distance to barricade at angle corresponding to J increments of azimuth angle THETA.
SBETA	$\sin(\text{BETA})$
SBS	$\sin^2(\text{BETA})$
SINA1	$\sin(\text{ALPH1})$
SII	Angle between barricade and R1.
SN	$\sin(\text{ETA})$
TH1	Angle to beginning of barricade segment being defined.
TH2	Angle to end of barricade segment being defined.
TS	$\tan(S1)$
TTA	Azimuth angle, THETA, using cylindrical barricade coordinates.
TTA1, etc.	Angles defining region containing trajectory, used to calculate number of steradians.

UF1, etc.	Maximum fragment weight, grams, etc.
VAL1	Absolute value of ALPH1.
VO(J)	Average fragment velocity in direction GAMMA.
VSQ	Velocity squared.
VSQD	Velocity squared divided by DEL.
VV(I)	Velocity vector.
VZER	Initial velocity.
V1	Velocity at start of a segment of trajectory.
V2	Velocity at end of a segment of trajectory.
WTPA	Weight per sq. ft. at impact areas.
W1, etc.	Minimum fragment weight, grams, etc.
XC	X coordinates of impact area.
XH	WIDTH of impact area.
XV(I)	Range vector.
X1, X2	Initial and end conditions for a segment of trajectory.
YC	Y coordinates of impact area.
YV	Length of impact area.
Y1, Y2	Initial and end conditions for a segment of trajectory.
ZW(J)	Height of barricade at distance R3(J).

4. PRINTOUT OF FRAGMENTATION PROGRAM


```

000160      FITH = ITH
000161      PITH = FITH / 57.30
C
C----- IF KFLAG = 0 INITIALIZE R1 AND ZW TO ZERO
C
000163      IF ( KFLAG .EQ. 0 ) GO TO 592
000165      GO TO 594
000169      992 00 593 I = 1 , JTHMX
000173      27(I) = 0.0
000174      593 7H(I) = 0.1
000179      992 IF ( KEEP2 .EQ. 1 ) GO TO 622
C
C-----INPUT TABLE 2 - BARRICADE DATA
C
C----- THETA IS THE ANGLE MEASURED FROM THE CENTERLINE OF THE OPEN SIDE
C----- OF A THREE SIDED BARRICADE
C
C----- ANGL IS THE ANGLE FROM THETA = ZERO TO THE CENTERLINE OF THE BOMP.
C----- MEASURE ANGL IN SAME DIRECTION AS PLUS THETA. (0.LE.ANGL.LE.+360 )
C
000177      PRINT 516
000202      DO 622 I = 1, NCD2
000204      READ 515, TH1, R1, TH2, R2, M9
000221      PRINT 517, TH1, R1, M9, TH2, R2, M9
C
C-----CONVERT INTEGER VALUES IN DEGREES TO NEAREST MULTIPLE OF ITH (IN-
C----- CREMENTS OF POLAR ANGLE )
C
000243      NTH1 = ( TH1 / FITH ) + 0.5
000245      NTH2 = ( TH2 / FITH ) + 0.5
000247      KTH1 = NTH1 * ITH
000252      KTH2 = NTH2 * ITH
C
C-----CONVERT INPUT ANGLES TH1 AND TH2 INTO RADIAN
C
000253      RTH1 = TH1 / 57.30
000255      RTH2 = TH2 / 57.30
C
C-----CONVERT ANGLES KTH1, KTH2, TO RADIAN
C
000257      FL1 = KTH1
000260      FL2 = KTH2
000262      RKTH1 = FL1 / 57.30
000264      RKTH2 = FL2 / 57.30
C
C-----CONVERT INTEGER VALUES OF KTH1 AND KTH2 TO INTEGER INCREMENTS FOR
C----- INDEXING PURPOSES
C
000264      J1 = NTH1 + 1
000266      J2 = NTH2 + 1
C
C-----COMPUTE ANGLES OF TRIANGLE MADE BY R1, R2, AND BARRICADE
C
000267      DTH = RTH2 - RTH1
000271      S1 = 0.5 * ( 3.14 - DTH )
000274      TS = TAN ( S1 )
000276      D1 = ATAN ( ( R1 - R2 ) / ( R2 + R1 ) ) * TS )
000278      PHI = S1 + D1
000280      S11 = S1 - D1
000282      D = R1 * ( SIN(DTH) / SIN(PHI) )
000284      ANGL = RKTH1
C
C-----SET HEIGHT OF BARRICADE FOR EACH INCR OF THETA FROM JTH1-JTH2

```

```

000320      DO 615 J = J1, J2
C-----COMPUTE ANGLE MADE BY R1 AND BARRICADE WALL
C
000322      DELTA = 3.14 - ( PHT + ( RTH2 - ANG ) )
C
C-----SET HEIGHT OF BARRICADE FOR DISTANCE R3(J)
C
000325      R3(J) = R2 * ( SIN(PHT) / SIN ( DELTA ) )
000326      WH(J) = HA
C
C-----CHECK FOR DUPLICATE VALUES OF J--IF THERE ARE TWO VALUES OF J ( IF
C      TWO VALUES OF TH1 OR TH2) USE VALUE THAT YIELDS SMALLEST R3(J)
C
000336      IF ( (J-JHLN).GT.0.02.(J-JHLN).LT.0. ) GO TO 612
000337      IF ( R3(J).LT.HLDR3 ) GO TO 612
000338      R3(J) = HLDR3
000339      WH(J) = HLDRW
000340      GO TO 614
000341      612      HLDR3 = R3(J)
000342      HLDRW = WH(J)
000343      JHLN = J
000344      ANG = ANG + PHT
000345      615      CONTINUE
000346      620      CONTINUE
C
C-----INPUT TABLE 3 - FRAGMENT DATA
C
000367      622      IF ( KEFP3.EQ.1 ) GO TO 650
000368      PRINT 925
C
000374      DO 630 N = 1, NNO3
000375      READ 525, GAMMA, AFM1, VO1, FPS1
000376      N2 = ( GAMMA / FITH ) + 1.5
000377      AFM(N2) = AFM1
000378      VO(N2) = VO1
000379      FPS(N2) = FPS1
000380      GAMMA = ( N2 - 1 ) * FITH
C
000385      PRINT 527, GAMMA, AFM(N2), VO(N2), FPS(N2)
C
000390      630      CONTINUE
C
C-----INPUT TABLE 4 - EXPERIMENTAL FRAGMENT DISPERSION DATA
C
000403      650 IF ( KEFP4.EQ.1 ) GO TO 660
000404      PRINT 929
C
000410      DO 655 K = 1, NNO4
000411      READ 530, XC, YC, XH, YH, NF1, W1, UW1, NF2, W2, UW2, NF3,
000412      1      W3, UW3
000413      PRINT 536, XC, YC, XH, YH, NF1, W1, UW1, NF2, W2, UW2, NF3,
000414      1      W3, UW3
000415      655      CONTINUE
C
000420      660 CALL TRAJ3
000421      GO TO 920
000422      999      CONTINUE
000423      PRINT 539
000424      END

```

```

SUBROUTINE TRAJ3
C
C----- SUBROUTINE TO CALCULATE TRAJECTORY OF FRAGMENTS
C
017553      COMMON ZH(360), AFH(360), VO(360), FPS(360), P3(360), JMAX ,
1          NMAX , MC3 , ANGD , JTHMX , JQMX , I9 , ITH , RITH , FITH,
2          TTA1 , TTA2 , FH(100) , XV(100) , VV(100) , NUM(100) , TN(100) ,
3          TM(100) , TX(100) , TV(100)
C
017559      1002 FORMAT ( 2F4.2 )
017555      1510 FORMAT ( //40H          TABLE 5. RANGE AND VELOCITY DATA ,/,
1          52H          THETA BETA RANGE,FT TMP VEL,FPS N
2          20H04H  AVG FRAG MASS,G , / )
017555      1520 FORMAT ( 9X, 2( 2X, F5.1 ), 3X, F4.1, 6X, F7.1, 2X, I8, 2X, F7.1 )
017555      1530 FORMAT(9X,2(2X,F5.1),30H  FRAGMENT DOES NOT CLEAR OBSTACLE )
017555      1540 FORMAT ( //777777 , 9X,2HAFH( , I3 ,3H) = , F12.3 , 4H(GRAMS) )
017555      1550 FORMAT ( 5X , 3HC = , E10.3 )
017555      1560 FORMAT ( 5X , 6HETA = , F8.0 , 3H(DEGREES) )
C
C      RHP IS A COMBINED SET OF CONSTANTS THAT INCLUDES AIR DENSITY
C-----RHP = .5 * PNO * 2.79
C      RHP FOR A TUMBLING CUBE IS APPROXIMATELY 0.000555
C
C      DEL IS INCREMENT FOR ALPHA (RADIAN) IN DETERMINING TRAJECTORY
C      OF FRAGMENT
C
C-----SET INITIAL VALUES
017555      G = 32.2
017556      RHP = .000555
017560      DTWR2 = ITH / 2.
C
C      CD = DRAG COEFFICIENT FOR FRAGMENT
C      TO GET ORDINARY FRICTION FREE TRAJECTORY SET CD = 0.0
C
C-----EFNR = EFFECTIVE NUMBER OF BOMBS IN BOMB STACK
C-----EFNR = 1 WILL SOLVE FOR THE EFFECT OF A SINGLE BOMB
C
017563      READ 1504 , CD , EFNR
C
C-----VARY POLAR ANGLE, THETA
C
017572      NR = 89 / I9
017575      JQMX = 2 * NR + 1
017600      JTHM1 = JTHMX - 1
C
C----- MAJOR LOOP -----
C----- INCREMENT AZIMUTH ANGLE, THETA, FROM 0 TO 360 DEGREES
C
017602      DO 1000 J = 1 , JTHM1
C
C      INITIAL BETA
C
017603      BETA = -NR * I9
017607      1640 DISTA = P3(J)
017610      HEITA = ZH(J)
C----- SET CONSTANTS
017612      RIR = I9 / 57.3
017614      TTA = (J-1) * ITH
017620      TTA1 = TTA - JTHM2
017621      TTA2 = TTA + JTHM2
017623      ETA = TTA - ANGD
017624      BETA = BETA / 37.3

```

```

007626      SN = SIN(BETA)
007631      SNS = SN*SN
007632      PRINT 1510
C
C----- MINOR LOOP -----
C----- INCREMENT DEPARTURE ANGLE, BETA, FROM -89 TO +89 DEGREES
C
007635      DO 1740 K = 1, JRMX
007637      BETA = BETA / 94.3
007640      CBETA = COS(BETA)
007642      SBETA = SIN(BETA)
007643      CBS = CBETA * CBETA
007644      SBS = SBETA * SBETA
C
C----- GAMMA IS THE ANGLE BETWEEN THE INITIAL VELOCITY OF THE
C          FRAGMENT AND THE CENTERLINE OF THE BOMB
C
007647      GAMMA = (ASIN((SBS + CBS * SNS) ** .5)) * 57.3
C          PRINT 1521, GAMMA
007657      1641 FORMAT (10X, F10.4)
C
C----- COMPUTE NEAREST NUMBER OF INCREMENTS OF THETA (ITH) IN GAMMA
C
007657      IGAMA = GAMMA / FITH + 1.5
C          PRINT 1665, IGAMA
007659      1665 FORMAT (10X, I9)
007654      FM(K) = AFM(IGAMA)
C
C----- SET INITIAL VELOCITY FOR THE FRAGMENT
C
007666      VZER = VO(IGAMA)
C----- SET DEL
C
007667      DEL = G * 1.01 * DIST2 / (VZER * VZER)
007672      N3 = IP / 2.
007674      BETA1 = BETA - 0.8
007675      BETA2 = BETA + 0.8
007677      RBTA1 = BETA1 / 57.3
007679      RBTA2 = BETA2 / 94.3
C
C----- COMPUTE THE NUMBER OF FRAGMENTS EJECTED IN DIRECTION OF TRAJECTORY
C----- INCLUDE THE EFFECTIVE NUMBER OF BOMBS
C
007702      NUM(K) = EPS(IGAMA) * RITH * (SIN(RBTA2) - SIN(RBTA1)) * EFMA
007713      ALPH1 = RBETA
007714      V1 = VZER
007716      X1 = 0.
007719      Y1 = HCR
C
C----- N3CL = -1 FRAGMENT HAS NOT CLEARED BARRICADE
C----- N3CL = +1 FRAGMENT HAS CLEARED BARRICADE
C
007720      N3CL = -1
007721      IF (WEITH.LT.0.1) N3CL = +1
C
007725      COSAL1 = COS(ALPH1)
007730      VSQ = V1 * V1
C
007731      C = R4P * CO / (FM(K) ** .33333)
C          PRINT 1551, C
007736      1551 SIN1 = SIN(ALPH1)
007737      1546 DELOG = DEL / C
007744      VSQD = VSQ * DELOG

```

```

017745      ALPH2 = ALPH1 - DEL
017747      COSAL2 = COS(ALPH2)

017709      V2 = ( V1 * COSAL1 - G * V1 * VSQD ) / COSAL2
017755      IF ( V2.GT.0. ) GO TO 1649
017760      DEL = DEL / 2.
017761      GO TO 1645
017762      1649 X2 = X1 + VSQD
017764      Y2 = Y1 + VSQD * SINAL1 / COSAL1

C
C
C      CHECK TO SEE IF PARTICLE HAS HIT THE GROUND INSIDE BARRICADE OR
C      HAS STRUCK THE BARRICADE WALL.
C
017767      IF (NACL ) 1650,1700,1700
017771      1650 IF(Y2) 1660,1670,1670
017773      1660 PRINT 1930 , TTA , BETA
010003      XV(K) = X1
010004      VV(K) = V1
010005      GO TO 1730
010007      1670 IF(DIST9 - Y2) 1680,1720,1720
010012      1680 IF(HEIGHT-Y2) 1690,1660,1660
010015      1690 NACL = 1
010016      GO TO 1720
010017      1700 IF(Y2) 1710,1720,1720
010021      1710 PRINT 1520 , TTA , BETA , X1 , V1 , NUM(K) , FM(K)
010041      XV(K) = X1
010042      VV(K) = V1
010044      GO TO 1730
010029      1420 ALPH1 = ALPH2
010045      COSAL1 = COSAL2
010050      V1 = V2
010091      X1 = X2
010053      Y1 = Y2
010054      VSQ = V1 * V1
010055      IF ( V1.GT.100. ) GO TO 1420
010061      DEL = 0.1
010062      GO TO 1645
010062      1725 DEL = G * 50. / VSQ
010064      VAL1 = ABS(ALPH1)
010066      IF ( VAL1.GE.0.7053 ) DEL=ABS(DEL*COSAL1/SINAL1)
010074      GO TO 1645
010075      1730 BETA = BETA + IS
010100      1740 CONTINUE
010102      CALL ORDEF
010103      1800 CONTINUE
010106      RETURN
010106      END

```

```

SUBROUTINE ORDER
C
C----- ARRANGE RANGES IN INCREASING ORDER OF MAGNITUDE
C
010339      COMMON ZH(350), AFH(350), VO(350), FPS(350), R3(350), JMAX ,
1          NMAX , MCR , ANGD , JTHMX , JBMX , TR , ITM , PITH , FITM ,
2          TTA1 , TTA2 , FM(150) , XV(150) , VV(150) , NUM(150) , TN(150) ,
3          TH(150) , TX(150) , TV(150)
C
010335      2535 FORMAT(//32H      TABLE 6. DISTRIBUTION DATA ,/,5X,9HTHETA(1)= ,
1          154.3 , 2140DEGREES      THETA(2)= , 54.3 , 4HDEGREES , / ,
2          25X , 7H RANGE 1 , 10H      RANGE 2 , 50H      IMP VEL,FPS      NUM/SQ FT
3          3      GRAMS/SQ FT      )
010339      2935 FORMAT ( 2X , 2F10.0 , F13.1 , 2(AX , E9.3 ) )
010335      DO 2790 NN = 2 , JBMX
010337      NN41 = NN - 1
010340      DO 2490 N = 1 , NN41
010342      IF ( XV(NN) - XV( N ) , 2750 , 2791 , 2790
010345      2750 NP1 = N + 1
010347      DO 2493 II = NP1 , NN
010356      ITM1 = II - 1
010357      TV(II) = VV(ITM1)
010359      TX(II) = XV(ITM1)
010362      TN(II) = NUM(ITM1)
010363      2753 TH(II) = FM(ITM1)
010369      VV(N) = VV(NN)
010371      XV(N) = XV(NN)
010372      NUM(N) = NUM(NN)
010374      FM(N) = FM(NN)
010376      DO 2754 I = NP1 , NN
010405      VV(I) = TV(I)
010406      XV(I) = TX(I)
010407      NUM(I) = TN(I)
010411      2754 FM(I) = TH(I)
010413      2490 CONTINUE
010421      PRINT 2535 , TTA1 , TTA2
010427      RA1 = 0.0
010430      DO 2795 I = 1 , JBMX
010432      IP1 = I + 1
010433      RA2 = ( XV(I) + XV(IP1) ) / 2.
010436      IF ( RA1.EQ.0. ) GO TO 2795
C---- CALCULATE AREA OF LANDING AREA AND NUMBER OF FRAGMENTS
C      PER SQ. FT. ( FRAG / SQ. FT. )
010440      AREA = XV(I) * RITH * ( RA2 - RA1 )
010443      IF(I.EQ.JBMX) GO TO 2797
010445      GO TO 2794
010446      2797 RA2 = 2. * XV(I)-RA1
010451      AREA = XV(I) * RITH * ( RA2 - RA1 )
010453      2794 IF ( AREA.LT.0.2 ) GO TO 2795
C
C      COMPUTE FRAGMENTS / SQ FT ( FRAG/SQ FT )
C
010457      DENS = NUM(I) / AREA
C
C
C-----COMPUTE WEIGHT/SQ. FT.      ( GRAMS/SQ FT )
C
010460      WTPA = DENS * FM(I)
C
010462      PRINT 2535 , RA1 , RA2 , VV(I) , DENS , WTPA
010477      2795 RA1 = RA2
010501      2796 CONTINUE
010503      RETURN

```

5. INPUT FORMAT

The input cards to a problem will depend on the problem being run and the number of variations to be considered in a run. The input to a single run or the first data set of a multiple run will include a card to describe the problem, a control card to instruct the memory to read data for the problem and set parameters, a series of cards containing data to define the barricade geometry surrounding a charge, a series of cards containing fragment initial condition in terms of polar bomb coordinates, and a card containing the typical drag coefficient for a bomb fragment and the number of effective bombs in the stack.

Subsequent data sets on multiple runs will include a card to describe the problem, a control card to instruct the memory storage to retain information from the previous run or to read new data for some or all of the data. If the barricade geometry is to be changed, a series of cards will be included to define the new geometry; otherwise, these cards are omitted. If the geometry of the bomb stack is to be changed, a series of cards containing the fragment initial conditions in terms of polar bomb coordinates will be included; otherwise, these cards are omitted. A card containing the drag coefficient and the number of effective bombs will be included in all data sets.

a. Description Card

Provisions are included to use the first card of each data set to describe in an alphanumeric format the problem being solved. The field for this format will be 80 spaces on one card.

b. Control Card

The second card in a data set will contain information as follows:

(1) KEEP2, I5 Format

In Columns 1-5 enter a zero (0) in Column 5 if barricade data is to be read during execution of the current problem. Enter a one (1) in Column 5 if barricade data is to be retained from the previous problem or if the problem is to be solved without a barricade.

(2) KEEP3, I5 Format

In Columns 6-10 enter a zero (0) in Column 10 if the fragment initial conditions are to be read from data cards during execution of the current problem. Enter a one (1) in Column 10 if fragment initial conditions are to be retained from the previous problem. A one (1) in Column 10 only applies on multiple runs and a zero (0) will be necessary on the initial problem of multiple runs and all single problem runs.

(3) KEEP4, I5 Format

In Columns 11-15 enter a one (1) in Column 15 if experimental fragment dispersion data is to be retained

from the previous problem. Otherwise, enter a zero (0) in Column 15. A one (1) in Column 15 only applies on multiple runs.

(4) NCD2, NCD3, NCD4, I5 Format

In Columns 16-20, 21-25, and 26-30, enter the number of data cards that are to be read containing barricade data, fragment initial conditions, and experimental dispersion data, respectively.

(5) KFLAG, I5 Format

In Column 35 enter a zero (0) when reading new barricade data or to solve the problem without a barricade. If, on a multiple run, barricade data from the previous run is to be retained, enter a one (1) in Column 35.

(6) ITH, I5 Format

In Column 36-40 enter the increment size for the azimuth angle, TTA. A small value for ITH will require larger numbers of fragment data cards to be read and more computations than large values, which are less accurate but faster. In general, a value of 20° for ITH will produce useful results and require reasonable computer time.

(7) IB, I5 Format

In Columns 41-45 enter the increment size for the departure angle, BETA. Small values for IB will yield more trajectories and impact points and produce a more accurate distribution, but more computer time will be required.

In general, a value of 10° for IB will produce useful results and require reasonable computer time.

(8) ANG, F5.0 Format

In Columns 46-50, enter the angle between TTA = zero (C) and the centerline out the nose of the bombs in the bomb stack. ANG will be measured CCW and lie between 0° and $+360^\circ$.

c. Barricade Data, 5F10.1 Format

Barricade data cards need to be included on single runs, initial problem of multiple runs, and on occasional problems of multiple runs when it is desired to change the barricade configuration. Each card will contain five (5) values to be read in a 5F5.1 Format. The data on the card will be the information necessary to define the finite number of linear segments representing the barricade. Each segment will require one (1) card. The card for each segment will contain the following information in the order presented.

(1) TH1, F5.1 Format

TH1 is the angle, degrees, to the start of the segment being defined.

(2) R1, F5.1 Format

R1 is the distance, ft., from the center of the bomb stack to the start of the segment being defined.

(3) TH2, F5.1 Format

TH2 is the angle, degrees, to the end of the segment being defined.

(4) R2, F5.1 Format

R2 is the distance, ft., from the center of the bomb

stack to the end of the segment being defined.

(5) HB, F5.1 Format

HB is the height, ft., of the segment being defined.

d. Fragment Initial Conditions

The cards described in this section are required only on single runs, initial problems of multiple runs and on intermediate problems of multiple runs when the fragment data is to be altered.

One data card will be required for each polar angle where the fragment initial conditions are to be read in. The input angles will begin with 0° and increase in increments equal to the increment of TTA, ITH, previously chosen. The number of card containing fragment initial conditions is equal to NCD2.

Each card will contain the following information:

(1) GAMMA, F10.0 Format

Enter in Columns 1-10 the polar angle, degrees, measured in spherical bomb coordinates from the nose of the bomb.

(2) AFM1, F10.0 Format

In Columns 11-20 enter the average value over the region $\text{GAMMA} \pm 1/2 \text{ ITH}$, for the fragment mass, grams, in the direction GAMMA.

(3) VOL, F10.0 Format

In Columns 21-30 enter the average value, over the region $\text{GAMMA} \pm 1/2 \text{ ITH}$, for the fragment velocity ft./sec., in the direction GAMMA.

(4) FPS1, F10.0 Format

In Columns 31-40 enter the average value, over the region $\text{GAMMA} \pm 1/2 \text{ ITH}$, for the number of fragments per steradian ejected by a single bomb in the direction GAMMA.

e. Experimental Fragment Dispersion Data

When experimental results are available for a problem being solved by the program, the experimental measurements may be read into the program to produce a printed record for comparison with the results predicted by the code. There will be one data card for each fragment recovery area. The information on each data card will be as follows:

(1) XC, F6.1 Format

Enter in Columns 1-7 the distance, ft., from the center of the bomb stack to the center of the recovery area measured parallel to the direction $\text{TTA} = \text{zero}$.

(2) YC, F6.1 Format

Enter in Columns 7-12 the distance, ft., from the center of the bomb stack to the center of the recovery area measured parallel to the direction of $\text{TTA} = 45^\circ$.

(3) XH, F6.1 Format

Enter in Columns 13-18 the dimension, ft., of the recovery area in the direction of XC.

(4) YV, F6.1 Format

Enter in Columns 19-24 the dimension, ft., of the recovery area in the direction of YC.

(5) NF1, NF2, NF3, I5 Format

Enter in Columns 25-29, 40-44, and 55-59 the number of fragments recovered in the recovery area in the heaviest weight class, second heaviest weight class, and third heaviest weight class, respectively.

(6) W1, W2, W3 F5.1 Format

Enter in Columns 30-34, 45-49, and 60-64 the minimum fragment weight, grams, in heaviest weight class, second heaviest weight class, and third heaviest weight class, respectively.

(7) UW1, UW2, UW3 F5.1 Format

Enter in Columns 35-39, 50-54, and 65-69 the maximum fragment weight, grams, in the heaviest weight class, second heaviest weight class, and third heaviest weight class, respectively. More than three weight ranges can be included by changing Formats 530 and 536 and by increasing the number of variables in Statements 650+3 and 650+4.

f. Drag Coefficient and Effective Number of Bombs in Stack
(CD and EFNB)

(1) CD, F8.2 Format

In Columns 1-8 enter the value of the drag coefficient to be read in a F8.2 Format. This card is required for each

problem of a multiple run and obviously for a single run. Setting drag coefficient equal to zero will solve for friction free trajectory. In general, CD will have a value between 0.3 and 2.0.

(2) EFNB, F8.2 Format

In Columns 9-16 enter the number of single bombs that must be exploded one at a time to produce the same fragment dispersion pattern as the bomb stack being modeled. In general, EFNB will be less than the actual number of bombs in the stack.

g. Blank Cards

After the last data set, include two blank data cards to terminate the run.

Notes on data sets

Normally a single run or the first problem of a multiple run will require data cards a, b, c, d, and f as a minimum. The inclusion of e is optional on any problem. These data cards will describe the problem and solve the dispersion pattern for a number of bombs in a specific barricade configuration.

If on the second problem of a multiple run the barricade geometry is to be changed and the bomb stack remains the same as the first problem, data cards a, b, c, and f would be included in the data set.

If, instead of changing the barricade on the second problem, the type of bomb is to be changed, data cards a, b, c, and f would be included in the data set.

h. Typical Set of Input Data

The data shown in Figure 32 are for a single run. All data cards discussed in this section are included with the exception of e.

COLUMN NUMBER										
5	10	15	20	25	30	35	40	45	50	55
blank										
blank										
.48	266.0									
180	40	1000	10000							
160	31	2554	7000							
140	23	4108	5000							
120	16	5662	3000							
100	9	7216	11000							
80	6	7552	8000							
60	10	6664	3000							
40	14	5776	3000							
20	17	4888	4000							
0	20	4000	5000							
228.0	67.3	296.6	55.9	11.0						
132.0	67.3	228.0	67.3	11.0						
63.3	55.9	132.0	67.3	11.0						
0	0	1	3	10	0	0	20	10270.0	4.4	
3 TEST CASE FOR FRAGM CHECKOUT										

Figure 32. Typical Input Data for Program FRAGM

6. OUTPUT FORMAT

a. Description of Problem

Across the top of the first page of printout for each problem one line of alphanumeric print is used to describe the problem being solved.

b. Table 1. Control Data.

This table prints a record of the variables and program options used for each problem.

(1) Table 1. Heading

Lines 1, 2 and 3 print the heading for the table columns. These headings appear as follows:

TABLE 1. CONTROL DATA

TABLE NUMBER

TABLE NUMBER
2 3 4

(2) Table 1. Data

Under these headings are printed the number 0 to indicate that new data are read into Tables 2, 3, or 4 on the current problem or a 1 to indicate that data from the preceding run of a multiple run is retained. If data is read into Tables 2, 3, and 4 on the current problem, the program prints

PRIOR DATA OPTIONS (1 = HOLD)	0	0	0
-------------------------------	---	---	---

(3) Table 1. Number of Cards

When data are read into Table 2, 3, or 4, the number of cards read into each table is printed. If 3, 10, and 7 data cards are read into Tables 2, 3, and 4, respectively, the program will print

NUM CARDS INPUT THIS PROBLEM	3	10	7
------------------------------	---	----	---

(4) Table 1. Barricade Data

If Barricade Data are not read into the current problem or to either omit the previous barricade and read new barricade or solve for the distribution without a barricade a 1 or 0, respectively, is printed with the following statement.

BARRICADE DATA (1 = NO)	0 or 1
-------------------------	--------

(5) Table 1. Increment Theta

The number of degrees used in the current problems for the increments on azimuth angle theta is printed as

INCREMENTS OF THETA, DEGREES	--
------------------------------	----

(6) Table 1. Increment Beta

The number of degrees used in the current problem for the increments on departure angle BETA is printed as

INCREMENTS OF BETA, DEGREES	--
-----------------------------	----

(7) Table 1. Angle

The angle measured from $\Theta = 0^\circ$ to the centerline out the nose of the bombs in the stack is printed as

ANGLE BETWEEN COORDINATES OF BOMB AND BARRICADE --

(8) Table 1. Height

The height of the geometric center of the bomb stack is printed as

HEIGHT OF STACK CENTER --

c. Table 2. Barricade Data

This table is printed only on problems where barricade data is read from data cards. If data are retained from the previous problem, this table is not printed

(1) Table 2. Heading

The heading for the table to contain data defining the geometry of the barricade is printed as

TABLE 2. BARRICADE DATA

THETA	DEGREES	DISTANCE, FT.	BARRICADE HEIGHT, FT.
-------	---------	---------------	-----------------------

(2) Table 2. Data

The data used to define a segment of the barricade geometry are printed in pairs for each segment. Data for segment 1, 2, ..., N, ..., are contained in lines 1 and 2

3 and 4, ..., 2N-1 and 2N, ..., respectively. The first line of information for a particular segment will print the angle to the start of the segment, the radial distance from the bomb stack geometric center to the start of the segment, and the height of the segment. The second line of information for a particular segment will print the angle to the end of the segment, the radial distance from the bomb stack geometric center to the end of the segment, and the height of the segment. The height of any segment is to be constant between its end points. When segment K meets segments K+1, the printed output for the first line of segment K+1 will be the same as the last line of segment K with the possible exception of the height.

d. Table 3. Fragment Data

This table is printed only on problems where the fragment data is to be read from data cards. If data is retained from the previous problem, this table is not printed.

(1) Table 3. Heading

This heading for the table to contain data defining the initial condition for the fragments ejected by a single bomb as a function of polar angle measured from the nose of the bomb, is printed as:

TABLE 3. FRAGMENT DATA

THETA, DEG (WRT BOMB COORD)	AVG FRAG MASS, GRAMS	INITIAL VEL, FPS	FRAGS PER STERADIAN
--------------------------------	-------------------------	---------------------	------------------------

(2) Table 2. Data

For each angle where data are input, starting with 0° and increasing in steps equal to the increment of theta to maximum of 180°, the program will print out the angles where the data are input. The fragment mass in grams, initial velocity in ft./sec., and the number of fragments per steradian are printed beside the appropriate angle to indicate the average initial condition used in the current problem at that angle.

e. Table 4. Experimental Fragment Dispersion Data

This table is printed on problems where there is experimental fragment dispersion data available that have been read into the program. If data are retained from the previous problem, this table is not printed.

(1) Table 4. Heading

The heading for Table 4 containing experimental fragment dispersion data is printed as:

TABLE 4. EXPERIMENTAL FRAGMENT DISPERSION DATA					
COORDINATES, FT.				NUM	WEIGHT RANGE
XC	YC	XH	YV		GRAMS

(2) Table 4. Data

For each recovery area of dimensions XH by YV at coordinates XC and YC the number of fragments per weight range is printed for the three heaviest fragment ranges.

f. Table 5. Range and Velocity Data

This table is printed for all problems run.

(1) Table 5. Heading

The heading for Table 5, Range and Velocity Data, is printed as:

TABLE 5. RANGE AND VELOCITY DATA

THETA	BETA	RANGE, FT.	IMP VEL, FPS	NUM	AVG FRAG MASS, G
-------	------	------------	--------------	-----	------------------

(2) Table 5. Data

For each combination of azimuth angle, theta, and departure angle, beta, the range to the impact point, ft., the impact velocity, ft./sec., number of fragments expected to impact at that range, and the average fragment mass, grams, are printed in tabular form. There will be one Table 5 for each azimuth angle, theta, where trajectories are computed and one entry in Table 5 for each value of departure angle, beta.

The entries for any single line of Table 5 will be in one of two forms.

(a) If the fragment does not clear the top of the barricade wall for the launch angles θ and β , the program will print the launch angles and indicate that the fragment does not clear the barricade. This appears as:

θ	β	FRAGMENT DOES NOT CLEAR BARRICADE
----------	---------	-----------------------------------

(b) If the fragment clears the barricade or if there is no barricade in the direction θ for the launch angles θ and β , the program will compute the range to the impact point, $X1$, impact velocity, $V1$, number of fragments expected to impact, NUM , and average fragment mass, FM .

The printed output appears as:

θ	β	$X1$	$V1$	NUM	FM
----------	---------	------	------	-------	------

g. Table 6

This table is printed for all problems run.

(1) Table 6. Heading

For each azimuth angle, θ , used in the current problem solution a Table 6 will be printed. Each Table 6 will give the distribution in a direction θ for an area bounded by lines symmetric about θ and separated by the angular increment of θ , ITH . Let θ be the azimuth angle and θ_1 , θ_2 , be the symmetric lines about θ . Then the Table 6 heading will be printed as:

TABLE 6. DISTRIBUTION DATA

THETA(1) = θ_1 DEGREES

THETA(2) = θ_2 DEGREES

RANGE 1	RANGE 2	IMP VEL, FPS	NUM/SQ FT	GRAMS/SQ FT
---------	---------	--------------	-----------	-------------

(2) Table 6. Data

Along an azimuth angle the impact ranges are computed at discrete points. From these discrete impact points

a representative impact area is defined by the angles θ_1 , and θ_2 mentioned in g.(1) and average ranges between impact points. For impact point number 1 call these ranges RA1 and RA2. Only impact areas where RA1 is greater than zero (0) are of interest. Therefore, for the first impact area $0 \leq RA1 \leq RA2$. In the printed Table 6 this would appear as:

RA1	RA2	V1	NPA	GPA
-----	-----	----	-----	-----

where RA1, RA2, NPA, and GPA are numbers corresponding to ranges defining the representative impact area, average impact velocity, number of fragments per sq. ft., and number of grams of fragments per sq. ft. in the impact area.

h. Typical Output

The following pages are indicative of the output format and type of information that is presented.

3 TEST CASE FOR FRAG CHECKOUT

TABLE 1. CONTROL DATA

	TABLE NUMBER		
PRIOR-DATA OPTICNS (1=HOLD)	2	3	4
NUM CARDS INPUT THIS PROBLEM	0	0	1
	3	10	0
BARRICADE DATA (1=NO)			0
INCREMENTS OF THETA, DEGREES			20
INCREMENTS OF BETA, DEGREES			10
ANGLE BETWEEN COORDINATES OF BOMB AND BARRICADE			270
HEIGHT OF STACK CENTER			4.4

TABLE 2. BARRICADE DATA

THETA, DEGREES	DISTANCE, FT	BARRICADE HEIGHT, FT
63.3	55.9	11.0
132.0	67.3	11.0
132.0	67.3	11.0
223.0	67.3	11.0
223.0	67.3	11.0
296.6	55.9	11.0
		11.0

TABLE 3. FRAGMENT DATA

THETA, DEG (WRT BOMB COORD)	AVG FRAG MASS, GRAMS	INITIAL VEL, FPS	FRAGS PER STERADIAN
0	20	4000	5000
20	17	4888	4000
40	14	5776	3000
60	10	6664	3000
80	6	7552	8000
100	9	7216	11000
120	16	5662	3000
140	23	4108	5000
160	31	2554	7000
180	40	1000	10000

TABLE 5. RANGE AND VELOCITY DATA

THETA	BETA	RANGE, FT	IMP VEL, FPS	NUM	AVG FRAG MASS, G
0.	-80.0	0.	7216.0	30929	9.0
0.	-70.0	0.	7552.0	44289	6.0
0.	-60.0	0.	7552.0	64739	6.0
0.	-50.0	0.	7552.0	83222	6.0
0.	-40.0	0.	7552.0	99177	6.0
0.	-30.0	0.	7552.0	112119	6.0
0.	-20.0	0.	7552.0	121655	6.0
0.	-10.0	0.	7552.0	127495	6.0
0.	0.	1100.0	497.8	129461	6.0
0.	10.0	1917.6	101.3	127495	6.0

0.	20.0	1970.6	113.4	121655	6.0
0.	30.0	1879.4	116.3	112119	6.0
0.	40.0	1699.7	117.0	99177	6.0
0.	50.0	1462.4	117.2	83222	6.0
0.	60.0	1177.9	117.2	64739	6.0
0.	70.0	831.1	117.3	44289	6.0
0.	80.0	487.0	125.5	30929	9.0

TABLE 6. DISTRIBUTION DATA

THETA(1) = -10.000 DEGREES		THETA(2) = 10.000 DEGREES			
RANGE 1	RANGE 2	IMP VEL, FPS	NUM/SQ FT	GRAMS/SQ FT	
244	659	125.5	4.379E-01	3.941E+00	
659	966	117.3	4.981E-01	2.909E+00	
966	1139	487.0	1.944E+00	1.167E+01	
1139	1320	117.2	8.689E-01	5.214E+00	
1320	1581	117.2	6.250E-01	3.750E+00	
1581	1790	117.0	8.019E-01	4.811E+00	
1790	1899	116.3	1.568E+00	9.409E+00	
1899	1944	101.3	4.177E+00	2.506E+01	
1944	1997	113.4	3.339E+00	2.803E+01	

TABLE 5. RANGE AND VELOCITY DATA

THETA	BETA	RANGE, FT	IMP VEL, FPS	NUM	AVG FRAG MASS, G
20.0	-80.0	0.	7552.0	22493	6.0
20.0	-70.0	0.	7552.0	44289	6.0
20.0	-60.0	0.	7552.0	64739	6.0
20.0	-50.0	0.	7552.0	83222	6.0
20.0	-40.0	0.	7552.0	99177	6.0
20.0	-30.0	0.	7552.0	112119	6.0
20.0	-20.0	0.	7552.0	121655	6.0
20.0	-10.0	0.	7552.0	127495	6.0
20.0	0.	1150.0	609.6	48548	10.0
20.0	10.0	1917.6	101.3	127495	6.0
20.0	20.0	1970.6	113.4	121655	6.0
20.0	30.0	1879.4	116.3	112119	6.0
20.0	40.0	1699.7	117.0	99177	6.0
20.0	50.0	1462.4	117.2	83222	6.0
20.0	60.0	1177.9	117.2	64739	6.0
20.0	70.0	831.1	117.3	44289	6.0
20.0	80.0	429.3	117.3	22493	6.0

TABLE 6. DISTRIBUTION DATA

THETA(1) = 10.000 DEGREES		THETA(2) = 30.000 DEGREES			
RANGE 1	RANGE 2	IMP VEL, FPS	NUM/SQ FT	GRAMS/SQ FT	
215	630	117.3	3.613E-01	2.168E+00	
630	991	117.3	4.237E-01	2.542E+00	
991	1164	609.6	6.974E-01	6.974E+00	
1164	1320	117.2	1.008E+00	1.040E+00	
1320	1581	117.2	6.250E-01	3.750E+00	
1581	1790	117.0	8.019E-01	4.811E+00	
1790	1899	116.3	1.568E+00	9.409E+00	
1899	1944	101.3	4.177E+00	2.506E+01	
1944	1997	113.4	3.339E+00	2.803E+01	

TABLE 5. RANGE AND VELOCITY DATA

THETA	BETA	RANGE, FT	IMP VEL, FPS	NUM	AVG FRAG MASS, G
40.0	-80.0	0.	7552.0	22493	6.0
40.0	-70.0	0.	7552.0	44289	6.0

40.0	-60.0	0.	7552.0	64739	6.0
40.0	-50.0	0.	6664.0	31208	10.0
40.0	-40.0	0.	6664.0	37191	10.0
40.0	-30.0	0.	6664.0	42044	10.0
40.0	-20.0	0.	6664.0	45620	10.0
40.0	-10.0	0.	6664.0	47810	10.0
40.0	0.	1150.0	689.3	48548	14.0
40.0	10.0	2199.1	111.5	47810	10.0
40.0	20.0	2253.0	122.6	45620	10.0
40.0	30.0	2155.8	126.2	42044	10.0
40.0	40.0	1958.3	127.3	37191	10.0
40.0	50.0	1648.0	127.6	31208	10.0
40.0	60.0	1177.9	117.2	64739	6.0
40.0	70.0	831.1	117.3	44289	6.0
40.0	80.0	429.3	117.3	22493	6.0

TABLE 4. DISTRIBUTION DATA

THETA(1) = 30.000DEGREES

THETA(2) = 50.000DEGREES

RANGE 1	RANGE 2	IMP VEL, FPS	NUM/SQ FT	GRAMS/SQ FT
215	630	117.3	3.613E-01	2.168E+00
630	991	117.3	4.237E-01	2.542E+00
991	1164	689.3	6.974E-01	9.764E+00
1164	1433	117.2	5.854E-01	3.512E+00
1433	1823	127.6	1.357E-01	1.357E+00
1823	2057	127.3	2.326E-01	2.326E+00
2057	2177	126.2	4.641E-01	4.641E+00
2177	2226	111.5	1.281E+00	1.281E+01
2226	2280	122.6	1.076E+00	1.076E+01

TABLE 5. RANGE AND VELOCITY DATA

THETA	BETA	RANGE, FT	IMP VEL, FPS	NUM	AVG FRAG MASS, G
60.0	-80.0	FRAGMENT DOES NOT CLEAR BARRICADE			
60.0	-70.0	FRAGMENT DOES NOT CLEAR BARRICADE			
60.0	-60.0	FRAGMENT DOES NOT CLEAR BARRICADE			
60.0	-50.0	FRAGMENT DOES NOT CLEAR BARRICADE			
60.0	-40.0	FRAGMENT DOES NOT CLEAR BARRICADE			
60.0	-30.0	FRAGMENT DOES NOT CLEAR BARRICADE			
60.0	-20.0	FRAGMENT DOES NOT CLEAR BARRICADE			
60.0	-10.0	FRAGMENT DOES NOT CLEAR BARRICADE			
60.0	0.	FRAGMENT DOES NOT CLEAR BARRICADE			
60.0	10.0	2354.5	117.2	47810	14.0
60.0	20.0	2427.0	129.2	45620	14.0
60.0	30.0	2324.6	133.0	42044	14.0
60.0	40.0	2119.9	134.5	37191	14.0
60.0	50.0	1696.7	127.6	31208	10.0
60.0	60.0	1355.6	127.6	24277	10.0
60.0	70.0	820.1	117.3	44289	6.0
60.0	80.0	379.4	117.3	22493	6.0

TABLE 6. DISTRIBUTION DATA

THETA(1) = 50.000DEGREES

THETA(2) = 70.000DEGREES

RANGE 1	RANGE 2	IMP VEL, FPS	NUM/SQ FT	GRAMS/SQ FT
190	600	117.3	4.142E-01	2.485E+00
600	1088	117.3	3.170E-01	1.902E+00
1088	1521	127.6	1.184E-01	1.184E+00
1521	1903	127.6	1.387E-01	1.387E+00
1903	2222	134.5	1.576E-01	2.206E+00
2222	2340	133.0	4.417E-01	6.183E+00
2340	2391	117.2	1.136E+00	1.590E+01
2391	2463	129.2	7.429E-01	1.040E+01

APPENDIX III

CRATER PROGRAM

1. FORTRAN PROGRAM DESCRIPTION

The program on cratering follows the theory summarized in Section IV-4. The basic values for the parameters that form part of the program are either assumed ($W_L = 500$ tons, $E_s^D = 0.3$, $\hat{\beta} = 0.3$) or result from the detonation of a 100-ton hemispherical bare charge on a silty clay at the Suffield Experimental Station ($D_a = 21$ ft., $R_a = 70$ ft., soil density = 94 lb/ft³).

New reference values for the charge weight, crater dimensions and soil density are read into the program by statement 45. The following statements compute new values for the dissipation ratio and the ejecta parameter according to the formulas given by Equations (123), (124), (125a) and (125b).

For charge weights that are part of the input data, the program computes apparent depths and radii according to Equations (117), (119), (120), (121a) and (121b). The only difficulty in this procedure is solving the transcendental equation (121a) for the ratio R_a/R_a^0 . The solution is obtained by means of the subroutine TRANS. Since a traditional iterative procedure did not work, it was necessary to write the equation in an alternate form. Suppose we define a function $FR(\hat{R})$ by

$$FR(\hat{R}) = \frac{K}{(E_s^D)^2} \left[1 - \frac{(1 - E_s^D)}{K^{1+\zeta}} (R^{4+\zeta}) \right]^2 - R \quad (III-1)$$

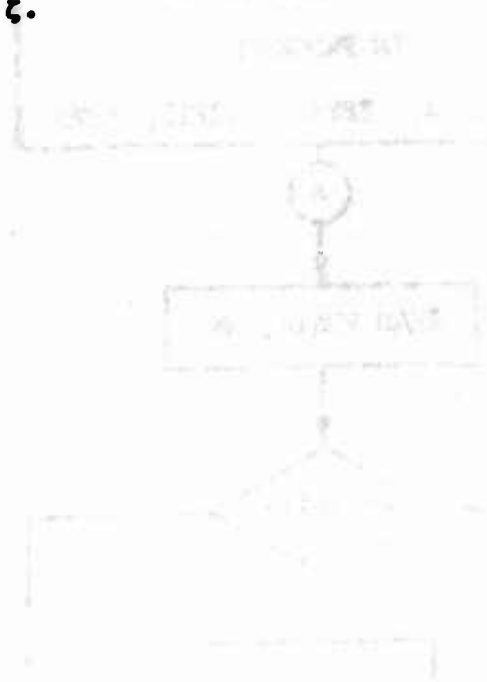
where

$$\hat{R} = R_a/R_a^0$$

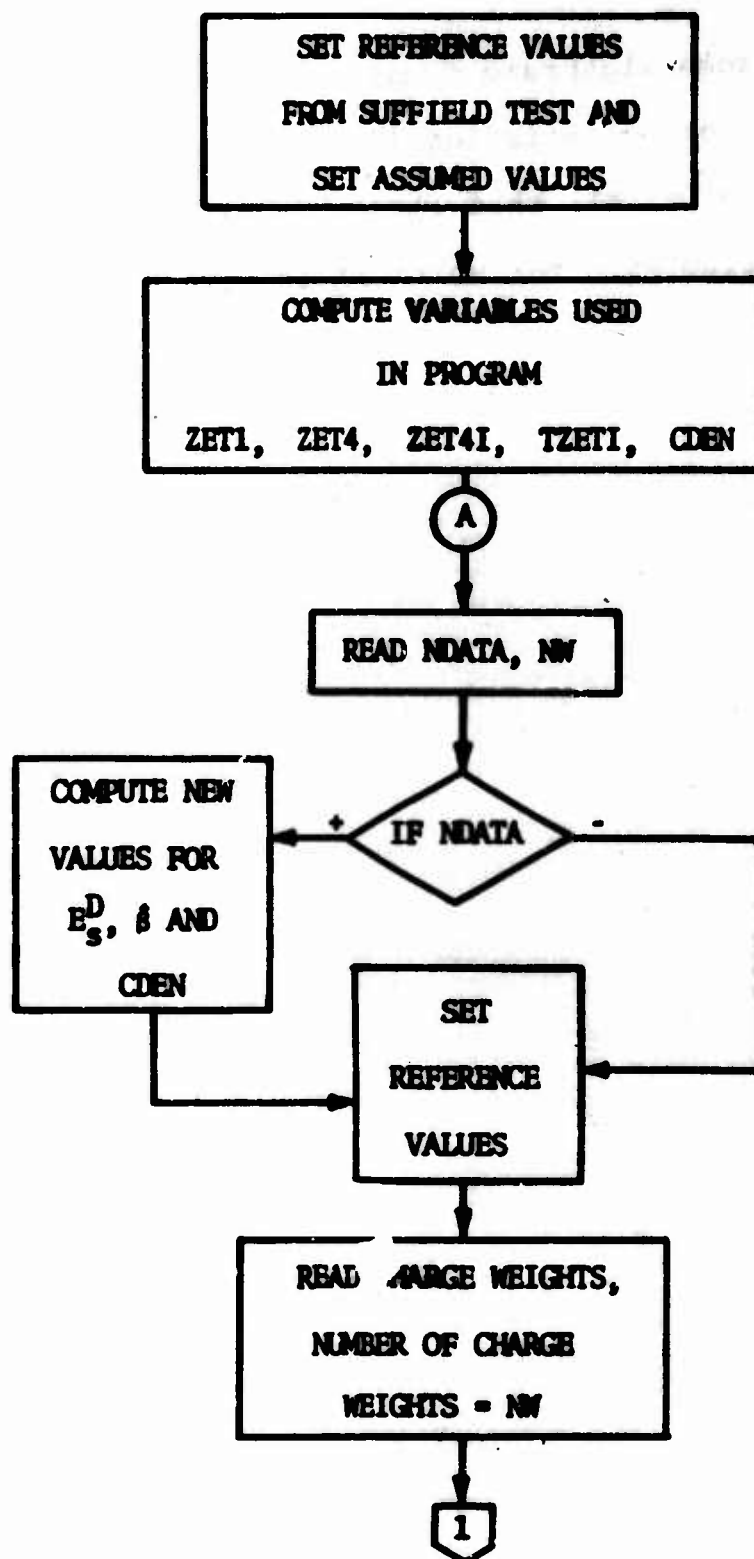
(III-2)

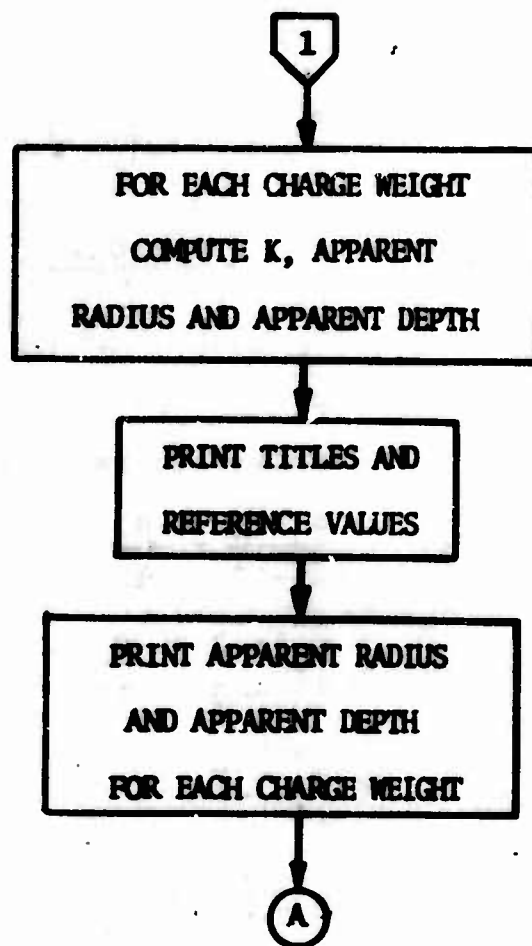
Then after some algebraic manipulations, it can be shown that Equation (121a) is satisfied if $FR(\hat{R})$ is zero.

Essentially, all that the subroutine TRANS does is to find that value of \hat{R} for which FR is zero for given values of K , E_s^D and ζ .



2. CRATER PROGRAM FLOW DIAGRAM





3. LIST OF VARIABLES IN CRATER PROGRAM

a. Main Program

<u>Program Variable</u>	<u>Description</u>
BETH	$\hat{\beta}$
BETHST	$\hat{\beta}^*$
BETREF	Reference value for $\hat{\beta}$
B1	$\frac{\hat{\beta} - 2}{\hat{\beta} - 3} - \frac{8}{15}$
B1ST	$\frac{\hat{\beta}^* - 2}{\hat{\beta}^* - 3} - \frac{8}{15}$
B2ST	$\frac{\hat{\beta}^* - 2}{\hat{\beta}^* - 3}$
CDEN	$2 - \left(\frac{W_o}{W_L}\right)^{1/3}$
CDEN1	$WREF * \left[2 - \frac{W_o}{W_L}\right]^{1/3}$
DEN	Weight density of earth media, ρg (lb./ft. ³)
DENREF	Reference value for density of earth media (lb./ft. ³)
DENST	New weight density of earth media, $\rho^* g$ (lb./ft. ³)
DREF	Reference value for apparent depth (ft.)
DT	D_a/D_a^o

<u>Program Variable</u>	<u>Description</u>
DV(I)	Apparent diameter vector
DZA	D_a^O (ft.)
DZAST	D_a^{*O} (ft.)
D1	$\frac{8}{15}$
D2	$\frac{1}{3}$
D5	C_{Fo}^*/C_{Fo}
D6	$(1 - E_s^{*D}) / (1 - E_s^D)$
D7	$\frac{\rho}{\rho^*} \left(\frac{R_a^O}{R_a^{*O}} \right) \left(\frac{D_a^O}{D_a^{*O}} \right)$
EDS	E_s^D
EDSREF	Reference value for dissipation ratio
EDSST	E_s^{*D}
K	K
NDATA	IF NDATA is positive, new reference values are to be read in
NW	Number of charge weights that are to be read in
RATDST	D_a^{*O}/D_a^O
RATRST	R_a^O/R_a^{*O}
RREF	Reference value for apparent radius (ft.)
RT	R_a/R_a^O
RV(I)	Apparent radius vector
RZA	R_a^O (ft.)

<u>Program Variable</u>	<u>Description</u>
RZAST	R_a^{*0}
TZETI	$1/2$
WL	W_L (tons)
WREF	Reference value for W_0
WV(I)	Charge weight vector
WZ	W_0 (tons)
WZST	W_0^* (tons)
ZETA	ζ
ZET1	$\zeta + 1$
ZET4	$\zeta + 4$
ZET4I	$1/(\zeta + 4)$

b. Subroutine TRANS

<u>Subroutine Variable</u>	<u>Description</u>
A	$K/(E_s^D)^2$
ALPHH	ζ
ALP11	$\zeta + 1$
ALP4II	$1/(\zeta + 4)$
ALP44	$\zeta + 4$
B	$(1 - E_s^D)/K^{\zeta+1}$
DEL	Absolute value of $FR(R)$
EDTT	E_s^D
FNEW, FN	New value of $FR(R)$
FP	Previous value of $FR(R)$

Subroutine VariableDescription

FR(R)	$\frac{K}{(E_s^D)^2} \left[1 - \frac{(1 - E_s^D)}{K^{\zeta+1}} R^{\zeta+4} \right]^2 - R$
KK	K
R	R_a/R_a^0
RP	Previous value of R
RNEW, RN	New value of R

4. PRINTOUT OF CRATER PROGRAM

```

PROGRAM CRATE ( INPUT , OUTPUT )
DIMENSION RV(25),RV(25),RV(25)
REAL K
000041 5 FORMAT (2110)
000041 10 FORMAT (H10.2)
000041 15 FORMAT (1H1.10A.34HREFERENCE PARAMETERS FOR THIS RUN //
000041 1 5X.17HREFERENCE YIELD = ,F7.2,5H TONS ,15X,
000041 2 5X.17HREFERENCE YIELD = ,F7.2,5H TONS //5X.16HAPPARENT DEPTH = ,
000041 3 5X.2,3H FT 10X.17HAPPARENT RADIUS = ,F6.2,3H FT //
000041 4 5X.19HDISSIPATION RATIO = ,F5.2,8X,6HZETA = ,
000041 5 5X.2,8X,6HZETA = ,F5.2,2///
000041 6 5X.3HAPPARENT RADIUS AND DEPTH VERSUS YIELD //
000041 7 5X.1H10X.7,10(TONS).10X.5HDEPTH 9X.6HRADIUS) //
000041 20 FORMAT (110.3F15.2)
C
C REFERENCE DATA FOR SOIL AND PROGRAM CONSTANTS.
000041 DATA W/500./, UZ/100./, UZA/21./, RZA/70./, ZETA/0.3/,
C 1 EDS/0.3/, BETH/3./, UEN/94./, U1/0.533333/, U2/0.333333/
C
000041 ZET1=ZETA*1.
000043 ZET2=ZETA*4.
000044 ZET3=1./ZET1
000045 ZET4=1./ZET1
000047 CUB=2.-((W/UL)*D2)
C
000055 40 READ 5,ADATA,N=
000064 IF (ADATA) GOTO 45
C
000066 45 READ 10,WZST,UZAST,RZAST,DENST
000104 RATDST=DZAST/UZAST
000105 RATST=DZAST/UZAST
000107 EDSST=EDS*((RATDST/RATST)**ZET1)
000113 US=(2.-((WZST/L)*D2))/EDS
000121 D6=(1.-EDSST)/(1.-EDS)
000125 D7=(DEN/DENST)*(RATST**3)/RATDST
000133 U1=(BETH-2.)/(L-ETH-3.)*U1
000141 U1ST=D5*D6*D7*UZAST/d7
000144 H2ST=H1ST*D1
000146 EL1ST=(3.-2S1-2.)/(H2ST-1.)
C
000152 WREF=WZST
000153 DEN-REF=DENST
000154 WREF=UZAST
000156 WREF=RZAST
000160 EDS-REF=EDSST
000161 U1-REF=U1ST
000163 CUB=2.-((WREF/L)*D2)
C
000170 50 TO 55
C
000171 50 WREF=WZ
000172 U1-REF=U1
000174 WREF=UZ
000175 WREF=RZ
000177 EDS-REF=EDS
000200 U1-REF=U1
C
000202 55 CUB=1.-CUB-REF

```

NOT REPRODUCIBLE

```

000204      READ 10,(MV(I),I=1,NW)
C
000216      DO 70 I=1,N
000220      K=(2.-((MV(I)/HL)**D2))*MV(I)/CDEN1
000225      RT=TRANS(K,EDSREF,ZETA,ZE1,ZETA,ZETA)
000233      JT=(RT**ZET1)/(K**ZETA)
000241      RV(I)=RT*RRREF
000245      70 DV(I)=DT*DREF
000251      PRINT 15,WREF,HL,DREF,RREF,EDSREF,ZETA,BETREF
000272      PRINT 20,(I,MV(I),DV(I),RV(I),I=1,NW)
000311      GO TO 40
000312      CALL EXIT
000313      END

```

```

FUNCTION TRANS(KK,EDTT,ALPHH,ALP11,ALP44,ALP411)
REAL KK
FR(X)=A*((1.-H*(R**ALP44))**2.0)-R
* FORMAT (1H0,10X,16HITERATION FAILED )
A=KK/(EDTT*EDTT)
H=(1.-EDTT)/(KK**ALP11)
II=0

```

```

C
000721      NP = 0.
000721      FP = A
000723      RN=(1./H)**ALP411
000726      FN = -RN
000727      5 II=II+1
000731      IF (20-II) 6,6,7
000733      6 PRINT 4
000742      TRANS=0.
000743      RETURN
000743      7 RNE = NP+FP*(RN-RP)/(FP-FN)
000750      FNE=FR(RNE)
000752      DEL=ABS(FNE)
000754      IF (DEL-0.002) 10,10,15
000756      10 TRANS=RNE
000760      RETURN
000760      15 IF (FNE) 16,16,20
000762      16 RN=RNE
000763      FN=FNE
000765      GO TO 5
000766      20 RP=RNE
000767      FP=FNE
000771      GO TO 5

```

```

C
000772      RETURN
000774      END

```

5. INPUT FORMAT

Each set of Input Data consists of either two or three groups of information. The integers NDATA and NW are read in on the first card according to the format 2I10. If NDATA is a positive integer, then the following new reference values are read in on the next card:

- a. WZST - the new reference charge W_0^* (tons),
- b. DZAST - the new reference apparent depth D_a^{*0} (ft.),
- c. RZAST - the new reference apparent radius R_a^{*0} (ft.),
- d. DENST - the new weight density of the earth media, ρ^*g (lb./ft.³).

The format for these variables is 4F10.2. If NDATA is negative or zero, this card is omitted.

The last group of input data consists of NW charge weights for which predicted values of apparent radii and depths are desired. The format for the charge weights is (8F10.2).

6. OUTPUT FORMAT

The output format is illustrated by the sample runs shown on the following pages. In addition to the reference values that formed part of the input, values for the dissipation ratio E_s^D and the ejecta parameter $\hat{\beta}$ (beta) are given. The apparent depth and radius for each of the charge weights are shown in the table following the reference parameters.

To obtain the ejecta depth at a given position, $\hat{\beta}$, and the apparent depth and radius are used in connection with Figure 28 of Section V.

REFERENCE PARAMETERS FOR THIS RUN

REFERENCE YIELD = 100.00 TONS

WL = 500.00 TONS

APPARENT DEPTH = 21.00 FT

APPARENT RADIUS = 70.00 FT

DISSIPATION RATIO = .30

ZETA = .30

HETA = 3.10

APPARENT RADIUS AND DEPTH VERSUS YIELD

I	Y (TONS)	DEPTH	RADIUS
1	10.00	14.72	32.76
2	20.00	16.76	42.11
3	30.00	17.89	48.27
4	40.00	18.66	52.96
5	50.00	19.25	56.84
6	70.00	20.11	63.31
7	100.00	21.00	70.00
8	200.00	22.66	84.83
9	300.00	23.57	94.98
10	400.00	24.16	100.75
11	500.00	24.62	105.97

REFERENCE PARAMETERS FOR THIS RUN

REFERENCE YIELD = 500.00 TONS

WL = 500.00 TONS

APPARENT DEPTH = 38.00 FT

APPARENT RADIUS = 79.00 FT

DISSIPATION RATIO = .66

ZETA = .30

BETA = 3.34

APPARENT RADIUS AND DEPTH VERSUS YIELD

I	W (TONS)	DEPTH	RADIUS
1	10.00	3.76	6.13
2	20.00	7.27	11.84
3	30.00	10.49	17.11
4	40.00	13.34	21.87
5	50.00	15.76	26.05
6	70.00	19.65	33.08
7	100.00	23.74	41.11
8	200.00	30.76	57.36
9	300.00	34.27	67.06
10	400.00	36.47	73.88
11	500.00	38.00	79.00

REFERENCES

1. Peterson, F. H.; Lemont, C. J.; Vergnolle, R. R.; High Explosive Storage Test - Big Papa, Technical Report No. AFWL-TR-67-132, Air Force Weapons Laboratory, Kirtland Air Force Base, New Mexico, May 1968.
2. Manual for Design of Protective Structures Used in Explosive Processing and Storage Facilities, Technical Report 3808, Picatinny Arsenal, Dover, New Jersey, November 1968.
3. Baker, W. E.; Grubbs, B. R.; Fitzgibbon, D. P.; (U) Non-Nuclear Weapons Effects on Protective Structures, Technical Report No. AFWL-TR-69-57, Air Force Weapons Laboratory, Kirtland Air Force Base, New Mexico, September 1969.
(SECRET)
4. Adams, C. L.; Sarmousakis, J. N.; Sperrazza, J.; Comparison of the Blast from Explosive Charges of Different Shapes, Report No. 681, Ballistic Research Laboratories, Aberdeen Proving Ground, Maryland, January 1949.
5. Cooper, C.A.; (U) Preliminary Warhead Terminal Ballistic Handbook, Part II - Warhead Terminal Ballistic Performance, NWL Report No. 1821, 15 August 1962.
6. Johnson, C.; and Smith, S. V.; Non-Nuclear Warhead Terminal Ballistic Handbook, Part II - Warhead Terminal Ballistic Performance, NWL Report No. 1864, U. S. Naval Weapons Laboratory, Dahlgren, Virginia, July 1964. (CONFIDENTIAL)

7. (U) Elements of Terminal Ballistics: Part I, Introduction, Kill Mechanisms and Vulnerability, AMCP 706-160, Headquarters, U. S. Army Material Command, November 1962.
8. Explosive Hazard of Rocket Launchings, Technical Report No. U-108:98, Aeronutronic Division of Ford Motor Company, November 30, 1960.
9. Shames, I. H.; Engineering Mechanics - Dynamics, Prentice-Hall, Inc., 1960.
10. Thomas, L. H.; Computing the Effects of Distance on Damage by Fragments, Report No. 468, Ballistics Research Laboratory, Aberdeen Proving Ground, Maryland.
11. Rindner, R. M.; Wachtell, S.; Safe Distances and Shielding for Prevention of Propagation by Fragment Impact (U), Technical Report No. DB-TR:6-60, Picatinny Arsenal, Dover, New Jersey, 1960. (CONFIDENTIAL)
12. Cratering from High Explosive Charges, Analysis of Crater Data, TR No. 2-547, U. S. Army Engineer Waterways Experiment Station, Corps of Engineers, Vicksburg, Mississippi, June 1961.
13. Rooke, A. D. Jr.; Chew, T. D.; Operation Snow Ball, Project 3.1, Crater Measurements and Earth Media Determinations, Interim Report, Miscellaneous Paper No. I-764, U. S. Army Engineer Waterways Experiment Station, Corps of Engineers, Vicksburg, Mississippi, December 1965.

14. Rooke, A. D. Jr.; Davis, L. K.; "Project 3.01, Monitor Crater Studies," Proceedings: Operation Distant Plain Symposium, Volume I (U), DASIAC Special Report 60, pp. 321-330, September 1967.
15. Diehl, C. H. H.; Pinnell, J. H.; Jones, G. H. S.; Crater and Ejecta Data from the Detonation of a 100 Ton Spherical Charge of TNT Tangential to the Surface (Distant Plain Shot 6) (U), Suffield Technical Note No. 208, Defense Research Establishment Suffield, Ralston, Alberta, August 1968.
16. Vortman, L. J.; Dimensions of a Crater from a 500-Ton TNT Hemisphere Detonated on Rock, SC-RR-65-277, Sandia Corporation, Albuquerque, New Mexico, July 1965.
17. Strange, J. N.; Hendron, A. J. Jr.; Method for Predicting the Shape of Explosion-Produced Craters, Miscellaneous Paper No. I-677, U. S. Army Engineer Waterways Experiment Station, Corps of Engineers, Vicksburg, Mississippi, October 1964.
18. Rooke, A. D. Jr.; Strange, J. N.; Techniques for Determining the Cratering Effects of Surface and Underground Explosions, Miscellaneous Paper No. I-778, U. S. Army Engineer Waterways Experiment Station, Corps of Engineers, Vicksburg, Mississippi, January 1966.

19. Gornak, G.; Preliminary Experiments for Crater Modeling in Controlled Soil Media, Report 1862, U. S. Army Engineer Research and Development Laboratories, Fort Belvoir, Virginia, June 1966.
20. Jones, G. H. S.; Some Comments on Cratering (U), Suffield Special Publication 22, Defense Research Board, Suffield Experimental Station, Ralston, Alberta, 22 April 1962.
21. Brode, H. L.; A Review of Nuclear Explosion Phenomena Pertinent to Protective Construction, R-425-PR, Prepared for United States Air Force Project Rand, The Rand Corporation, Santa Monica, California, May 1964.
22. Effects of Air Blast, Ground Shock, and Cratering on Hardened Structures, AFSCM 500-8, Air Force Systems Command Manual, Headquarters, Air Force Systems Command, Andrews Air Force Base, Washington, D. C. 20331, 1 March 1967.
23. Project STAGECOACH, 20-Ton HE Cratering Experiments in Desert Alluvium, SC-4596 (RR), Sandia Corporation, Albuquerque, New Mexico, Final Report, May 1962.
24. Fung, Y. C.; Foundations of Solid Mechanics, Prentice-Hall, Inc., 1965.

UNCLASSIFIED

Security Classification

DOCUMENT CONTROL DATA - R & D

(Security classification of title, body of abstract and indexing annotation must be entered when the overall report is classified)

1. ORIGINATING ACTIVITY (Corporate author) Mechanics Research, Inc. Albuquerque, New Mexico 87106		5a. REPORT SECURITY CLASSIFICATION Unclassified	
		5b. GROUP	
3. REPORT TITLE ANALYTICAL MODEL FOR HIGH EXPLOSIVE MUNITIONS STORAGE			
4. DESCRIPTIVE NOTES (Type of report and inclusive dates) February 1969 through March 1970			
6. AUTHOR(S) (First name, middle initial, last name) H. L. Schreyer, L. E. Romeberg			
8. REPORT DATE June 1970		7a. TOTAL NO. OF PAGES 256	7b. NO. OF REFS 24
9a. CONTRACT OR GRANT NO. F29601-69-C-0034 0034		9b. ORIGINATOR'S REPORT NUMBER(S) AFWL-TR-70-20	
a. PROJECT NO. 1598			
c. Task 12		9c. OTHER REPORT NO(S) (Any other numbers that may be assigned this report)	
10. DISTRIBUTION STATEMENT This document is subject to special export controls and each transmittal to foreign governments or foreign nationals may be made only with prior approval of AFWL (WLCT), Kirtland AFB, NM 87117. Distribution is limited because of the technology discussed in the report.			
11. SUPPLEMENTARY NOTES		12. SPONSORING MILITARY ACTIVITY AFWL (WLCT) Kirtland AFB, NM 87117	
13. ABSTRACT (Distribution Limitation Statement No. 2) Analytical models and subsequent computer codes have been developed for predicting peak overpressure, positive unit impulse, the distribution and impact velocity of bomb fragments, crater dimensions and ejecta thickness from the detonations of typical bomb stacks used by the Air Force. These models consider aboveground barricaded stacks with an equivalent net weight high-explosive range of 10 to 500 tons of TNT. The peak overpressure and impulse from a detonation are obtained by modifying the known results of a bare hemispherical charge to take into account the stack and barricade geometries and the interaction effect of bombs. Fragment dispersion patterns are predicted by combining experimental results for single bombs and using the trajectory equations for the motion of a steel fragment in air. By using basic principles and experimental data, crater and ejecta dimensions are predicted. Based on output from the computer codes, illustrative examples are given together with recommendations for future tests to obtain needed data. Programs for optimizing munition storage areas are also suggested.			

DD FORM 1 NOV 61 1473

UNCLASSIFIED
Security Classification

~~UNCLASSIFIED~~
~~Security Classification~~

14

KEY WORDS

LINE A

LINK

LINE 6

NOTE

WT

ROLE

WY

SOLE

Munitions storage
Mathematical model
Analytical model
Conventional explosives
Fragmentation

AFBC-HOLLOMAN AFB, NMEX

UNCLASSIFIED
Security Classification